

Electronic Thesis and Dissertation Repository

---

11-18-2020 3:00 PM

## An investigation of the adsorption mechanism of an aliphatic nitrile (TECFLOTE S11) on sulphide mineral surfaces.

Trevor Holness, *The University of Western Ontario*

Supervisor: Hart, Brian. R, *The University of Western Ontario*

Co-Supervisor: Linnen, Robert. L., *The University of Western Ontario*

A thesis submitted in partial fulfillment of the requirements for the Master of Science degree in Geology

© Trevor Holness 2020

Follow this and additional works at: <https://ir.lib.uwo.ca/etd>

 Part of the [Other Earth Sciences Commons](#)

---

### Recommended Citation

Holness, Trevor, "An investigation of the adsorption mechanism of an aliphatic nitrile (TECFLOTE S11) on sulphide mineral surfaces." (2020). *Electronic Thesis and Dissertation Repository*. 7507.  
<https://ir.lib.uwo.ca/etd/7507>

This Dissertation/Thesis is brought to you for free and open access by Scholarship@Western. It has been accepted for inclusion in Electronic Thesis and Dissertation Repository by an authorized administrator of Scholarship@Western. For more information, please contact [wlsadmin@uwo.ca](mailto:wlsadmin@uwo.ca).

## Abstract

As grades of new base metal deposits decline and environmental restrictions on their extraction, increase, the mining industry is looking for new methods of processing minerals. This thesis, investigates the manner in which an aliphatic nitrile (TECFLOTE S11) is adsorbed onto the surface of sulphide mineral surfaces, to understand how TECFLOTE S11 can improve the extraction of base metals from their ores.

Bench tests, including micro-flotation, were conducted and their products examined by Time of Flight – Secondary Ion Mass Spectrometry (ToF-SIMS) to establish where the TECFLOTE S11 was adsorbed onto the mineral surface. The tests showed that the adsorption of TECFLOTE S11 onto chalcopyrite was greater than on to pyrite surfaces. While the results did not provide a definitive model for the adsorption of TECFLOTE S11 on sulphide mineral surfaces, a number of attachment mechanisms are proposed.

## Keywords

TECFLOTE S11, flotation, chalcopyrite, nitrile, collectors

## Summary for Lay Audience

When copper is extracted from its ore, the extracted rock is crushed and ground to the consistency of coarse flour, before it is pulped with water to create a slurry. Specialized chemicals called collectors are added to the slurry. The collector alters the surface chemistry of the copper mineral surface so that it does not mix well with water, which is called hydrophobic. When air is blown through the slurry, the now hydrophobic copper mineral, adheres to the air bubbles and floats to the surface of the slurry. This process is called froth flotation.

For almost a century, the mineral processing industry, has relied on sulphur-based chemicals called xanthates, to be the workhorse collector in the flotation of copper minerals. In 2018, a new family of collectors (TECFLOTE) were introduced to improve the efficiency of the flotation process and produce a higher copper content to the finished product. TECFLOTE is different from xanthates in that the sulphur atoms are replaced by a carbon atom that is triple-bonded to a nitrogen atom, which is called a nitrile.

Bench tests involving various methods of mixing the TECFLOTE chemical with copper sulphide (chalcopyrite) minerals were conducted and the surface of the sulphide mineral examined by Time of Flight-Secondary Ion Mass Spectrometry (ToF-SIMS) to determine the adsorption of TECFLOTE on the mineral surface. ToF-SIMS, bombards the surface with ions from a heated bismuth source, to eject ions from the surface being examined. The time for these secondary ions to reach a detector is measured and the ions identified because lighter ions travel faster than heavier ions.

The investigation determined that TECFLOTE, adsorbs onto the chalcopyrite in quantities larger than the amount that is adsorbed onto iron sulphide (pyrite) surfaces. This difference in adsorption allows chalcopyrite to be selectively separated from pyrite and produce a high-grade copper end-product. The investigation also found that the method of introducing the TECFLOTE to the slurry affected its adsorption on the chalcopyrite surfaces, which permitted a model of the adsorption mechanism of TECFLOTE to be developed.

## Acknowledgments

I would like to express my appreciation to:

Dr. Brian Hart for his guidance and support. I especially appreciate his having rekindled in me, my love for the mining and particularly the mineral processing industry. It has been an honour to be his “last graduate student.”

Dr. Bob Linnen, for his academic guidance and for his wellbeing checks during the pandemic.

Dr. Carolyn Hill, for her assistance in loading samples into the ToF-SIMS and SEM-EDX analyzers.

Ms. Baian Almusned for her assistance with the use of the SEM.

Nouryon for the supply of the samples of the TECFLOTE chemicals.

All the staff at Surface Science Western (SSW) for their hospitality, while I was conducting the surface analysis portions of my research.

Last but by no means least, the person, without whom none of this would be possible, my wife Rose Anne, who has supported and encouraged me throughout our married life.

## Table of Contents

Abstract.....	ii
Keywords.....	iii
Summary for Lay Audience .....	iv
Acknowledgments.....	v
Table of Contents.....	vi
List of Figures .....	x
List of Tables .....	xiv
List of Appendices (where applicable).....	xvii
Glossary and Abbreviations .....	xviii
1. Introduction .....	1
1.1 History of Froth Flotation .....	3
1.1.1 First period (1860-1920).....	4
1.1.2 Second period (1920-1950) .....	4
1.1.3 Third period (1951-2000).....	5
1.1.4 Fourth period (2001- present) .....	5
1.2 Thesis Objectives.....	6
1.3 Thesis Overview .....	7
1.4 References .....	8
2 Chemistry and Physics of Flotation.....	9
2.1 Physics of Froth Flotation .....	9

2.1.1 Contact Angle.....	9
2.1.2 Contact angle and flotation. ....	11
2.1.3 Contact angle and flotation kinetics .....	12
2.2. Particle-Bubble attachment.....	13
2.2.1 Bubble trajectory. ....	13
2.2.2 Film Drainage .....	18
2.2.3 Summary .....	21
2.3. Thermodynamics of Flotation.....	21
2.3.1 Summary .....	26
2.4. Chemistry of Froth Flotation.....	26
2.4.1 Electrochemistry .....	26
2.4.1.1 Electrical Double Layer .....	27
2.4.1.2 Hydration of Surfaces .....	31
2.4.1.3 Galvanic interaction between iron and sulphide minerals.....	34
2.4.1.4 Summary .....	37
2.5. Electrochemistry of Sulphide flotation. ....	38
2.5.1 Cathodic reduction of Oxygen .....	38
2.5.2 Electrochemistry and surface hydrophobicity.....	38
2.5.3 Summary .....	39
2.6. Reaction between flotation chemicals (Collectors) and Sulphide minerals..	40
2.6.1 Thiol Collector Coatings on Sulphides .....	46
2.6.2 Summary .....	49
2.7. Activation mechanisms for selective flotation of pyrite and sphalerite. ....	50
2.7.1 Activation of sphalerite.....	50

2.7.2 Cu(OH) <sub>2</sub> activation.....	53
2.7.3 Zeta potential and isoelectric point (iep) .....	54
2.7.4 Effect of sphalerite iron concentration on copper activation. ....	56
2.7.5 Copper activation of pyrite. ....	57
2.7.6 Cu(II) and Cu(OH) <sub>2</sub> activation.....	58
2.7.7 Mixed pyrite and sphalerite flotation .....	59
2.7.8 Summary .....	62
2.8. Amine flotation of potash ores.....	63
2.9. Conclusions .....	64
2.10. References. ....	66
3 Methodology.....	76
3.1 Materials used.....	76
3.1.1 Sulphide Minerals .....	76
3.2 Research Methodology .....	77
3.2.1 Conditioning tests.....	77
3.2.2 Micro-flotation Tests .....	78
3.2.3 Column flotation tests .....	80
3.2.4 Time of Flight Secondary Ion Mass spectrometry (ToF-SIMS).....	81
3.2.5 Scanning Electron Microscope-Energy Dispersive X-ray Spectroscopy (SEM-EDX).....	83
3.3 Data Generation and Presentation .....	84
3.3.1 ToF-SIMS .....	84
3.3.2 TOF-SIMS surface chemistry data presentation .....	85
3.3.3 SEM-EDX.....	86
3.4 Metallurgical balances .....	87



3.5 References .....	89
4. Results and Discussion.....	91
4.1 Experimental results .....	98
4.1.1 Conditioning tests .....	98
4.1.2 Column tests .....	102
4.1.3 Micro-flotation tests .....	106
4.2 Discussion.....	114
4.2.1 Distribution mechanism.....	114
4.2.2 Adsorption mechanism .....	116
4.2.3 Selectivity of TECFLOTE S11 for chalcopyrite instead of pyrite.....	118
4.3 Summary .....	120
4.4 References .....	121
5 Conclusions .....	123
6 Future Work.....	125
Appendix 1. Test data .....	127
Appendix 2. Permissions to Reproduce .....	134
Curriculum Vitae .....	136

## List of Figures

Figure 1.1 Cross section of typical flotation cell.....	2.
Figure 1.2 Daily tonnage of copper ores milled .....	4.
Figure 1.3 Representation of TECFLOTE S10 molecule.....	6.
Figure 1.4 Representation of TECFLOTE S11molecule. ....	6.
Figure 2.1. Surface Tension of bubble on mineral surface showing the surface tension forces.	10.
Figure 2.2 Three-zone model of particle-bubble interaction around the surface of a bubble.	15.
Figure 2.3. Observed trajectories of spherical particles.....	16.
Figure 2.4. Observed trajectories around a bubble, coloured by their instantaneous speeds.	17.
Figure 2.5. Position of particle A relative to bubble surface over time .....	18.
Figure 2.6 Instantaneous dynamic contact angle, following primary hole formation for two bubbles of different radii.....	20.
Figure 2.7. Attachment of particle (S) to bubble (G) in water (L).....	23.
Figure 2.8. Mechanism of bubble attachment:.....	25.
Figure 2.9. Mechanism of bubble attachment: .....	25.
Figure 2.10.(a) Stern model of electrical double layer. (b). Change in potential with distance from solid surface. ....	28.
Figure 2.11. Compression of the double layer by indifferent electrolytes.....	29.
Figure 2.12. Oxidation and reduction reactions, with an electron migrating from the cathode to the anode site. ....	30.

Figure 2.13. Polar nature of water molecule.....	32.
Figure 2.14. Hydrogen bonding properties of water with silica. ....	32.
Figure 2.15. Hydration of metal sulphide surface.....	33.
Figure 2.16. Effect of dissolved oxygen on hydration of metal sulphide surface. ....	34.
Figure 2.17. A schematic representation of the electrochemical cell formed when ferrous grinding media is in contact with sulphide minerals .....	35.
Figure 2.18. Current-potential curves for the reduction of a xanthate collector to diethyldixathogen on platinum.....	39.
Figure 2.19. General structure of flotation collector and adsorption mechanism .....	40.
Figure 2.20. Classification of flotation collectors.....	41.
Figure 2.21. Chemical structure of most popular sulfydryl collectors .....	42.
Figure 2.22. Precipitation regions of cuprous ethyl xanthate. ....	46.
Figure 2.23. Schematic of sphalerite copper activation showing the various simultaneous processes likely to occur under different activation conditions. ....	52.
Figure 2.24. The position of the Cu on the surface of the sphalerite lattice is shown as indicated by the XAFS results .....	53.
Figure 2.25. Zeta potential of sphalerite at increasing pH.....	55.
Figure 2.26. Adsorption and dixanthogen formation on unactivated pyrite surface .....	57.
Figure 3.1. Siwek micro-flotation tube. From (Leja, 1982).....	79.
Figure 3-2. Mass spectrum in the region from 58 to 66.5 amu.....	.82.
Figure 3-3. ToF-SIMS output: (a) Distribution of Cu <sup>+</sup> ions on grain surfaces; (b) Selected ROI; (c) Spectrum of Cu <sup>+</sup> of an ROI.....	84.

Figure 3.4. Example of box and whisker plot with explanation of the legend.....	85.
Figure 4.1 (a) ToF-SIMS spectra of TECFLOTE S11 showing negative secondary ion fragments between amu 0 and 50.....	93.
Figure 4.1 (b) ToF-SIMS spectra of TECFLOTE S11 showing negative secondary ion fragments between amu 50 and 100.....	94.
Figure 4.1 (c) ToF-SIMS spectra of TECFLOTE S11 showing negative secondary ion fragments between amu 100 and 150.....	95.
Figure 4.1 (d) ToF-SIMS spectra of TECFLOTE S11 showing negative secondary ion fragments between amu 150 and 200 .....	96.
Figure 4.1 (e) ToF-SIMS spectra of TECFLOTE S11 showing negation secondary ion fragments between amu 200 and 233 .....	97.
Figure 4.2 Box plots of normalized intensity for mass positions identified as representative of TECFLOTE S11.....	99.
Figure 4.3 Box plots of normalize intensity of negative ion mass positions from conditioning tests compared to baseline tests.....	100.
Figure 4.4. Box plot of TECFLOTE S11 ion intensities on pyrite grains with (green) and without CuSO <sub>4</sub> (blue) .....	101.
Figure 4.5. Comparison of TECFLOTE S11 intensity on chalcopyrite grains from column flotation tests.....	104.
Figure 4.6. Comparison of TECFLOTE S11 intensities obtained in column flotation tests, .before washing (blue) and after washing (green) with conditioning tests (yellow).....	105.
Figure 4.7. Mass recovery of the concentrate and tails, the Cu grade and the non-mass corrected Cu recovery for the microflotation test samples performed at four different pH's.....	107.

Figure 4.8. TECFLOTE S11 ion intensities on concentrate and tailings portions from micro-flotation tests at (a) pH 6.7, (b) pH 8.1, (c) pH 9.5 and (d) pH 10.9. ....	108.
Figure 4.9. Median ion intensity of TECFLOTE S11 at amu 149, on microflotation concentrate (green), tailings (blue) compared to weighted % recovery (purple line).....	109.
Figure 4.10. General structure and adsorption mechanism of flotation collector.....	111.
Figure 4.11. Comparison of TECFLOTE S11 surface intensities on chalcopyrite grains from concentrates between the micro-flotation tests (solid colour) and column tests before washing (hashed areas) areas at approximately pH 9.5 .....	113.
Figure 4.12 Comparison of TECFLOTE S11 between micro-flotation tests and conditioning tests.....	114.

## List of Tables

Table 3.1. Composition of "synthetic ores" used in investigations.	76
Table 3.2 Elemental content of sample of the tailings from micro-flotation test, conducted at pH 6.7, with statistics, as measured by EDX used in estimating the recoveries.	87
Table 4.1 TECFLOTE S11 labels and associated amu. * denotes spectrum used for illustrative purposes.	92
Table 4.2. Metallurgical results from the microflotation tests.	106
Table A1. Conditioning tests +ve ions on Chalcopyrite grains. Baseline.....	128
Table A2. Conditioning tests -ve ions on Chalcopyrite grains. Baseline.....	128
Table A3. Conditioning tests +ve ions on Pyrite grains. Baseline.....	128
Table A4. Conditioning tests -ve ions on Pyrite grains. Baseline.....	128
Table A5. Conditioning tests +ve ion loadings on Chalcopyrite grains.....	128
Table A6. Conditioning tests. -ve ion loadings on Chalcopyrite grains.....	128
Table A7. Conditioning tests. +ve ions on Pyrite grains.....	128
Table A8. Conditioning tests -ve ions on Pyrite grains.....	129
Table A9. Conditioning tests with addition of CuSO <sub>4</sub> -ve loadings on Chalcopyrite.....	129
Table A10. Conditioning tests with addition of CuSO <sub>4</sub> +ve ion loadings on Chalcopyrite.....	129
Table A11. Conditioning test with addition of CuSO <sub>4</sub> -ve ions loading on Pyrite grains.....	129
Table A12. Conditioning tests with addition of CuSO <sub>4</sub> +ve ion loadings on Pyrite grains.....	129
Table A13. Micro-flotation tests -ve ion loadings on concentrate pH 6.7.....	129
Table A14. Micro-flotation tests TECFLOTE S11 -ve ion loadings on concentrate pH 6.7.....	129

Table A15.	Micro-flotation tests +ve ion loadings on concentrate pH 6.7.....	129
Table A16.	Micro-flotation tests TECFLOTE S11 +ve ion loadings on concentrate pH 6.7.....	130
Table A17.	Microflotation tests. -ve ions loading on tailings pH 6.7.....	130
Table A18.	Microflotation tests. TECFLOTE S11 -ve ions loading on tailings pH 6.7.....	130
Table A19.	Micro-flotation tests. +ve ion loadings on tailings. pH 6.7.....	130
Table A20.	Micro-flotation tests. TECFLOTE S11 +ve ion loadings on tailings. pH 6.7.....	130
Table A21.	Micro-flotation tests. -ve ion loadings on concentrate. pH 8.1.....	130
Table A22.	Micro-flotation tests. TECFLOTE S11 -ve ion loadings on concentrate. pH 8.1... ..	130
Table A23.	Micro-flotation tests. +ve ion loadings on concentrate. pH 8.1.....	130
Table A24.	Micro-flotation tests TECFLOTE S11 +ve ion loadings on concentrate. pH 8.1.....	131
Table A25.	Micro-flotation tests +ve ion loadings on tailings pH 8.1.....	131
Table A26.	Micro-flotation tests -ve ion loadings on tailings pH 8.1.....	131
Table A27.	Micro-flotation tests TECFLOTE S11 -ve ion loadings on tailings pH 8.1.....	131
Table A28.	Micro-flotation tests TECFLOTE S11 +ve ion loadings on tailings pH 8.1.....	131
Table A29.	Microflotation tests. -ve ion loadings on concentrate. pH 9.5.....	131
Table A30.	Microflotation tests. TECFLOTE S11 -ve ion loadings on concentrate. pH 9.5.....	131
Table A31.	Micro-flotation tests. +ve ion loadings on concentrate. pH 9.5.....	131
Table A32.	Micro-flotation tests. TECFLOTE S11 +ve ion loadings on concentrate. pH 9.5 .....	132
Table A33.	Micro-flotation tests. -ve ion loadings on tailings. pH 9.5.....	132
Table A34.	Micro-flotation tests. TECFLOTE S11 -ve ion loadings on tailings. pH 9.5.....	132

Table A35	Micro-flotation tests. +ve ions loadings on tailings. pH 9.5.....	132
Table A36.	Micro-flotation tests. TECFLOTE S11 +ve ions loadings on tailings. pH 9.5.....	132
Table A37.	Micro-flotation tests. -ve ion loadings on concentrate. pH 10.9.....	132
Table A38.	Micro-flotation tests. TECFLOTE S11 -ve ion loadings on concentrate. pH 10.9 ..	132
Table A39.	Micro-flotation tests. +ve ion loadings on concentrate. pH 10.9.....	132
Table A40.	Micro-flotation tests. TECFLOTE S11 +ve ion loadings on concentrate. pH 10.9...	133
Table A41.	Micro-flotation tests. -ve ion loadings on tailings. pH 10.9.....	133
Table A42.	Micro-flotation tests. TECFLOTE S11 -ve ion loadings on tailings. pH 10.9.....	133
Table A43.	Micro-flotation tests. +ve ion loadings on tailings. pH 10.9.....	133
Table A44.	Micro-flotation tests. TECFLOTE S11 +ve ion loadings on tailings. pH 10.9.....	133
Table A45	Column flotation tests -ve ion loadings unwashed grains.....	133
Table A46	Column flotation tests. +ve ion loadings unwashed grains.....	133
Table A47.	Column flotation tests. -ve ion loadings washed grains.....	133
Table A48.	Column flotation tests. +ve ion loading washed grains.....	134
Table A49.	Micro-flotation tests tailings EDX values.....	134
Table A50.	Micro-flotation tests. Metallurgical balance.....	134



## List of Appendices (where applicable)

Appendix 1: Test Data .....	123
Appendix 2: Permissions to reproduce.....	129

## Glossary and Abbreviations

Adsorption	Physiochemical reaction between mineral surface and collector whereby collector adheres to a surface. A new chemical phase is created at the surface, or a surface charge created.
Beneficiation	Process where valuable minerals are separated from non-value minerals.
Cleaners	The final stage of flotation process where the final concentrate grade is improved.
Collector	Chemical (surfactant) added to make a mineral surface hydrophobic
Concentrate	The fraction of feed that is extracted by a process
Feed	Untreated ore
Gangue	Material of no commercial value, rejected in processing.
Grade	Metal content of the flotation fraction
Recovery	Wt % of metal in a concentrate as % of metal in the feed
Roughers	The first cells in the flotation circuit. Mostly fully liberated grains are collected.
Tails or tailings	The fraction of feed that is not extracted in a processing stage. Contains gangue and unwanted minerals.
<b>Abbreviations</b>	
A	Surface area of a solid
DTPI	Diisobutyl dithiophosphate
Eh	Oxidation potential
EXAFS	X-Ray absorption fine structure

FTIR-ATR	Fourier Transform Infra-Red -Attenued Total Reflection
G	Surface free energy
MIBC	Methyl isobutyl carbinol
R	Gas constant or hydrocarbon chain
ROI	Region Of Interest
SHE	Standard Hydrogen Electrode
T	temperature
ToF-SIMS	Time of Flight-Secondary Ion Mass Spectrometry
TPC	Three-Phase Contact
TPLC	Three-Phase Line of Contact
XAS	X-Ray Absorption Spectroscopy

---

*“The metallurgist has been the geologist’s best friend, and the geologist in turn has been able to help convert the metallurgist’s ideas into the concrete form of an increased ore supply”*

*P. Billingsly a mining geologist. 1928*

---

(Fuerstenau et al., 2007)

## 1. Introduction

Froth flotation, generally referred to as flotation, is a technique for the beneficiation of mineral ores. The process is essentially one of physical separation where the value-added phases are selectively separated from the waste or gangue phases. The process relies heavily on the physical and chemical differences between the various minerals within the ore. The process of selective mineral flotation of the ore depends upon the differences in the affinity for water on the mineral surfaces. Mineral surfaces that attract water, are referred to as hydrophilic or wettable and those that repel water are referred to as hydrophobic. Flotation separation involves ensuring that the surfaces of the minerals to be floated are rendered hydrophobic. Few mineral surfaces are naturally hydrophobic; however, most minerals will show some degree of hydrophobicity under certain conditions of pH and Eh. Froth flotation is the most commonly used process for the beneficiation of metal sulphide minerals. It is also used in the processing of gold, coal, apatite, various silicate and oxide ores, as well as de-inking paper and waste water purification.

The process of mineral separation by froth flotation commences with comminution: crushing, grinding and sizing of the ore constituents to a size where ideally, each particle is composed solely of either the valuable or gangue material. This step is referred to as liberation and is essential to ensuring that the particles entering the flotation process are capable of being separated. It is also critical that the comminution limits the generation of fine material that can be problematic in the flotation process.

The liberated mineral particles are mixed with water and form a suspension with the fluid, referred to as a pulp. The process of flotation separation begins with the introduction of air or gas to the pulp. Some of the solid species whose surfaces are naturally hydrophobic adhere to the gas bubbles, others adhere to the bubbles due to induced hydrophobicity through the addition of chemical reagents (referred to as collectors) which are adsorbed onto their surface. The remainder of the species whose surface are not hydrophobic remain suspended within the pulp.

The gas bubbles with the adhering mineral particles, rise to the surface of the pulp, where the froth is scraped off into the launder of the flotation machine.

The products of the concentration by froth flotation are called, concentrates and tails. The valuable minerals in the concentrate are further treated by other metallurgical processes, such as leaching or smelting. The tails or tailings are either shuttled to another section of the beneficiation or are discarded to a tailings disposal area.

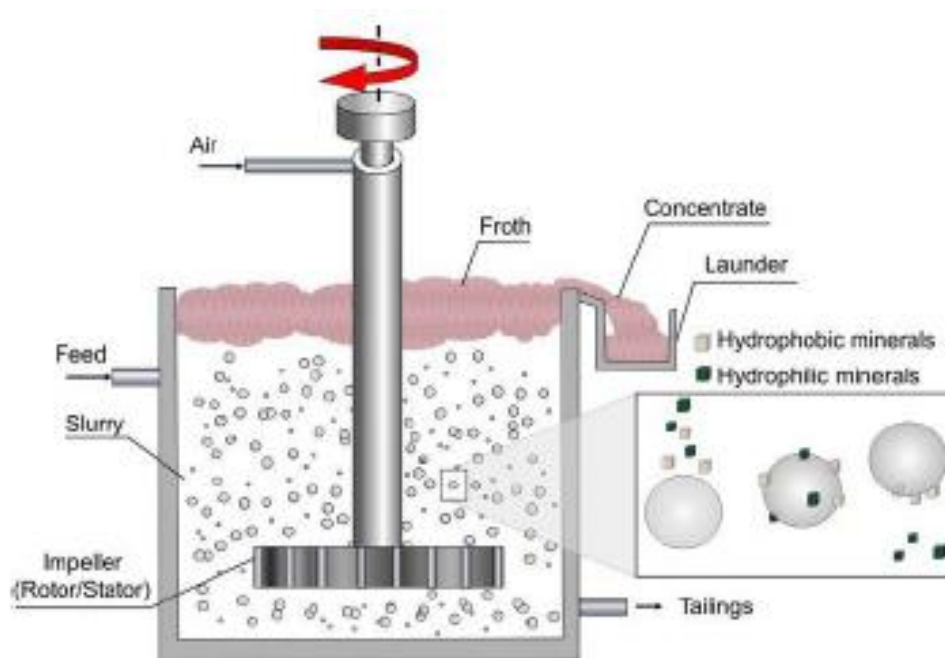


Figure 1.1 Cross section of typical flotation cell, the insert shows the valuable minerals sticking to air bubbles and rising to the surface. Gangue minerals remain suspended in the slurry.

Reprinted from *Mineral Processing Technology* (p.285-360). By B.A. Wills and J.A. Finch, 2015, Butterworth-Heinemann. Copyright 2015 by Elsevier. Reprinted with permission

Most inorganic particles have a hydrophilic surface, and as such, are not floatable. To attach the mineral surface to an air bubble, requires the displacement of a water film between their surfaces. This is partially achieved using surfactants designed to render specific mineral surfaces hydrophobic. Collectors, so called because the surfactant allows the valuable mineral to be collected whilst the non-valuable minerals are rejected, are usually long chain hydrocarbon molecules containing a polar group. The polar headgroup of the collector becomes absorbed onto the mineral surface with the hydrocarbon chain being presented to the aqueous phase. The later, being hydrophobic, attaches to the introduced air bubbles and the mineral/collector complex is then removed from the pulp through collector induced flotation.

## 1.1 History of Froth Flotation

Flotation, has been used by the mineral processing and waste water treatment industries since the 19<sup>th</sup> century. The first patent was issued in Dresden to Gebrueber Bessel in 1877 for the concentration of graphite, using nonpolar oils (Fuerstenau et al., 2007). In 1911, James M. Hyde used flotation in the US for copper sulphide concentration at Butte and Superior Copper Company. However, it was not until 1923 that widespread utilization was started. This resulted in an increase in concentrate grades, but also a decrease in mining cutoff grades and increase in mineral reserves (Fuerstenau et al., 2007)

From a small beginning of 45.94 Mt of sulphide ores being treated in the U.S. in 1926, the total tonnage of flotation treated sulphide ores rose to 142.32 Mt in 1960 and to 260.98 Mt in 1980 (Fuerstenau et al., 2007). Most of the ores treated were copper and the copper recoveries increased from 87.4% to 91.2%. Furthermore, the size of the concentrators have increased exponentially from 100-300 tonnes/day in 1930 to 1000-30,000 tonnes/day in the 1960s (Crabtree and Vincent, 1962) to 20,000-60,000 tonnes/day in the 1980s with some mills in the

100,000-175,000 tonnes/day range (Leja, 1982) Figure 1-2. Future predictions indicate that concentrators will process up to 365,000 tonnes/day.

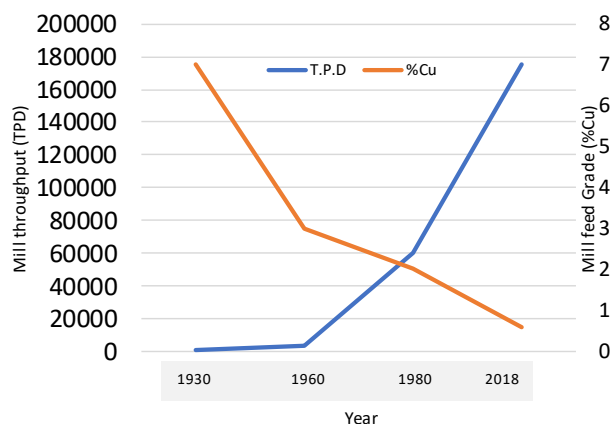


Figure 1.2 Daily tonnage of copper ores milled (T.P.D, left axis), has steadily increased, whilst the 00 grade (%Cu, right axis) has decreased.

Adapted from *Froth Flotation. 50<sup>th</sup>*

*Anniversary Volume* (p. 23) by M.C.

Fuerstenau, 1962, the American Institute of Mining, Metallurgy and Petroleum Engineers, Inc. Copyright by the American Institute of Mining, Metallurgy and Petroleum Engineers, Inc.

At the same time as the use of froth flotation was gaining popularity, the search for new chemical reagents for improving flotation performance was advancing. Nagaraj and Farinato (2016) in their paper on the evolution of flotation chemistry, postulated a continuum of evolution. A summary of flotation reagent development is given below.

### 1.1.1 First period (1860-1920)

This period is characterized by process improvement designed to reduce the consumption of oils used as the main flotation collectors. The research method was strictly trial and error of any readily available chemical. As a result, it was found that alkaline circuits lead to lower reagent consumption in sulphide flotation. Also, that the best sulphide collectors contained either nitrogen and/or sulphur atoms (Nagaraj & Farinato, 2016).

### 1.1.2 Second period (1920-1950)

Research during this period, focused on screening chemicals which were in use in other industries, to use as building blocks for new flotation chemical families. Many of the chemicals which were developed in this period, are still in use today, including the workhorses of the



industry, namely, xanthates, dithiophosphates and mercaptobenzoates. All of these contain either sulphur and/or nitrogen atoms (Nagaraj & Farinato, 2016).

### 1.1.3 Third period (1951-2000)

As the understanding of organic, polymer and coordination chemistry increased, reagents were designed for specific challenges experienced by the mineral processing industry. The concept of donor-acceptor reactions led to the development of collectors based on the reactions resulting from a redistribution of valence electrons. The role of the functional group became the predominant factor over the attributes of charge, solubility, hydrolysable or oxidizable etc. (Nagaraj and Farinato, 2016).

### 1.1.4 Fourth period (2001- present)

The failure rate of new product introductions was high due to the selection of new flotation reagents being subjective, being based mainly on personal preference with no standards of practice. The need to control the froth zone, which is central to flotation was recognized during this period. However, the dynamics of particle flow through a network of liquid lamellae is still unavailable. (Nagaraj and Farinato, 2016). Underlying the research, is the recognition that reagent development is driven by industry needs before there is a basic understanding of the theory of the interaction between the mineral and the reagent (Adamson and Gast, 1997; Nagaraj and Farinato, 2016).

In 2018, Akzo Nobel, now renamed Nouryon, introduced a family of flotation collectors for sulphide minerals, under the tradename TECFLOTE. The TECFLOTE collectors are non-ionic and immiscible with water, making them completely different from the thiol collectors currently used for sulphide mineral flotation.

The reagent used as a model for aliphatic nitrile collectors is TECFLOTE S11. The TECFLOTE family of collectors are manufactured by Nouryon Chemicals B.V., headquartered in The Netherlands. The chemical structure of the TECFLOTE family consists of a triple bonded CN functional group attached to organic chains of various length (number of carbon atoms). TECFLOTE S10 has 12-16 carbon atoms (Figure 1.3) whereas TECFLOTE S11 has 36 carbon atoms (Figure 1.4). Both variants are immiscible with water and consequently when introduced

into a mineral slurry, the collector spreads across the water/air interface rather than dissolving in water as do the more commonly used thiol group of flotation collectors, for example the xanthates (Lewis and Lima, 2018). Nouryon, claims that the use of TECFLOTE collectors result in higher grade and recoveries than do xanthate collectors (Lewis and Lima, 2018). As well as improving rougher grades, TECFLOTE also improves the flotation of fines (Lewis et al.,2019).

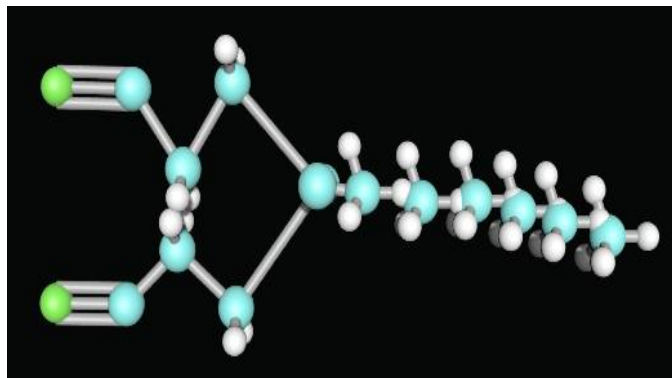


Figure 1.3 Representation of TECFLOTE S10 molecule. Carbon atoms are blue. Hydrogen atoms are white and nitrogen green.

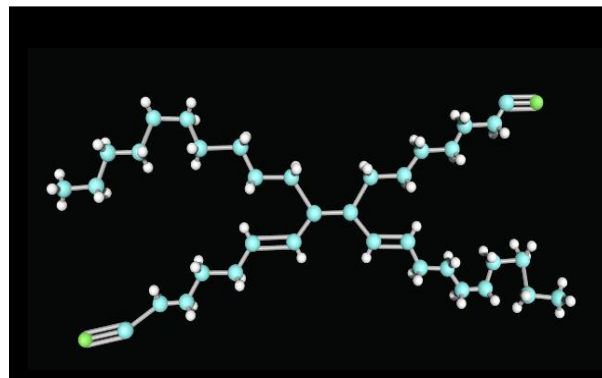


Figure 1.4 Representation of TECFLOTE S11 molecule. Carbon atoms are blue, Hydrogen atoms are white and nitrogen green.

## 1.2 Thesis Objectives

Although the TECFLOTE collectors have been shown to improve grade and recovery in a mill environment (Lewis, et al., 2019; Lewis and Lima, 2018), little research has been conducted into the reasons for the improved performance besides these plant trials.

The overall goal of the thesis is to better understand the role of the TECFLOTE family of collectors (specifically TECFLOTE S11) in the flotation recovery of the sulphide minerals chalcopyrite and pyrite. The thesis will, through a series of laboratory tests, attempt to identify some of the factors giving rise to the test outcomes. The data generated will be used to develop

an adsorption model which can be used towards the continued improvement of the flotation response. The adsorption model consists of two parts: Collector distribution, or how the collector is delivered to the mineral surface and; Surface attachment, which describes how the collector is attached to the mineral surface, rendering the surface hydrophobic to allow flotation. This thesis concentrates on the collector distribution portion of the mechanism and the surface attachment will be speculated upon. To this end, three series of experiments (conditioning, column flotation and micro-flotation) will be conducted to:

- 1) Establish if there is a preference of TECFLOTE S11 for chalcopyrite over pyrite.
- 2) Establish the distribution mechanism of TECFLOTE S11 as a collector in the flotation of sulphide minerals.
- 3) Ascertain the relationship between TECFLOTE S11 concentration on the chalcopyrite surface and flotation recoveries.

TECFLOTE S11<sup>TM</sup> was chosen over TECFLOTE S10 as the model aliphatic nitrile collector, because the TECFLOTE S10<sup>TM</sup> was diluted with 10% acetyl nitrile (ACN) and so the pure TECFLOTE S11, eliminated the presence of ACN as a variable.

## 1.3 Thesis Overview

Chapter 1 presents a background to froth flotation, the history of froth flotation and the evolution of reagents in the froth flotation process.

Chapter 2 reviews the chemistry and physics of froth flotation as described in the literature.

Chapter 3 defines the research methods and instrumentation used to conduct the experiments.

Chapter 4 discusses the results of the experiments conducted in the investigation.

Chapter 5 summarizes the main findings and conclusions of the research and suggests future work that needs to be conducted.

## 1.4 References

- Adamson, A. and Gast, A. P. (1997). *Physical Chemistry of Surfaces* (6th ed.). New York: John Wiley & Sons.
- Crabtree, E.H., Vincent, J. D. (1962). *Froth Flotation. 50th Anniversary Volume*. (D. W. Fuerstenau, Ed.). New York: American institute of Mining, Metallurgical and Petroleum Engineers.
- Fuerstenau, M. C., Graeme, J., & Yoon, R. H. (2007). *Froth Flotation: A Century of Innovation. Flotation Chemistry*.
- Leja, J. (1982). *Surface Chemistry of Froth Flotation* (First). New York: Plenum.
- Lewis, A., Bolin N-J., Malm, Svensson, M., Lima, O. (2019). Analysis of the rougher-scavenger bank using Tecflote S11 at Boliden Aitik. In *Flotation '19*.
- Lewis, A. and Lima, O. (2018). Tecflote- New collector for Sulfide Flotation. In *Procemin Geomet* (pp. 321–333). Santiago, Chile.
- Nagaraj, D.R. and Farinato, R. S. (2016). Evolution of flotation chemistry and chemicals: A century of innovations and the lingering challenges. *Minerals Engineering*, 96–97, 2–14.
- Nagaraj, D. R., & Farinato, R. S. (2016). Evolution of flotation chemistry and chemicals: A century of innovations and the lingering challenges. *Minerals Engineering*.  
<https://doi.org/10.1016/j.mineng.2016.06.019>
- Wills and Finch. (2015). *Mineral Processing Technology* (8th ed.). Butterworth-Heinemann.

## 2 Chemistry and Physics of Flotation

This chapter reviews the literature as to the physics and chemistry of froth flotation. Because of the predominance of the use of xanthates in current flotation practice, the discussions are therefore xanthate-centric. The discussion of the separation of sphalerite from pyrite is included to illustrate the changes that occur at the sulphide surface when copper is added to activate the sphalerite surface.

### 2.1 Physics of Froth Flotation

The wettability, or more specifically, the non-wettability of mineral surfaces is critical to the absorption of chemicals on the mineral surfaces. Wettability is generally measured by the angle between the mineral surface and the air bubble to which it makes contact. This contact angle can be measured accurately in the laboratory, but presents difficulties in a flotation system, because of particle shape and size. This section reviews the development of the equations related to contact angle measurement and their effects on practical flotation conditions are discussed.

#### 2.1.1 Contact Angle

For there to be a displacement of water from the mineral surface, there must be a finite contact angle at the gas, liquid and mineral interface. (Rao, 2004). Measurement of the contact angle is the measurement most often used to indicate or determine the wettability of a minerals surface. If there is no reaction or adsorption of the liquid by the mineral surface, it is known as inert wetting or non-reactive. If the wetting process is influenced by a reaction or absorption of the liquid and mineral surface, then it is known as reactive wetting. For a contact angle to be formed the interfacial tensions of the three phases must be in equilibrium. (Figure.2.1)

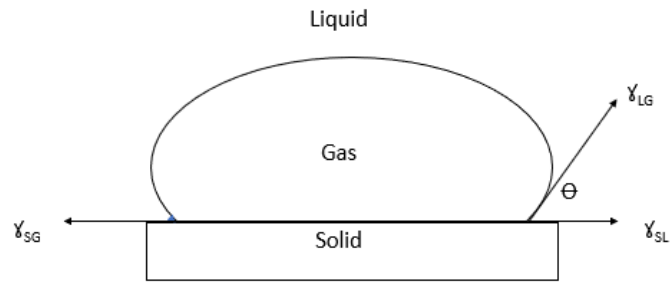


Figure 2.1. Surface Tension of bubble on mineral surface showing the surface tension forces. Adapted from “A review of factors that affect contact angle and implications for flotation practice” by T.T. Chau, 2009, *Advances in Colloid and Interface Science*. 150,2

From the above figure the relationship between the 3 phases is:

$$\gamma_{LG} = \gamma_{SL} + \gamma_{LG} \cos \Theta \quad (1)$$

Where:  $\gamma_{SG}$  is the solid-gas surface tension,  $\gamma_{SL}$  is the solid-liquid interfacial tension and  $\gamma_{LG}$  is the liquid-gas surface tension.  $\Theta$  is known as Young’s contact angle and equation (1) is known as Young’s equation. (Chau, Bruckard, Koh, & Nguyen, 2009). The equation holds true, if the following conditions of the solid surface are:

- Smooth,
- Flat,
- Homogeneous,
- Inert,
- Insoluble,
- Non-reactive,
- Non-porous and
- Non-deformable.

Such a surface is referred to as an ideal surface. However, most surfaces do not meet these conditions, so the measured contact angle is referred to as the apparent contact angle  $\Theta_{app}$ . The apparent contact angle does not have a unique value but rather exists within a range, with the highest value being called the advancing contact angle and the lowest the receding contact angle. The difference between them is called the contact hysteresis.

Researchers have postulated various versions of Young's formula to account for the non-ideal conditions that Young's formula would not cover. Wenzel (1949) investigated the effect of roughness on the static contact angle measurement. He found that roughness caused a hydrophilic fluid to act as more hydrophobic and conversely, a hydrophobic fluid to act as if it was more hydrophilic. One shortcoming of Wenzel's approach is the assumption that the surface features are insignificant to the drop dimensions, regardless of the drop dimensions. (Chau et al., 2009)

On a non-homogeneous surface, (Cassie and Baxter, 1944), found that the apparent contact angle is related to the ideal contact angle by the equation

$$\cos \Theta_c = f_1 \cos \Theta_1 + f_2 \cos \Theta_2 \quad (2)$$

where  $f_1$  is the fractional area of the surface with contact angle  $\Theta_1$ ,  $f_2$  is the fractional area of the surface with contact angle  $\Theta_2$  and  $\Theta_c$  is the Cassie contact angle. The equation is further reduced to the Cassie-Baxter equation for a porous surface, viz.

$$\cos \Theta_c = f_1 \cos \Theta_1 - f_2 \quad (3)$$

Where  $f_2$  is the fraction of air spaces when  $\cos \Theta_2 = -1$ .

This equation is constrained, but better than the Wenzel approximation for real surfaces; however, the difficulty is in the measurement of  $f_1$  and  $f_2$  for rough surfaces.

### 2.1.2 Contact angle and flotation.

For the flotation of sulphide minerals, contact angles are typically between 60 and 80° where floated with weak xanthates (2-3 carbon atoms in the hydrocarbon chain) for base metals, or strong xanthates (6 carbon atoms) for sulphides containing gold and other precious metals. Non-

sulphide minerals can be floated with similar contact angles using collectors with hydrocarbon chains of 12-18 carbon atoms. (Chau et al., 2009). The flotation normally is improved when the pH is slightly alkaline.

### 2.1.3 Contact angle and flotation kinetics

Collection of mineral particles takes place as air bubbles rise in the flotation cell. The efficiency of collection is determined by the balance between the attachment of the minerals to the bubbles when they collide and the later detachment of the particle from the bubbles.

Successful particle-bubble attachment depends on three factors, the thinning of the intervening liquid film to a critical thickness for it to rupture, formation of a three-phase contact (TPC) and the liquid film rupture itself. (Chau et al., 2009). The expansion of the TPC line to form stable bubble-particle aggregates is a function of the hydrophobicity of solid surfaces measured by the Young contact angle, the line tension and TPC mobility on the mineral surface. (Stechemesser and Nguyen, 1999).

Stresses created by shear, or turbulence in the flotation cell, cause the particles to detach themselves from the bubbles. The maximum size of particle that could remain attached to a bubble may be calculated from the contact angle (Nguyen, 2003). For chalcopyrite, assuming a contact angle of  $60^\circ$ , (Jameson, Ngyen and Ata, 2007) calculated a maximum floatable particle size of  $512\mu\text{m}$ , well aligned with practical flotation practice.

Contact angle measurement may quantify the wetting behaviour, but obtaining consistent contact angle values is difficult, due to factors such as surface roughness, heterogeneity and particle size. There is no rigid quantitative correlation between contact angle and flotation rate recovery. (Chau, 2009)



## 2.2. Particle-Bubble attachment

The role of bubble kinetics governs the attachment of mineral particles to a bubble rising in a mineral ore slurry. This section reviews the three-stage process of the attachment of the particle to the bubble, the trajectory of the bubble with respect to the mineral particle and the eventual attachment and detachment of the particle.

The displacement of aqueous solutions from the surface of mineral particles by a gas phase is an essential step in the froth flotation process. As a gas bubble interacts with a mineral particle, the intervening liquid film must thin and rupture, establishing a stable three phase contact line. (TPC).(Newcombe,1994). The particle-bubble attachment along with the mineral surface and flotation collector, form the tripartite of froth flotation.

There have been two mechanisms proposed for the interaction of bubbles and particles. Taggart proposed the gas-supersaturation theory, where the bubbles created by the impellor of the flotation cell, were super-saturated with gas, which precipitated on the hydrophobic surfaces of the metal sulphide particles and then floated to the surface (Sutherland, 1948). Gaudin (1932) postulated a theory of collision between the bubble and particle, which resulted in attachment of the particle to the bubble resulting in subsequent flotation (Dai, Fornasiero, & Ralston, 2000). With the two authorities in mineral dressing taking opposing views to mechanism of bubble attachment, it was several years before the collision theory came to the fore and was accepted as the model for the widely accepted mechanism. (Dai et al., 2000)

### 2.2.1 Bubble trajectory.

The theory was further enhanced by the introduction of the three-zone model (Derjaguin and Dukhin, 1961).

In zone 1, (Figure 2.2), far from the bubble, hydrodynamic forces are dominant. The hydrodynamic forces sweep a particle around the bubble, giving it no chance of collision. Meanwhile, the bubble rises towards the surface driven by inertial and gravitational forces. In zone 2, the liquid flows around the bubble, creating a tangential stream which sweeps adsorbed ions or surfactants downwards along the bubble surface from the top half to the bottom. The result is that ions are non-uniformly concentrated at the rear of the bubble, with a strong electrical field being created between the upper surface and particles which collide with the bubble. The forces controlling the particle motion are a combination of hydrodynamic, diffusional and electrophoretic. For this reason, Zone 2 is referred to as the diffusiophoretic zone (Dai et al., 2000).

In zone 3, surface forces come into play once the liquid film has thinned to below a few hundred nanometers (Ralston, Fornasiero, & Hayes, 1999). From a thermodynamic point of view, the free energy of a liquid film, differs from that of the bulk phase from which it is formed. The excess free energy may be referred to as the “disjoining force” and represent the difference between the pressure in the bubble and the pressure of the liquid adjacent to the solid surface (Ralston et al., 1999).

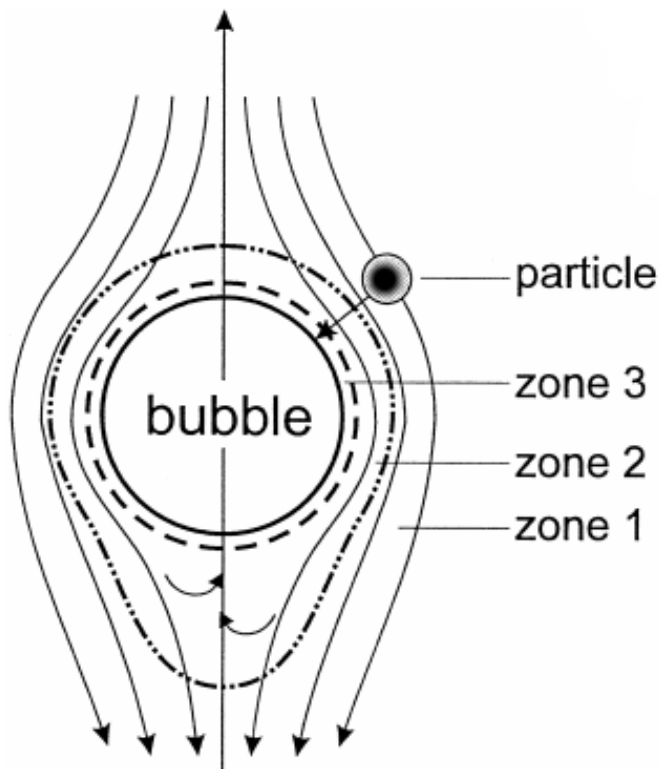


Figure 2.2 Three-zone model of particle-bubble interaction around the surface of a bubble. Adapted from “Theory of flotation of small and medium size particles by B.V.Derjaguin and S.S. Dukhin. 1961, *Transactions of the Institute of Mining and Metallurgy*, 70, pC221-246, Copyright by Taylor and Francis 1961.

When a particle collides with a bubble, it will deviate from its original trajectory and then slide over the bubbles surface, before attaching or falling away from the rear of the bubble, dependent on the sliding time. The bubble has to be fully mobile to allow the particle to slide.

Figure 2.3, shows the trajectories of spherical particles falling under gravity around a stationary near spherical bubble.

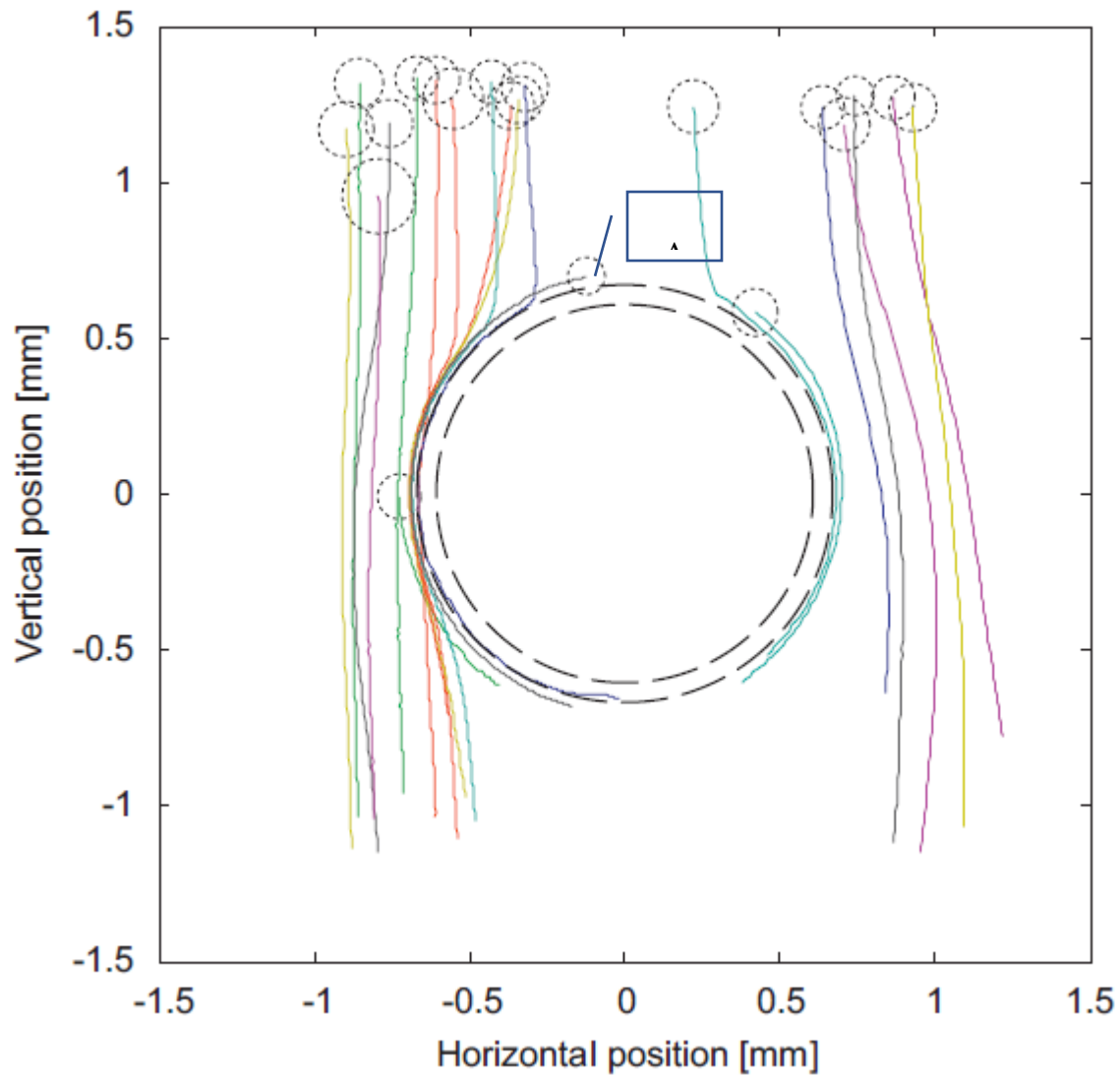


Figure 2.3. Observed trajectories of spherical particles. The coloured lines trace the particle paths. The particle size is indicated by the dotted outline, whilst the dashed lines represent the bubble sizes. A is the particle whose trajectory is discussed in Figure 2.5. Reprinted from “Particle–bubble interaction and attachment in flotation” by D.I. Verrelli et al., 2011, *Chemical Engineering Science*, 66(23), Copyright 2011 by Elsevier. Reprinted with permission.

Some particles deviate around the bubble without even coming close. The deviation is more obvious when the separation is the same magnitude as the particle diameter. Other particles slide over the bubble and move towards the bottom of the bubble. (Verrelli et al., 2011).

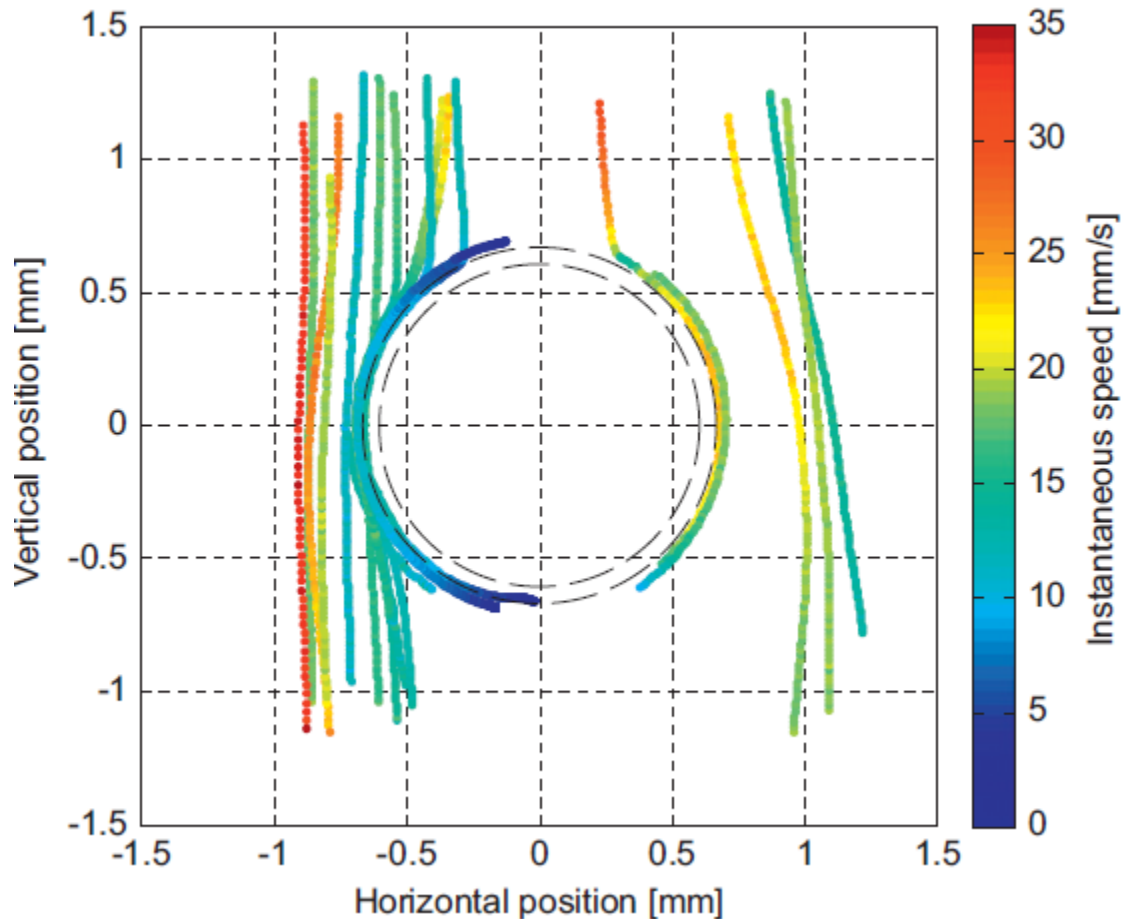


Figure 2.4. Observed trajectories around a bubble, coloured by their instantaneous speeds.

Reprinted from “Particle–bubble interaction and attachment in flotation” by D.I. Verrelli et al., 2011, *Chemical Engineering Science*, 66(23), Copyright 2011 by Elsevier Science Ltd..

Reprinted with permission.

Figure 2.4 shows the observed trajectories of particles around a spherical bubble, with colours to indicate their velocities. Those particles which did not approach the bubble close enough to slide over the surface, show little to no change in their velocity. When a particle slides over the bubble

surface, it slows down appreciably when sliding over the more horizontal portions and speeds up when it reaches the more vertical section (Verrelli et al., 2011). Addition of a surfactant will cause more of a change in particle motion following attachment due to the reduction in bubble surface mobility (Manor, Vakarelski, Stevens, Grieser, Dagastine, Chan, 2008).

As a particle approaches a bubble, it slows down due to the hydrodynamic resistance of the liquid as it is forced out of the ever-narrowing gap between the particle and bubble. As the particle disengages from the bubble surface, its motion is slowed by the hydrodynamic resistance created by the flow of water into the resultant gap between particle and bubble.

The particle shown in Figure 2.5 starting nearest the apex of the bubble (Particle A in Figure 2.3), demonstrated a “jump-in” towards the centre of the bubble, after a short period of sliding.

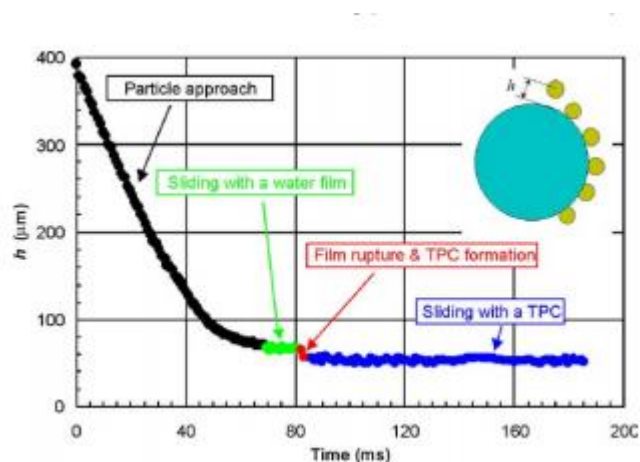


Figure 2.5. Position of particle A relative to bubble surface over time This phenomenon is attributed to the rupture of the thin film and formation of the TPC, as marked in red in Figure 2.5 Reprinted from “Movement of fine particles on an air bubble surface using high-speed video microscopy”, by A.V. Nguyen and G.M. Evans, 2004, *Journal of Colloid and interface Science*, 273 (1), p.275. Copyright 2004 by Elsevier. Reprinted with permission.

## 2.2.2 Film Drainage

Bubble-particle attachment occurs in three stages;

- The thinning of the intervening liquid film to a critical thickness where it ruptures,
- The formation of a three-phase contact (TPC) when the film ruptures

- The expansion of the three-phase contact to form a stable wetting perimeter

Each of these three stages have a characteristic time associated with them. The sum of them must be less than the contact time of the particle with the bubble to allow attachment to take place and thus allow flotation. Total contact time is generally  $10^{-2}$  sec or less (Ralston et al., 1999). Induction time is the time required for the bubble-particle attachment to take place. The film rupture is almost instantaneous, so the induction time is the sum of the film drainage and TPC time.

The shape of a bubble pressed against a surface is not uniform. Liquid drains away from the edges of the film quickly and a thicker dimple of liquid is trapped in the centre, due to the deformable nature of the bubble. The rate of drainage is dependent on the salt concentration, with the drainage rate at the centre of the bubble, decreasing with increasing salt concentration, while the reverse is true at the edge or boundary ring (Hewitt, Fornasiero, Ralston, Fisher, 1993). This may be explained by the decrease in electrostatic repulsion with increasing salt concentration, permitting the film to drain more rapidly at the boundary ring. The controlling factor in the drainage is therefore the rate at which the aqueous solution can pass through the boundary ring.

In their study of the kinetics of the TPC line rupture, (Newcombe and Ralston, 1994) found that for silica surfaces, both clean and coated with long-chain hydrocarbons:

- Large bubbles spread more rapidly, in the initial stages of spreading than do small bubbles but require a longer time to achieve the final wetting perimeter.
- For the same initial bubble size, initial spreading rates are higher as the contact angle  $\Theta$  increases, however, the final equilibrium state is achieved in approximately the same time.
- For bubbles of any radius, the final approach to the stable spread state is slow.

The mechanism apparently involves the formation of a primary hole, which forms within nanoseconds and expands at extremely high velocities. Subsequent to the formation of the hole, the expansion rate of the TPCL may dictate whether or not bubble-particle adhesion can occur,

because the capillary force acting on that the TPCL must increase rapidly enough to counteract the detaching forces acting on the bubble-particle aggregate. (Crawford and Ralston. 1988)

Where a large and a small bubble are just contacting a hydrophobic surface, Figure 2.6.

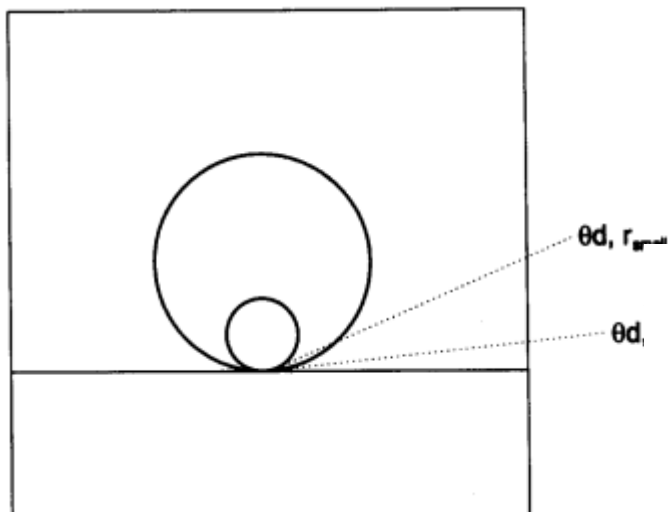


Figure 2.6 Instantaneous dynamic contact angle, following primary hole formation for two bubbles of different radii. Reprinted from G. Newcombe and J. Ralston, 1994, *Minerals Engineering*, 7(7), p. 901. Copyright 1994 Elsevier Science Ltd. Reprinted with permission.

At the instant when a primary hole forms, just prior to the TPCL movement, one may reasonably suppose the initial tiny area of contact is the same. Thus, the dynamic contact angle immediately after the primary hole formation would be expected to be larger for the smaller bubble. The value of the difference between the dynamic and static cosines of the contact angle, will be greater for the larger bubble and the initial spreading velocity will be higher. The distance required for TPCL spreading to the stable state is not as great as for the larger bubble, so that the overall time required for spreading is less.

The force required to achieve a given velocity on a surface covered with long chain molecules exceeds that when short chain species are present, i.e., it is more difficult for a bubble to spread over the former surface. This suggests that influence the chemical structure of the collector molecule used in flotation will influence the TPCL kinetics and hence might be used to enhance selectivity differences.



### 2.2.3 Summary

For there to be adhesion between a rising bubble and a mineral particle, the particle must be close enough to the bubble, so that surface forces come into play. Once contact is made, the particle slides over the surface of the bubble until the intervening fluid film thins and ruptures, creating a triple point of contact before the particle detaches itself from the bottom of the bubble.

For the film to rupture, a minute hole must form in the bubble at the point of contact between the bubble and mineral particle. This hole then expands until it reaches the TPC line. Smaller bubbles are more efficient at collecting particles because their faster spreading causes the maximum capillary force to be achieved more rapidly for the smaller bubble and achieve a stable bubble-particle aggregate in a shorter time than for a larger bubble.

## 2.3. Thermodynamics of Flotation

In extracting valuable minerals from the mineral ore, froth flotation relies on the collision of gas bubbles with the mineral particles. To achieve the attachment of the mineral particles to the gas bubble, surfactants referred to as collectors, are added to the ore slurry to render the mineral surface(s) hydrophobic. The attached active agent (collector) renders the particle surface hydrophobic which then drives the particle towards a solution/gas interface of a bubble where it attaches and can be removed from the liquid (Laskowski, 2007). In order to better understand factors governing bubble – particle attachment the following section describes the interaction of the dominant phases, pulp (liquid), particles (solids) and bubbles (gas), in a thermodynamic context.

The adsorption density of surfactants ( $\Gamma$ ) is interrelated with the solution/gas interfacial tension as given by the Gibbs adsorption equation (Laskowski, 2007).

$$\delta\gamma = -\Gamma\delta\mu \quad (1)$$

The chemical potential of component  $i$  is as follows:

$$\mu_i = \mu_i^\circ + RT \ln a_i \quad (2)$$

where  $\mu_i^\circ$  and  $a_i$  are the standard chemical potential and thermodynamic activity of compound  $i$ ,  $R$  is the gas constant and  $T$  is the temperature (Laskowski, 2007).

Given that  $a=fc$  (where  $c$  is concentration and  $f$  is the free energy coefficient) for dilute solutions  $c$  approaches 0, and  $f$  approaches 1,  $a=c$ , thus

$$\delta\mu = RT\delta\ln a$$

which approximates  $RT\delta\ln c$ . (3)

Therefore, for dilute solutions, the Gibbs equation may be expressed as:

$$\Gamma = -(1/RT) (\delta\gamma/\delta\ln c) = -(1/2.3RT) (\delta\gamma/\delta\log c) \quad (4)$$

Since surface active compounds prefer (by definition) the gas/liquid interface, in a flotation system, such surface active agents tend to accumulate at the surface of bubbles (Laskowski, 2007). For organic surface-active compounds or agents, the hydrocarbon chains penetrate into the gaseous phase, whereas the polar group remains on the liquid side of the interface. This preferred orientation satisfies the van der Waals attraction forces between the non-polar groups and the dipole attraction forces between the polar groups and the polar solvent molecules. (de Bruyn and Agar, 1962)

For the following discussion surface tension ( $\gamma$ ) is substituted for the surface free energy, (Adam, 1938). When a particle collides with a bubble and successfully attaches to the bubble, the particle floats to the surface of the froth. Consider the simplified situation demonstrated in Figure 2.7 before and after particle attachment to a bubble.

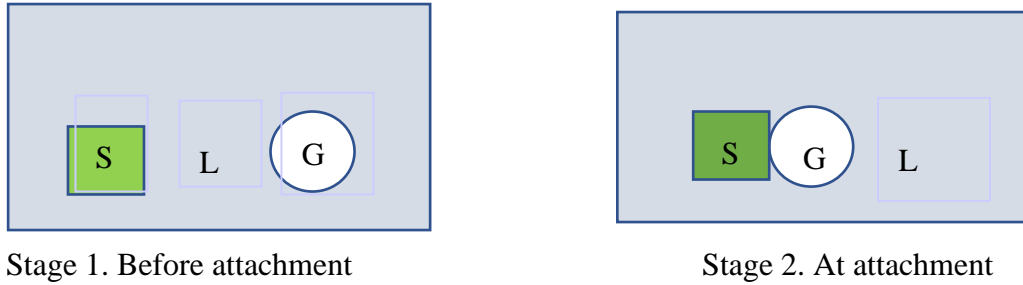


Figure 2.7. Attachment of particle (S) to bubble (G) in water (L). (Adapted from Laskowski 1989)

At constant temperature, pressure and concentration, the change in surface free energy ( $\Delta G$ ) during the attachment process is negative (Laskowski, 1989).

$$\Delta G = G_2 - G_1 = G_2^s - G_1^s = \gamma_{SG} - \gamma_{SL} - \gamma_{LG} < 0 \quad (5)$$

Where  $G_1$  and  $G_2$  are Gibbs free energies of the system before and after attachment (Stages 1 & 2).  $G_1^s$  and  $G_2^s$  are the corresponding surface free energies which may be equated to  $G_1$  and  $G_2$ , as only the surface portion of the system's surface free energy changes during the process;  $\gamma_{SG}$ ,  $\gamma_{SL}$  and  $\gamma_{LG}$  are the surface tensions of the surface/gas, surface/liquid and liquid/gas interfaces respectively (Laskowski, 1989)

The more negative the value of  $\Delta G$ , the greater the probability of the dewetting of the particle. Also, Young's equation may be written as

$$\cos\Theta = (\gamma_{SG} - \gamma_{SL}) / \gamma_{LG} \quad (6)$$

For a hydrophilic surface,  $\Theta = 0$ ,  $\cos\Theta = 1$  and  $\gamma_{SG} - \gamma_{SL} = \gamma_{LG}$ . The contact angle can only increase if  $\gamma_{SG}$  decreases more than  $\gamma_{SL}$ , so that  $\gamma_{SG} - \gamma_{SL} < \gamma_{LG}$ , which may only happen if  $\Gamma_{SG} > \Gamma_{SL}$ , where  $\Gamma_{SG}$  and  $\Gamma_{SL}$  are the adsorptions at the solid/gas and solid/ liquid interfaces. (Laskowski, 2007). From this it may be concluded that an increase in the contact angle results from the adsorption of the surfactant being greater at the solid-gas interface than at the solid liquid interface.(Laskowski, 2007)

Laskowski (1989) lays out the thermodynamics of the attachment of a particle to a bubble in the presence of surfactants as follows;

“The flotation system comprises mineral particles and air bubbles suspended in an aqueous solution”

$$G^s = A\gamma \quad (7)$$

And the surface free energy changes by

$$\delta G^s = A\delta\gamma + \gamma\delta A \quad (8)$$

where  $A$  is the surface area of the solid particles and air bubbles, and  $\gamma$  denotes the corresponding surface tensions. According to equation (8), the surface free energy of the system can be lowered by decreasing interfacial surface tensions by adsorption of some surfactants, at the interfaces, or by decreasing the surface area of the dispersed phases by attachment of particles to bubbles. (Aggregation of particles and coalescence of bubbles is neglected here).

In the presence of surfactants which adsorb at all involved interfaces, the surface tensions and the contact angle on mineral grain surfaces will be altered and initially a hydrophilic particle will be rendered hydrophobic. The contact angle will increase and the particle will become floatable.

Higher surfactant adsorption at the solid/gas interface than at the solid/liquid and liquid/gas interfaces can be explained by the penetration of the surfactant layers absorbed at the particle/solution and bubble/solution interfaces at the moment of particle-to-bubble attachment as postulated by Leja and Schulman (1954) (Figures 2.8 & 2.9).

As the adsorption density of collector at the solid-liquid interface is increased, the contact angle between the solid and gas, will increase, making the surface more hydrophobic. Eventually, equilibrium will be reached between the amount of collector adsorbed onto the mineral surface and the collector molecules in the pulp (Figure 2.8).

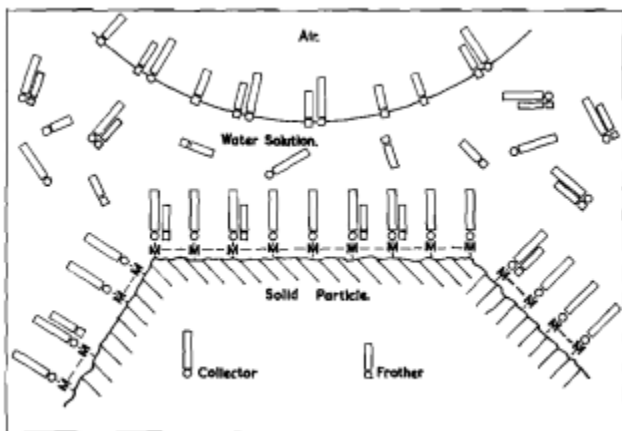


Figure 2.8. Mechanism of bubble attachment: bubble approaching a collector-coated solid surface; diffused monolayers of associated and unassociated molecules at interfaces and in solution. Reprinted from “Flotation Theory: molecular interactions between frothers and collectors at solid-liquid-air interfaces.” by J. Leja and J.H. Schulman, 195, *Transactions AIME* 199, p.227. Copyright 1954 by Minerals, Metals & Materials Society. Reprinted with permission.

As an air bubble approaches and contacts the mineral surface, the collector molecules at the air/water interface, are absorbed onto the mineral surface increasing the hydrophobic nature of the mineral (Figure 2.9). The collector layer at the bubble surface becomes more condensed and the link between the particle and bubble is stabilized. (Leja and Schulman, 1954)

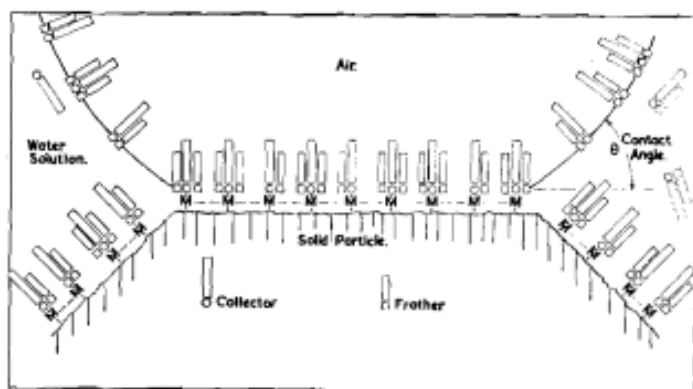


Figure 2.9. Mechanism of bubble attachment: adherence of an air bubble established through the penetration of the monolayer at the solid/liquid interface by the monolayer at the air/liquid interface. Reprinted from “Flotation Theory: molecular interactions between frothers and collectors at solid-liquid-air interfaces.” by J. Leja and J.H. Schulman, 195, *Transactions AIME* 199, p.227. Copyright 1954 by Minerals, Metals & Materials society. Reprinted with permission

If too much collector is present, conditions for the formation of a micelle exist. Micelles are defined as “a colloidal sized group of organic ions, which have their linked hydrocarbon chains oriented inward, with the charged headgroups orientated outward to the water” (Aplan and Fuerstenau, 1962). In these circumstances the extensive micelle formation will render the bubble surface stabilized essentially armoured and unable to attach to the mineral surface, (Leja and Schulman, 1954). Experiments have established that collector molecules primarily absorb onto corners and edges of scratches in the mineral surface, where the surface free energy is minimum and the adsorption energy is at a maximum.(Beischer, 1953; Smart et al., 2000).

### 2.3.1 Summary

In the section, the role of the bubbles in the distribution of the collector molecules through the system and to the mineral surface was outlined. Previously, the role of the bubble has been overlooked by researchers, largely due to the greatest efforts focused towards sulphide mineral recovery and the interaction with water soluble thiol collectors. However, with renewed evaluation of phosphate, oxide and silicate ore flotation using amine-based collectors, the role of the bubble has been identified as significant for water immiscible collector distribution and mineral particle interaction. In the context of sulphide flotation using TECFLOTE S11 a model similar to that of phosphate flotation using amines may be operating.

## 2.4. Chemistry of Froth Flotation

### 2.4.1 Electrochemistry

Most metal sulphides exhibit semiconducting properties, allowing either the acceptance or donation of electrons. These characteristics, can change the surface chemistry of the mineral and lead to either increased or decreased floatability of the minerals. This section reviews the theory behind the electrical double layer, as well as the hydration of the surface. This is followed by a review of the galvanic interaction between iron, both as elemental iron and as pyrite, and sulphide mineral and the effects on the flotation of the sulphide minerals.

### 2.4.1.1 Electrical Double Layer

In preparing the correct size distribution for the flotation circuit to promote the attachment of mineral grains to the bubbles, the ore must be crushed and ground. In doing so, the fresh mineral surfaces obtain an electrical charge due to the breakage of surface bonds and internal structural disruptions (Chander et al., 1975). Surface charge may also be subsequently modified by the adsorption of ions. The surface may remain uncharged if only the Van de Waals bonds of the lattice are broken and there are no electrons, ions or dipoles, i.e. mobile charges, in the system (Rao, 2004). When mobile charges are present, the interface becomes charged.

When a mineral is immersed in water, an electrical double layer is created as the charged species in the water try to establish equilibrium by migrating across the mineral/water interface. The electrical charge on the mineral surface, becomes balanced by the liquid which is equal and opposite to the charge on the mineral surface. (Fuerstenau and Urbina, 1988)

If we consider a negatively charged plane surface in water, it may acquire a uniform positive charge by contact with the liquid containing positive and negative ions. In doing so the surface develops a potential of  $\psi_0$ , which decreases with distance into the solution (Adamson and Gast, 1997). At any point in the electric double-layer solution, the potential energy is defined as:  $ze\psi$ , where  $z$  is the valence and  $e$  is the charge on the electron (Rao, 2004). This situation exists in most flotation systems. There is a transfer of charged species across the interface which acts as a semi-permeable membrane, causing the solution to equilibrate because of the saturation of the water by the ions derived from the solid surface.

The electrical double-layer that exists is demonstrated below. Figure 2.10a is the solid positively charged surface with negative or counter ions attracted to the surface that extend into the solution. Figure 2.10b shows how the potential declines with distance from the surface. The

closest distance ( $\delta$ ) of approach of the counter ions is referred to as the Stern layer.

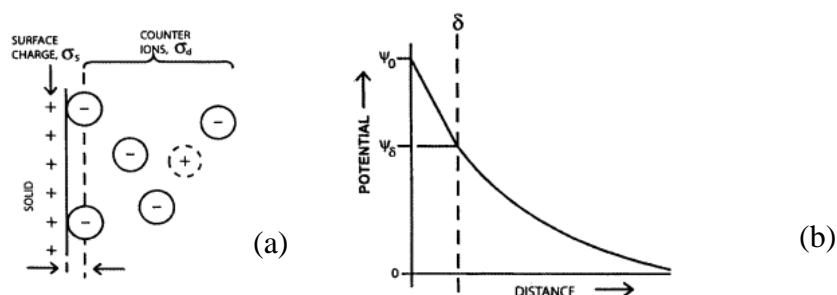


Figure 2.10.(a) Stern model of electrical double layer. (b). Change in potential with distance from solid surface.  $\delta$  denotes location of Stern layer. Reprinted from *Surface Chemistry of Flotation* (p.212), by S.R. Rao, 2004, Plenum. Copyright 2004 by Springer Nature. Reprinted with permission.

When a particle moves in an electric field, the layer of liquid in contact with the particle, moves at the same velocity as the particle. Where the liquid starts to move at a different velocity to the particle is referred to as the surface of shear. The potential at the surface of shear is called the zeta potential.

The potential of the double layer is controlled by ions from the solid. With ionic solids, the surface charge is derived from the preference for one of the lattice ions sites on the solid as opposed to the aqueous phase (Rao, 2004). The ionic species that passes through the two phases is called the potential determining ion. Their concentration in the aqueous phase determines the magnitude and sign of the zeta potential. (Rao, 2004).  $H^+$  and  $OH^-$  are principle potential determining ions of oxide minerals. The surface charge is created by the disassociation of surface hydroxyls resulting from their interaction with water. (Yopps, and Fuerstenau. 1964). This interaction will result in a change in the pH of the solution.

The zero point of charge or zero charge point is reached at the pH where an equal number of positive and negative surface sites are present and the surface is uncharged with respect to the solution.

Other ions may act as counterions, they only affect the magnitude of the zeta potential because they are adsorbed electrostatically. Because of this, they are referred to as indifferent



ions. The indifferent ions do not migrate between the solid and solution phases, changing the zeta potential of the solution instead of the surface charge of the solid, because they occur in the diffuse layer. If the concentration of indifferent ions is increased, the double layer collapses and the zeta potential ceases to exist, while the surface remains charged. (Rao, 2004) This phenomenon, is called double layer compression. The compression is increased with an increase in the valence of the ions (Figure 2.11).

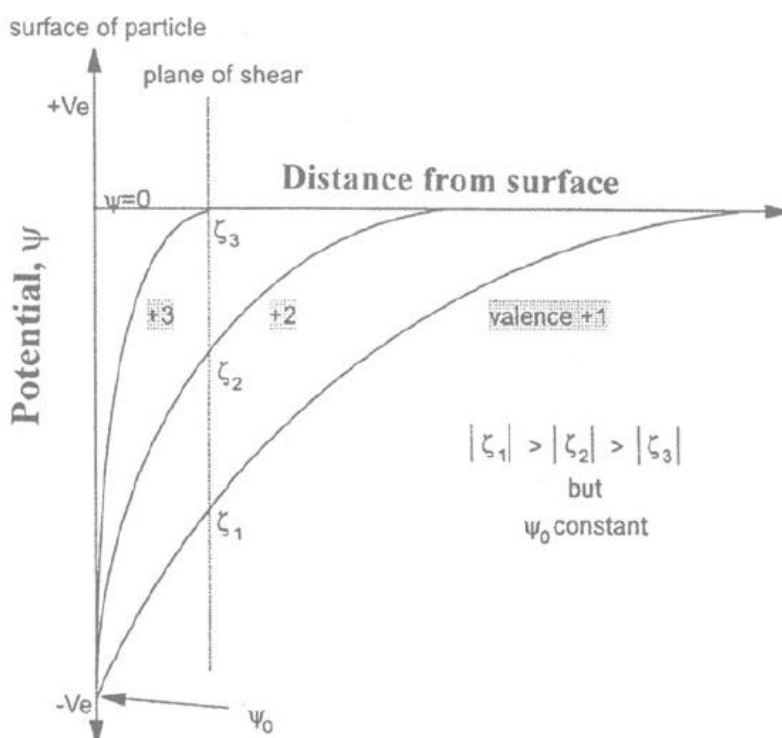


Figure 2.11. Compression of the double layer by indifferent electrolytes. The potential decays more rapidly in the presence of high valence cations. Reprinted from *Surface Chemistry of Flotation* (p.216), by S.R. Rao, 2004, Plenum. Copyright 2004 by Springer Nature. Reprinted with permission.

Surface active ions (surfactants) may be absorbed by chemisorption rather than by electrostatic forces. Being chemically active, they bond to surface sites and are called specifically adsorbing

ions. The charge of these ions may exceed the surface charge when adsorbed in the Stern plane, which leads to a charge reversal of the surface. Chemisorption involves the transfer of charge across the interface (Rao, 2004). This charge may be an electronic exchange between the substrate and adsorbate, or it can be by an ion transfer that is accompanied by a partial or complete neutralization. Unlike electrons, that can cross the energy barrier by tunneling, ions are held in the Stern layer, until they acquire the necessary energy to pass the barrier and incorporate themselves in the solid (Rao, 2004). When there is a charge transfer or ion exchange between the mineral (electrode) and the electrolyte, either a reducing (cathodic) or oxidizing (anionic) process may occur. Both oxidizing and reducing reactions may take place at different locations on the same solid surface. (Figure 2.9)

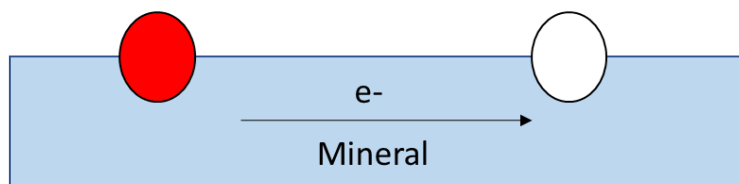
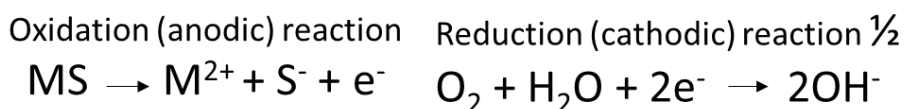
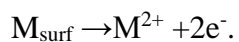


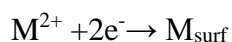
Figure 2.12. Oxidation and reduction reactions may take place at different portions of the same mineral surface, with an electron migrating from the cathode to the anode site. Adapted from J. A. Finch ,(2019) Slide 23

Figure 2.12, is a simplistic representation of the mixed potential reaction, the redox reaction of monosulphide minerals may involve as many as 7 steps, while for disulphide minerals there may be as many as eight. (Rimstidt & Vaughan, 2003)

When a metallic surface is immersed in a solution containing its ions, metallic ions go into solution with the oxidation reaction.



The reduction reaction is the reverse.



Similarly, when the electrolyte contains metal ions that are different from the mineral surface, deposition is possible. This is known as underpotential deposition. The attachment of these ions may be stronger than that of the like ions on the same metal surface. (Buckley and Woods, 1997).

#### 2.4.1.2 Hydration of Surfaces

Molecules of water adsorb onto all surfaces, especially a freshly formed polar solid surface, such as that formed by wet grinding prior to flotation, forming a hydration layer. Most insoluble metal oxides form a surface hydroxyl group by dissociative chemisorption, on top of which molecular water is adsorbed. (Rao, 2004)

Solids other than the metal oxides do not form surface hydroxyl groups by dissociative chemisorption, but all solids adsorb water to the extent of forming numerous multilayers when the partial pressure approaches saturation.

The adsorption of water molecules onto surfaces is due to the polar nature of water. A water molecule is composed of a hydrogen atom and two oxygen atoms. Each hydrogen atom is covalently bonded to the oxygen atoms by a shared pair of electrons. The oxygen atoms have two unshared pairs of electrons, resulting in 4 pairs of electrons surrounding the oxygen atoms, two pairs involved in covalent bonds with hydrogen, and two unshared pairs on the opposite side of the oxygen atom. Causing the oxygen to be "electronegative" or electron "loving" atom compared with hydrogen.

The uneven electron density distribution causes the water molecule to be polar, Water has a partial negative charge ( $\delta^{-}$ ) near the oxygen atom due the unshared pairs of electrons, and

partial positive charges ( $\delta^+$ ) near the hydrogen atoms. (Figure 2.13). This imbalance of charge leads to water molecules hydrogen bonding with each other and other polar species

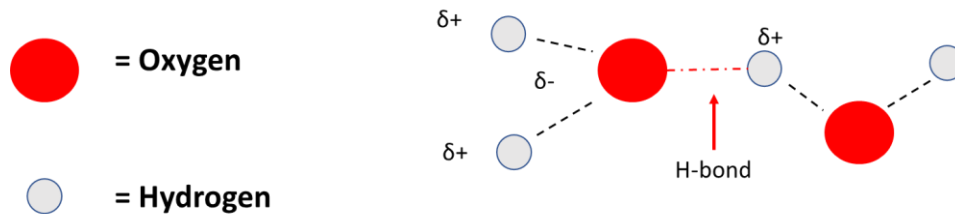


Figure 2.13 Polar nature of water molecule. Adapted from J. A. Finch ,(2019) Slide 9

When water comes into contact with a fresh mineral surface such as silica, the surface becomes hydrated as the silicon atom and oxygen atoms form a covalent bond, while one of the hydrogen atoms bonds covalently with an oxygen atom on the mineral surface. The remaining hydrogen atom forms a hydrogen bond with a water molecule, thus rendering the silica surface hydrophilic. (Figure 2.14)

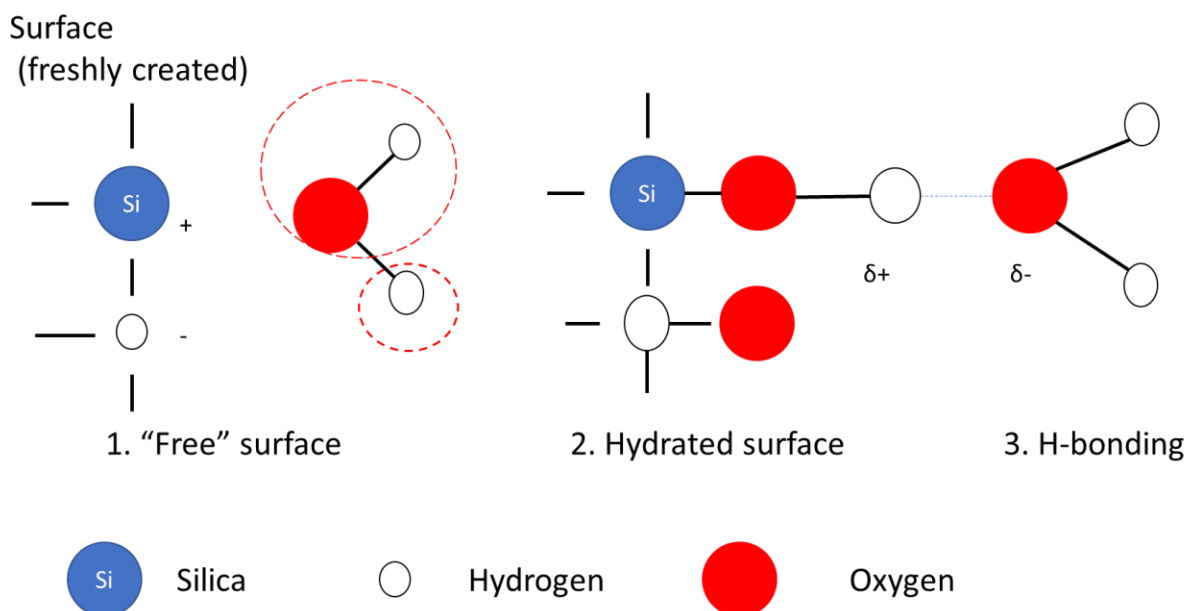


Figure 2.14. Hydrogen bonding properties of water with silica. Adapted from J. A. Finch ,(2019) Slide 10

A similar situation occurs between water and metal sulphide surfaces. An oxygen atom will form a covalent bond with the positively charged metal atom (e.g.  $\text{Cu}^{2+}$  or  $\text{Fe}^{2+}$ ) to form the metal hydroxide. A hydrogen atom will form a covalent bond with a negatively charged Sulphur ion at the mineral surface. The remaining oxygen atom will hydrogen bond with a water molecule and the surface will be rendered hydrophilic. (Figure 2.15)

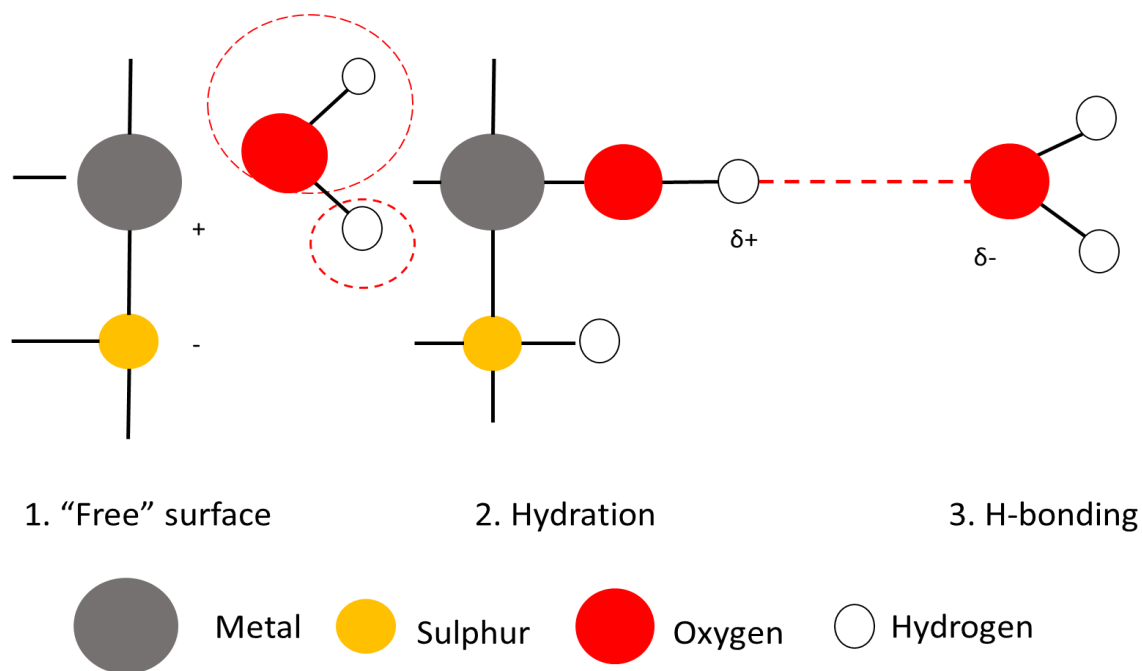


Figure 2.15. Hydration of metal sulphide surface. Adapted from J. A. Finch ,(2019) Slide 11

This representation of the hydration of metal surfaces, is rather simplistic and does not account for the presence of oxygen in the water. In most mineral processing environments, oxygen is dissolved in the process water. In this situation, the metal ion will bond with the hydrogen ion, which will form the metal hydroxide, the hydrogen which can then bond with a water molecule. However, the sulphur ion will not bond with the remaining hydrogen ion, but will bond with an oxygen molecule dissolved in the water, with the oxygen atoms free to form hydrogen bonds with other water molecules. The surface of the mineral will then become hydrophilic. (Figure 2.16).

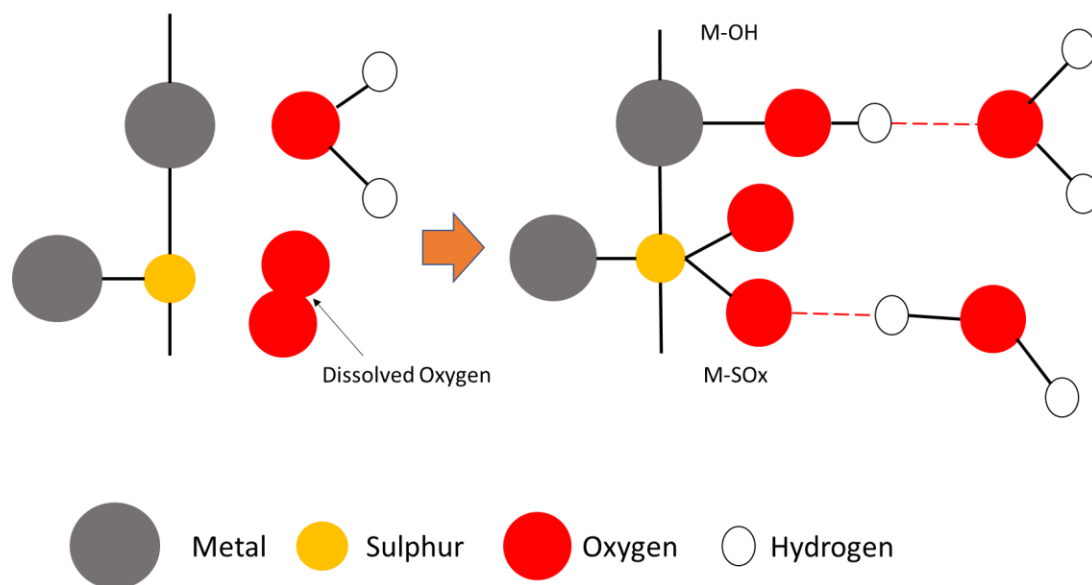


Figure 2.16. Effect of dissolved oxygen on hydration of metal sulphide surface. Adapted from J. A. Finch, (2019) Slide 12

With non-polar surfaces, such as carbon, coal, bitumen and oils or hydrocarbons, the oxygen cannot bond to the surface atoms, so the surface is hydrophobic.

#### 2.4.1.3 Galvanic interaction between iron and sulphide minerals.

Most sulphide minerals are more noble, i.e., have higher rest potentials, than forged steel used in grinding media. As a result, a galvanic couple is created between the sulphide mineral and the grinding media. This galvanic couple increases the corrosion rate of the forged steel and creates iron oxy-hydroxide species which precipitate onto the surfaces of the sulphide minerals thereby effecting their floatability. (Greet, Kinal, Steiner, 2005).

Whenever sulphide minerals are brought into contact with ferrous metal grinding media, galvanic interactions occur. Generally, the grinding media acts as the anode, because it has the lowest rest potential, with the sulphide minerals acting as the cathode. The grinding media

undergoes oxidation, while the sulphide minerals undergo oxygen reduction, as per the following equations: (Figure 2.17).

At the cathode:  $\frac{1}{2}\text{O}_2 + \text{H}_2\text{O} + 2\text{e}^- \rightarrow 2\text{OH}^-$

At the anode:  $\text{Fe} \rightarrow \text{Fe}^{2+} + 2\text{e}^-$

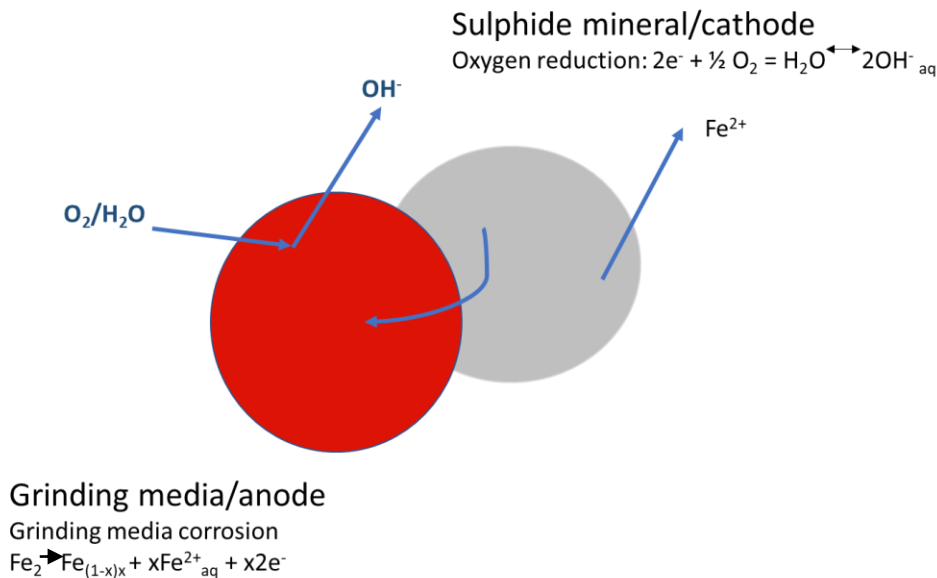


Figure 2.17. A schematic representation of the electrochemical cell formed when ferrous metal grinding media is in contact with sulphide minerals, within and aqueous medium. Adapted from *Centenary of Froth Flotation* (p.967), by C.J. Greet et al., 2005, AIME. 2005. Copyright AIME 2005.

The ferrous ions react with the hydroxyl ions to produce iron oxy-hydroxyl species on the sulphide mineral surfaces. These hydrophilic products coat the sulphide mineral surfaces and may affect their floatability. Control of the iron in the processing system becomes paramount. (Finch, Rao and Nasset, 2007).

The role of oxygen must also be considered. Increasing oxygen levels in the pulp significantly increases the level of corrosion of the forged steel grinding media, in the presence of electroactive minerals such as pyrrhotite and magnetite. (Iwasaki et al., 1985). The rate of corrosion of carbon steel increases markedly when chalcopyrite is ground in the presence of

oxygen. (Isaacson, 1989). However, when the grinding media is changed to high chrome white iron, the corrosion rate is reduced when chalcopyrite is ground in an oxygen environment.

The move to autogenous grinding, where the ore acts as the grinding medium, will also help reduce the galvanic interaction effect on flotation. Fossberg, E, Sundberg, S. and Hongxin, (1988) found that the use of autogenous grinding had a marked difference in the pulp chemistry of complex sulphide ores. The Eh of the pulp was less reducing and the dissolved oxygen concentrations higher, enhancing the flotation performance, with chalcopyrite being selectively floated from pyrite. The copper recovery was improved by as much as 10 percentage points when autogenous grinding was employed. Similar results were found for a copper-nickel ore when autogenous grinding was used instead of steel grinding media. (Iwasaki et al. 1983).

Similar results may be obtained by substituting high chrome steel for forged steel. The Eh is increased to more oxidizing potentials while the pH remains approximately constant. The pulp became more oxidizing as the chrome content of the grinding media was increased. (Greet et al., 2005). It appears that there is a correlation between the less reducing Eh, decreased oxygen demand and decrease iron. (Greet et al., 2005)

The results of a long-run plant trial indicate that the switch from forged steel grinding media to high chrome steel was economically feasible, resulting in net savings of US\$8,030,000 per annum. (Greet et al., 2005)

Galvanic cells exist between sulphide minerals in a slurry. The mineral with the higher rest potential acts as the cathode and the mineral with the lower rest potential, the anode. When a galvanic contact between pyrite and sphalerite is created, the pyrite recovery increased in the presence of sphalerite, whereas the sphalerite recovery decreased in the presence of pyrite. (Rao and Finch, 1988)

In the galvanic cell of pyrite and galena, the pyrite acts as the cathode and galena as the anode, as the galena is more electrochemically active than pyrite. The recovery of galena in a mixture of galena and pyrite, decreased in comparison to the flotation of the individual mineral particles. The zeta potential of the galena changes significantly, while that of the pyrite increases when the two minerals were mixed together. (Qin, 2015) Recovery of pyrite increases with the amount of



galena, due to the increased lead species on the pyrite surface as a consequence of the galvanic contact with the galena.(Allahkarami, Poor and Rezai, 2017).

When nitrogen was used as the gas, the amount of oxygen dissolved in the pulp was decreased, which weakened the galvanic interaction between the minerals, resulting in an increase in the floatability of the pyrite. (Rao and Finch, 1988; Qin, 2015)

In the galvanic reaction between these two minerals, the galvanic contact is related to an increased dissolution of the galena. The metal ions hydrolyse forming either hydroxo-complexes or precipitated hydroxides, which adsorb onto the mineral surfaces, making them hydrophilic. (Senior and Trahar, 1991). As pyrite is more noble than galena under all conditions, in any galvanic contact between the two minerals, the preferential anodic oxidation can be expected to occur on the galena surface.

When there is contact between pyrite and galena, there is a release of  $Pb^{2+}$  ions into the solution as a result of the anodic dissolution of galena, activating the pyrite surfaces onto which the collector is adsorbed.

#### 2.4.1.4 Summary

The surface of a mineral in water is complex, with an electrical charge being established at or close to the mineral surface. This charge, allows for reduction-oxidation (redox) reactions to take place on the surface. These mixed potential reactions with water molecules permit the hydrolysis of the surface because of the polar nature of water. It is this reaction that makes the mineral surface hydrophilic.

The redox reaction at the mineral surface, also occurs between the sulphide minerals and the steel grinding media, which leads to the formation of iron hydroxides on the sulphide mineral surface, rendering them less hydrophobic and thus are detrimental to the floatability of the minerals.

The redox reaction also occurs because of a similar galvanic contact between two sulphide minerals, resulting in the release of metal ions into the solution leading to the inadvertent activation of the higher noble mineral.

## 2.5. Electrochemistry of Sulphide flotation.

Sulphides are electrical conductors and act both as a source and a sink for electrons, allowing electrode reactions at the mineral surface. One of the most important of these reactions to the flotation process, is that of the reduction of oxygen. It is this reaction which result in production of the chemical species that render the sulphide mineral surfaces hydrophobic. This section discusses the role of oxygen in the flotation process and the reduction of xanthate to dixanthogen

### 2.5.1 Cathodic reduction of Oxygen

The reduction of oxygen has long been recognized as the most important cathodic reduction involving the flotation of sulphide minerals. Hydrogen peroxide on sulphide minerals results from the grinding of sphalerite minerals with pyrite and mild steel balls (Xia et al., 2017) and that grinding produces a low oxidizing environment creating a greater proportion of metal oxides on the sphalerite surface, resulting in the depression of sphalerite flotation. It has been reported that the reaction between hydrogen peroxide and xanthates results in the replacement of the C=S group with C=O, monothiocarbonates being formed. (Reid, 1962).

### 2.5.2 Electrochemistry and surface hydrophobicity.

Dependent on the test conditions, xanthate ions can be specifically adsorbed, chemisorbed by a charge transfer process, or metal xanthates can grow on the mineral surface and dixanthogen can be formed. (Buckley and Woods, 1997). The extent to which these species enhance, depress or have no influence on the mineral floatability is fundamental to flotation and varies significantly between mineral species. The contact angle measurement has been used as a measure of the wettability of the mineral surface and as such its hydrophobicity. (Gardner and Woods, 1974)

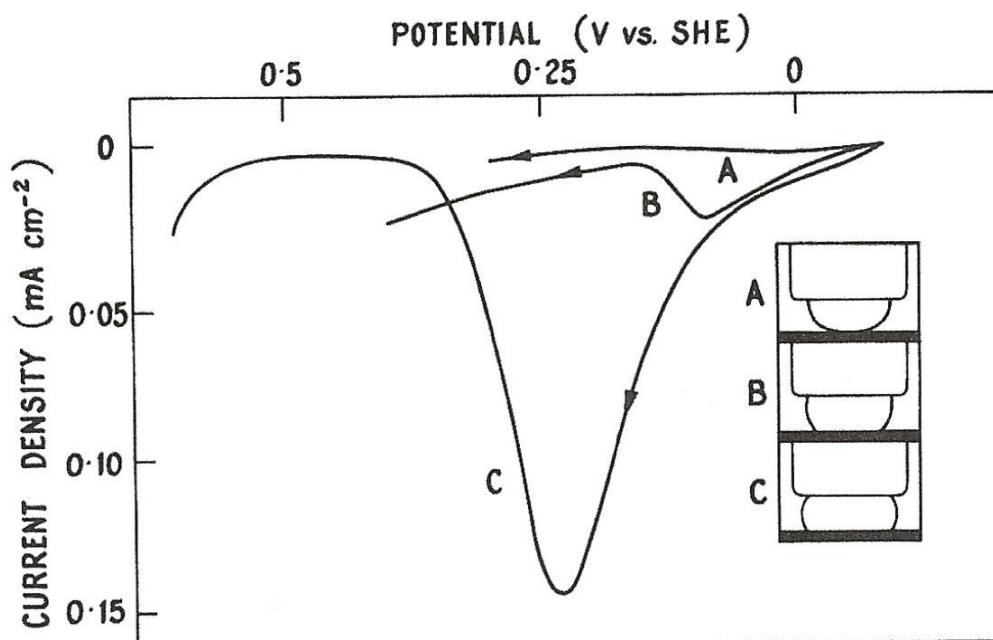


Figure 2.18. Current-potential curves for the reduction of a xanthate collector to diethyldixanthogen on platinum. Curve A, 10°, B, 60° and C 75°. Reprinted from “An electrochemical investigation of Contact Angle and of Flotation in the presence of alkyl xanthates. 1 Platinum and Gold Surfaces.” By J.R. Gardner and R. Woods, 1974, *Aust. J. Chem* 2142. Copyright CSIRO. Reprinted with permission.

Figure 2.18 shows the voltammogram obtained for platinum and the contact angles obtained in response to an increase in current density. The reduction of xanthate to dixanthogen on the surface clearly renders the surface hydrophobic. Xanthate ions adsorbed onto platinum at potentials cathodic to dixanthogen formation, show contact angles in the region close to zero. This data indicates that specifically adsorbed xanthate ions do not make the surface hydrophobic and that there is some requirement for the formation of dixanthogen in order to render the surface hydrophilic.

### 2.5.3 Summary

The role chemical reactions at the mineral surface, is pivotal to the flotation nature of mineral particles. Oxygen may cause the creation of iron hydroxides, which deposit on sphalerite

mineral surfaces, rendering them unfloatable. Similarly, the reduction of xanthate ions to dithiolenes, will have a detrimental effect on flotation as the dithiolenes will render the surface hydrophilic.

## 2.6. Reaction between flotation chemicals (Collectors) and Sulphide minerals.

To assist in making a specific mineral surface hydrophobic, one or more reagents are added to the ground ore slurry before it enters the flotation process. This section discusses the structure and characteristics of collectors used in the flotation of sulphide minerals.

Typically, these reagents are referred to as promoters or collectors. The general structure of the collector is shown in Figure 2.19.

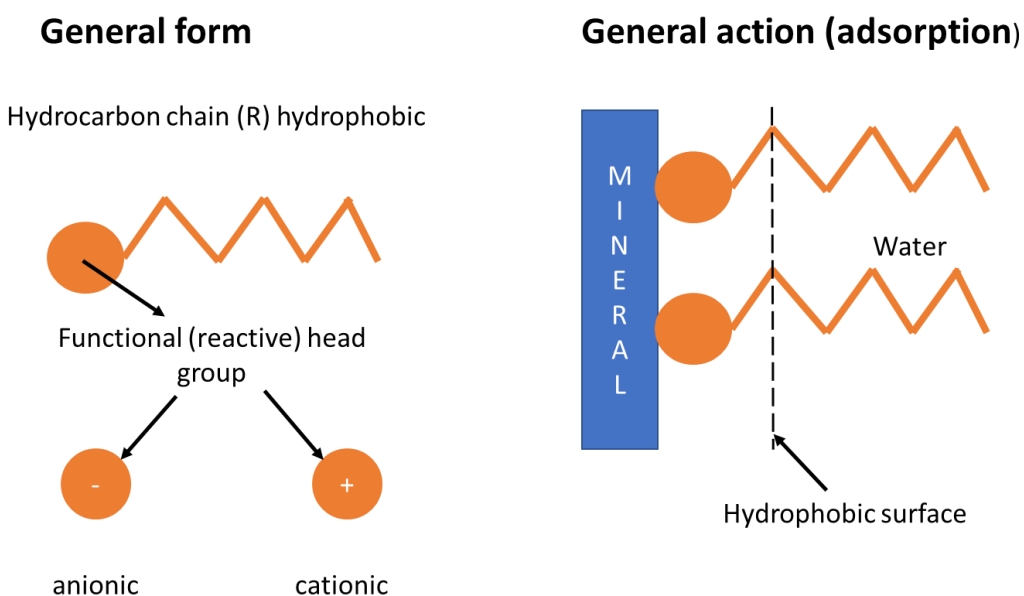


Figure 2.19. General structure of flotation collector and adsorption mechanism. Adapted from J.A. Finch, 2019. Slide 16

The collector consists of a hydrocarbon chain that is hydrophobic, attached to an anionic headgroup. The ionic headgroup, having an electrical charge, will then be adsorbed onto the surface of the mineral at either an anionic or cathodic site, depending on the ionic charge of the

ionic headgroup. The hydrocarbon chain is orientated towards the aqueous phase of the slurry, thus allowing easier attachment to the rising air bubbles and eventual collection of the selected mineral.

The composition of the hydrocarbon chain and the ionic headgroup will depend on the mineral to be collected. Collectors may be classified as in Figure 2.20.

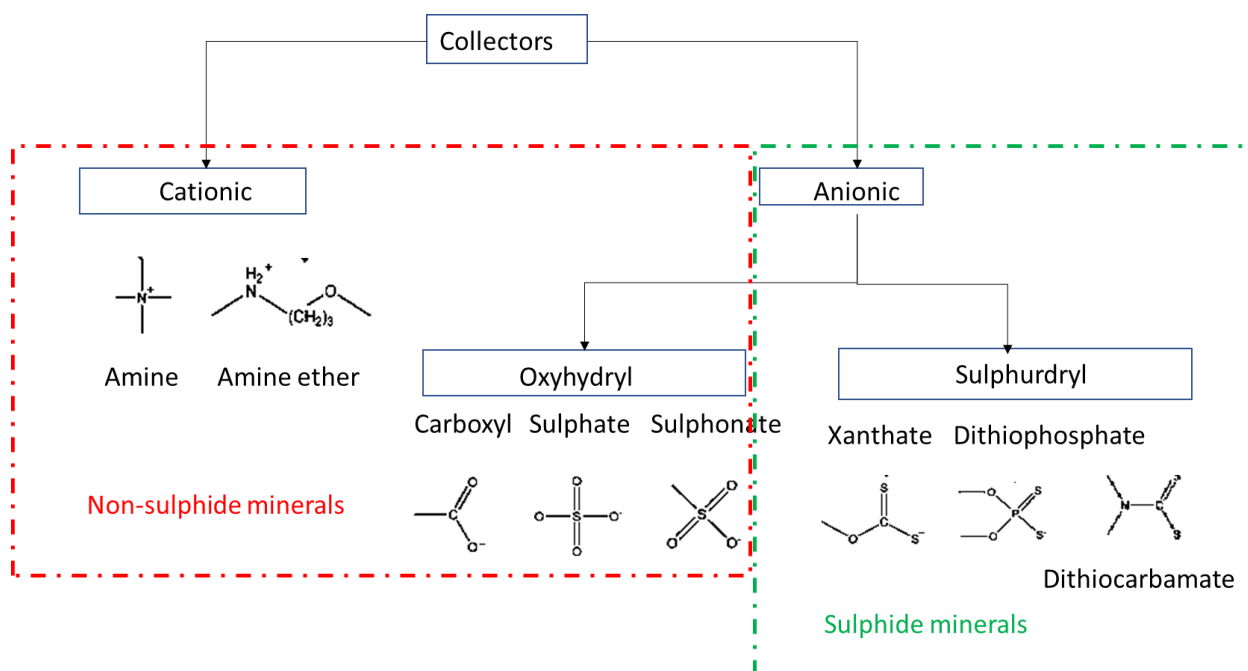


Figure 2.20. Classification of flotation collectors. Adapted from J.A. Finch, 2019. Slide 17.

The first level of classification is based on charge. The cationic collectors are positively charged and are based on nitrogen ions and are used mainly for the flotation of phosphate ores. The anionic collectors are negatively charged and are further classified as oxyhydroxyl or sulphydryl. Oxyhydroxyl collectors are based on the oxygen ion and are used mainly for flotation of oxide minerals, such as hematite, cassiterite and corundum. (Somasundaran, 2004). The anionic collectors of the sulphydryl group are based on the sulphur ion and are used in the beneficiation of sulphide minerals worldwide. The best known and most widely used of the sulphydryl or thiol collectors are the xanthate family of chemicals. The worldwide usage of xanthates in 2018 was

80-85,000 tons, with 12-15,000 tons of di-thiophosphates and 6-8,000 tons of thionocarbamates. (Chidley, 2019)

The chemical structure of selected collectors is shown in Figure 2.21 below.

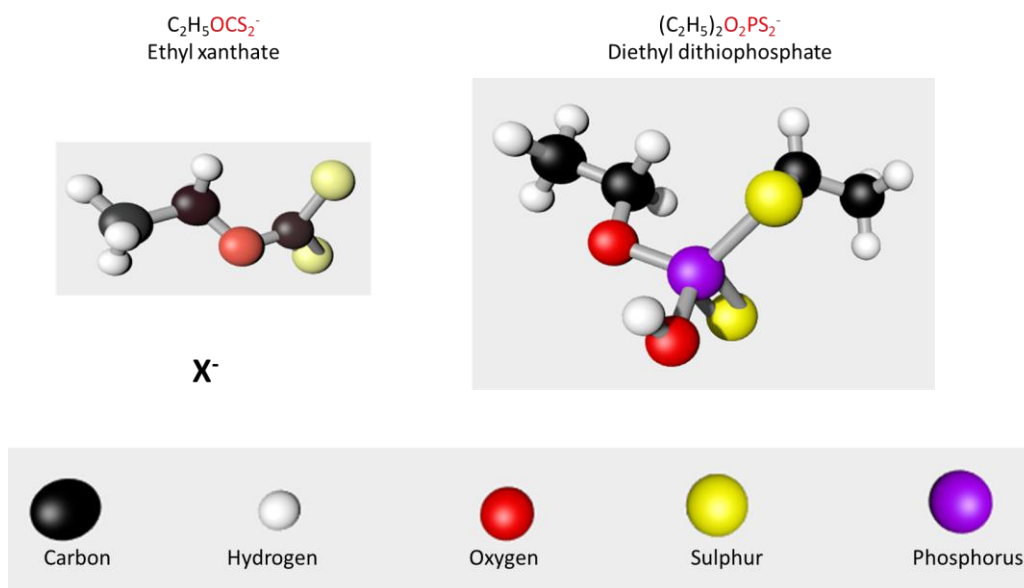


Figure 2.21. Chemical structure of most popular sulfydryl collectors. Adapted from J.A. Finch, 2019. Slide 18.

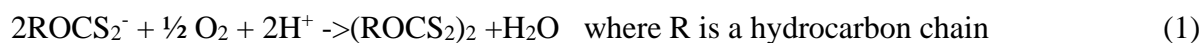
While the collector action of thiol-type surfactants represents such an important portion of the industry, it is the most studied but one of the controversial topics of research. For example, the rendering of galena surfaces hydrophobic, could be caused by: (Poling, 1976):

- Lead ethyl xanthate, as a 1:2 complex,
- Lead ethyl xanthate as a 1:1 complex
- Ethyl dixanthogen as a physiosorbed film
- Mixed lead ethyl xanthate plus ethyl dixanthogen
- Ethyl xanthic acid
- Elemental Sulphur
- Sulphur-dixanthate
- Absorbed ethyl xanthate anions.

Thiol-type collectors generally exhibit a high level of chemical reactivity for metal ions. They do not absorb actively at the air/liquid interface, because of their short hydrocarbon chains.

Xanthate anions can be oxidized to dixanthogen either homogeneously by oxidizing agents such as  $\text{H}_2\text{O}_2$ , or heterogeneously or electrocatalytically on an electrode surface. The longer the hydrocarbon chain, the easier the xanthate ions are oxidized. Without catalysts, dissolved oxygen is ineffective in oxidizing xanthate anions to dixanthogen. (Finkelstein, 1967). The formation of dixanthogen is believed by many to be paramount in the flotation of sulphides. The identification of dixanthogen on mineral surfaces has largely been anecdotal, with direct identification somewhat lacking. Never the less its development has been deemed critical in the sulphide recovery process.

The oxidation of xanthate to dixanthogen, is as follows:



Actually, takes place as two separate, simultaneous electrode processes. The anodic oxidation would be



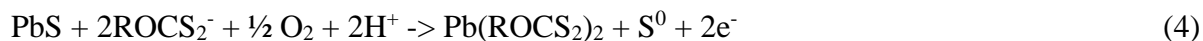
And the cathodic reaction, the reduction of oxygen,



The sulphide surface acts as a catalyst for the formation of dixanthogen (Woods, 2007).

Chemisorption can occur in a similar electrochemical way, with the surface acting as a reactant.

For example:



Involves the anodic reaction



With the cathodic reduction of oxygen being equation (3).

These electrochemical reactions, may be likened to the corrosion of metals, where the dissolution and formation of passive layers that are known to take place by electrode process mechanisms. Some researchers have likened the adsorption of xanthates on the mineral surface to the corrosion reaction, although with a faster rate of reaction. (Poling, 2007).

There is a potential at which the process is in equilibrium; as the potential is increased in the anodic direction from the reversible value, the rate of the anodic reaction (2), i.e., oxidation of xanthate to dixanthogen, would be increased and similarly the reduction of dixanthogen to xanthate will be accelerated if the potential is reversed with an movement in the cathodic direction.

For reaction (1) or (4) to proceed, in which the anodic and cathodic components are different processes, there must be a potential, called a mixed potential, at which the two processes can proceed at a finite rate. Both the anodic cathodic processes occur at the same potential and hence a uniform surface can support both reactions.

Oxidation of the xanthate to its disulfide state only occurs on those minerals that have a rest potential above that of the reversible potential for disulphide formation. In the case of potassium ethyl xanthate, the rest potential for formation of the dixanthogen is 0.13 v. which is exceeded by the rest potentials of pyrite, arsenopyrite, pyrrhotite and chalcopyrite. (Allison and Finkelstein, N.P., 1971). Below this potential, the metal xanthates are formed.

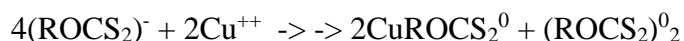
The reaction favoured at pH values relevant to flotation is the formation of the metal xanthate, with the release of thiosulphate ions into the solution. (Woods, 2007). One of the problems with interpreting the results of electrochemical equilibria, is that the measurements are performed on bulk species, whereas flotation systems deal in monolayer quantities. Consequently, the properties of the monolayer generated at the sulphide surface during flotation, can differ from subsequent layers.



Work by Tolun and Kitchener (1964) with polarographic techniques, generated large quantities of product on the electrode, much greater than the monolayers that induce flotation. Also, this method did not detect charges transfer adsorption processes.

Ethyl xanthate is oxidized to diethyl dixanthogen on platinum and gold electrodes (Tolun and Kitchener, 1964). In the absence of xanthates, current flows because of the adsorption and desorption of hydrogen below 0 V and the adsorption and desorption of oxygen above 0 v, both absorbates being derived by charge-transfer from the solvent, water. When xanthates are present, the absorption of hydrogen and oxygen is inhibited by adsorption of xanthate ions. Above 0.2 v, xanthate is oxidized to dixanthogen and an anodic current is passed. (Winter and Woods, 1973). Xanthate ions are produced when the current is reversed.

Dixanthogen is one of the most prevalent non-polar species of all the xanthate reaction products. Dixanthogen is also formed by the reaction of xanthate ions with dissolved metal ion, such as  $\text{Cu}^{++}$  as follows



Both the dixanthogen and cuprous xanthate precipitate out of solution (Poling, 1976).

Formation of the metal xanthate complex, can reduce the polar characteristics of the xanthate group. The overall polar-nonpolar character of the metal xanthate complex should be dependent on the alkyl chain length and the metal. The nature of the metal appears to be more significant than the hydrocarbon chain length in determining the polar/non-polar character (Poling, 1976).

Figure 2.22 shows the results of mixing potassium ethyl xanthate with  $\text{CuSO}_4$  in solution

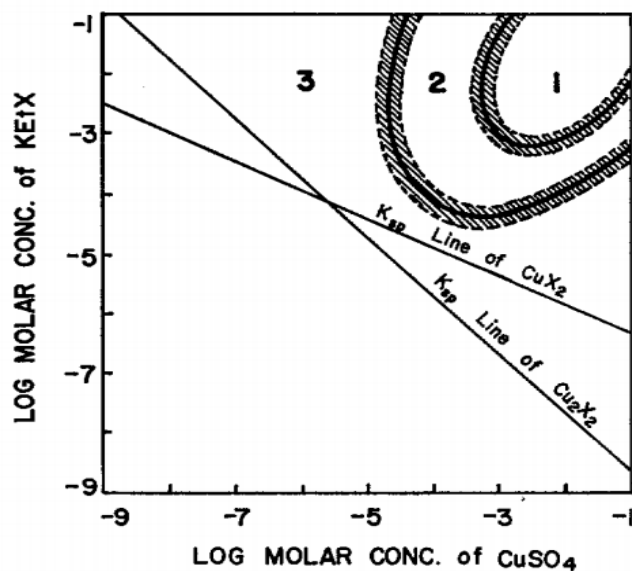


Figure 2.22. Precipitation regions of cuprous ethyl xanthate, showing regions of: (1) high turbidity, (2) low turbidity, (3) turbidity not observed. Reprinted from “Precipitation and Stability of Copper Ethyl Xanthate in Hot Acid and Alkaline Solutions”, by N. Sheikh and J. Leja, 1974, *Journal of Colloid and Surface Interfaces* 47(2), p.302. Copyright Elsevier Science Ltd.

Coarse precipitates of cuprous ethyl xanthate rapidly form in region 1. In region 2, the precipitate remains in the colloidal state, while no precipitate is detected in region 3.

Spectrophotometric analysis indicated that the species in region 3 was an apparently soluble  $\text{Cu Xanthate}^+$  (Poling, 1976).

### 2.6.1 Thiol Collector Coatings on Sulphides

Basic research on thiol/sulphide interactions was conducted using contact angle measurements. Preliminary studies showed that the hydrocarbon chain was the determinant of the maximum contact angle attained. The maximum contact angle was believed to occur when the collector coverage was a complete monolayer. This led to the inference that the thiol collectors were attached to the mineral surface through their polar groups. However, contact angles are not necessarily the best indicators of the mineral floatability.

Collector coverage can exceed the loading associated with a close-packed monolayer if the sulphide surface is heavily oxidized or if dissolved oxygen is available during the conditioning phase. The complete monolayer coverage is of little significance for many of the thiol collectors (Sutherland and Wark, 1955). Partial monolayer coverage of metal xanthates, or mixed with dixanthogens appear capable of creating the necessary hydrophobicity for active flotation. Microautoradiography by Plaskin, (1957) has showed that adsorbed collectors on the mineral surfaces has a typical non-uniform distribution. This non-uniform distribution on the surface of galena was correlated with electrochemical heterogeneity on the mineral surfaces, with xanthates concentrated in areas of high surface free energy, created by cracks, pits and hollows, which acted as anodic sites for collector attachment (Plaskin, 1957).

A study of the chemical nature of adsorbed xanthates was performed by high energy electron diffraction. (Hagihara and Uchikoshi, 1954). Galena faces interacted with xanthates to produce diffraction patterns indicative of lead-xanthate species. Highly pre-oxidized galena surfaces exhibited patterns attributed to lead xanthate crystals as well as the absorbed species. Dixanthogen may have been present, but could have been removed when the sample was subjected to the high vacuum conditions of the analytical technique. Furthermore, the incident electron beam may have heated the  $\text{PbS}_2\text{O}_3$  oxidation product to  $\text{PbSO}_4$  on the galena surface (Leja, Little and Poling, 1963). Lead ethyl xanthate has been reported as not floatable (Mellgren, 1966) Three mechanisms for adsorption of thiol collectors on sulphide minerals were proposed (Poling, 1976):

- Chemical precipitation of insoluble metal xanthates.
- Ion exchange and competition of thiol-collector anions for previously absorbed  $\text{OH}^-$ ,  $\text{SH}^-$  or  $\text{S}_x\text{O}_y^{n-}$  ions
- Neutral collector molecule theory, which attempted to explain how xanthates in solution present as anions, absorbed on negatively charged sulphide mineral surfaces by first hydrolyzing to neutral xanthic acid species.

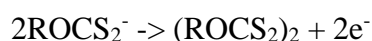
In the last 50 years more attention has been paid to the role oxygen plays in the flotation process. Oxygen is recognized as being needed for thiol collectors to convert the sulphide surface to a hydrophobic state and thus allow flotation. Oxidation occurs during the grinding of sulphide ores and has been found to deplete the dissolved oxygen content of the slurries. As a result, the plant

practice of installing conditioning tanks prior to the flotation circuit, has been established (Konigsmann, 1973).

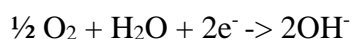
Metal sulphides are generally semiconductors. Changes in the stoichiometric makeup, presence of impurities and imperfections in the lattice, can change their bulk electronic properties. For example, lead rich galena acts as an n-type semiconductor, while sulphur rich galena has the electrical conductivity of a p-type semiconductor. Electron accepting adsorbates should be capable of chemisorption on n-type semiconductors (O<sub>2</sub> on Pb). Conversely, electron donating (reducing) adsorbates should readily chemisorb on p-type semiconductors. Xanthates, which are electron donating reducing agents, will donate electrons to the surface they chemisorb to and may end up as metal xanthates complexes and/or dixanthogen molecules (Poling, 1976). Oxidation can also change galena from an n-type to a p-type semiconductor, which should enable to chemisorption of xanthate, although other researchers have found that the amount of ethyl xanthate on both n and p type samples was the same. (Poling, 1976)

The electrochemical theory behind adsorption of thiol collectors has been drawn from the electrochemical theory of corrosion. This theory states that the sum of the rates of all oxidation reactions must equal the sum of the rates of all reduction reactions. With corrosion, the only oxidation reaction is the oxidation of the metal, with M<sup>0</sup> oxidizing to M<sup>+</sup> or M<sup>2+</sup>. Electrons released by the corrosion, are often consumed by reduction of oxygen on neighbouring sites to form OH<sup>-</sup> ions or H<sub>2</sub>O<sub>2</sub> or H<sub>2</sub>O. The metal adopts a “mixed-potential” between the reversible potential of these two reactions. Oxygen can be reduced on any exposed site, thus, the entire surface of a corroding metal, will be at a “mixed potential”(Poling, 1976).

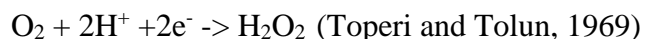
Applying this theory to the adsorption of thiol collectors, the anodic oxidation of xanthate,



Should balance the cathodic reduction of oxygen.



Or



The latter is supported by (Xia, Hart, Chen, Furlotte and Gingras, 2017).

A necessary condition of the formation of dixanthogen, is that the “mixed-potential” must be anodic to the equilibrium potential of xanthate/dixanthogen (Poling, 1976).

The application of corrosion theory may be only partially appropriate to describe the sulphide flotation system. There is evidence that some sulphides, such as galena and sphalerite do not adopt a single “mixed- potential” (Eadington and Prosser, 1968); (Fleming and Kitchener, 1965). Other observations made, include: anionic sites appear to absorb more thiol collector ions than cathodic sites, chemisorption of the thiol collectors polarize these anionic sites to potentials more cathodic than the original cathodic sites. Many of the electrons donated to the solid appear to be localized at the anodic adsorption sites. The increase in the number of electrons transferred to the solid during chemisorption does not balance with the amount of reduction ions of adsorbed oxygen. (Poling, 1976) .

## 2.6.2 Summary

In summary:

Xanthate and several other thiol collectors react with most transition metal cations to form mineral surface complexes of low solubility. Many of these complexes exhibit floatability in the absence of disulphide oxidation products. When covalent metal-sulphur bonds are formed, the partial conversion of the sulphur atoms in the thiol polar groups to non-polar behavior, creates the insolubility and hydrophobicity.

Fractional coverage by chemisorbed transition metal thiolates are often enough to create hydrophobicity on the sulphide surfaces. Under practical conditions, hydrophobicity should be attainable in absence of the disulphide.

Few minerals which have conductivities and rest potentials above the thiol/disulphide reversible potentials, can become covered by disulphide oxidation products, thus for a few minerals, oxygen appears to act electrochemically as a cathodic reactant.

The roles played by oxygen in thiol-collector-sulphide interactions are not necessarily the same for all sulphide minerals. Most sulphide minerals that float with thiol collectors appear to be incapable of acting as electrocatalysts for significant oxidation of thiols to disulphides. For these minerals, the still highly necessary oxygen might consume excess electrons donated to the solid during the formation of metal-thiolate complexes. This function might enable chemisorption of

collector to proceed far enough to confer floatability within practical time limits. Oxygen might also alter the chemical nature of the sulphide surface to facilitate thiol chemisorption through metal-thiolate formation. This same mechanism of oxidation may reduce the degree of hydration of the sulphide surfaces and thereby facilitate collector adsorption.(Poling, 1976)

## 2.7. Activation mechanisms for selective flotation of pyrite and sphalerite.

This section is presented here to provide an understanding of the mechanism of collector attachment to the activated mineral surface, that allows for the selective separation of sphalerite from pyrite.

Some of the more common value-added ore minerals in polymetallic sulphide ore deposits include pyrite ( $\text{FeS}_2$ ) and sphalerite ( $\text{Zn,FeS}$ ). Both occur alone and intermixed with other minerals such as chalcopyrite ( $\text{CuFeS}_2$ ), galena ( $\text{PbS}$ ) and gold ( $\text{Au}$ ). Typically, in these deposits, their relative proportions are low ( $\sim < 5\%$ ) and need to be separated and concentrated free of contaminants to a grade that the end-user (smelter) will accept without penalty. For the most part the separation process involves selective flotation and the following discusses some of the key factors affecting the flotation behavior of pyrite and sphalerite.

Metal sulphide minerals are for the most part weakly polar in nature, thus have a hydrophilic surface. Collectors, such as xanthates, dithiocarbamates and dithiophosphates are used to create hydrophobic mineral surfaces thereby facilitating their floatability.

This section reviews some of the research into the activation of sphalerite and its subsequent flotation.

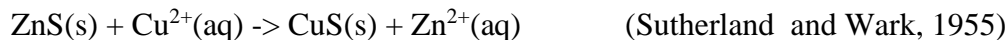
### 2.7.1 Activation of sphalerite

Sphalerite does not respond well to short chain thiol collectors, because the zinc xanthate complex is not stable (Leppinen, 1990). To activate the surface of the sphalerite, the surface

needs to be enhanced to allow the adsorption of the xanthate collector (Wills, 1997). To this end, it is normal to add cupric ions to the slurry before flotation. Cupric sulphate or nitrate are the copper compounds most widely used for this purpose. Other heavy metals, such as lead, silver, cadmium and  $\text{Fe}^{2+}$  or  $\text{Fe}^{3+}$ , may also be used, but generally are not because of the cost or the existence of these ions in the sphalerite lattice or in the process water. When sphalerite is mixed with other minerals, addition of the activator, may also activate other minerals, such as pyrite, allowing it to be floated along with the sphalerite reducing the grade of the final zinc concentrate

A typical mill process for a mixed base metal ore of chalcopyrite, galena, sphalerite and pyrite, would be to float the chalcopyrite and galena as a bulk concentrate. Copper sulphate would then be added to the tailings and the zinc floated leaving the pyrite to be discharged with the gangue as tailings.

It has been well established that copper activation of sphalerite is a result of an ion exchange mechanism, with copper substituting for zinc on a 1:1 basis, releasing  $\text{Zn}^{2+}$  ions into solution. (Finkelstein, 1997).



The Cu(II) on the sphalerite surface is subsequently reduced to Cu(I) with the oxidation of the surface sulphide. Xanthates then react with the resultant copper sulphide, increasing the flotation response (Patrick et al., 1999).

Hydrophobic species such as polysulphides ( $\text{S}_n^{2-}$ ) and elemental sulphur ( $\text{S}_n^0$ ) appear to dominate at mildly acidic conditions while hydrophilic species such as hydroxides of copper and zinc along with some sulphite/sulphates occur at higher pH values. Polysulphides or elemental sulphur form as a result of oxidation of the metal deficient sulphide on the sphalerite surface (Popov and Vucinic, 1990);(Prestidge, Skinner and Ralston, 1997). These hydrophobic species can lead to collectorless flotation at low pH (Finkelstein, 1997);(Popov and Vucinic, 1990).

Impurities such as copper and iron may diffuse from the bulk to the surface and under acidic conditions may contribute to collectorless flotation of sphalerite. (Buckley et al., 1989). This occurs because the migration of bulk cationic impurities from the zinc dissolution to the metal

deficient sphalerite surface, can induce collector attachment and self-activation of the sphalerite surface. (Fornasiero and Ralston, 2006)

The processes involved in the activation of sphalerite are shown in Figure 2.23 below.

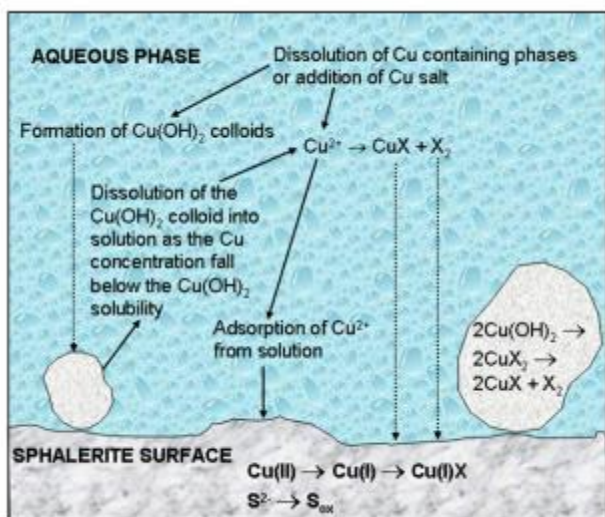
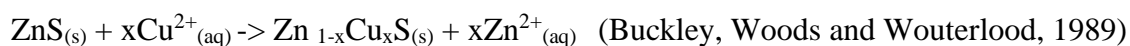


Figure 2.23. Schematic of sphalerite copper activation showing the various simultaneous processes likely to occur under different activation conditions. Reprinted from “A review of the fundamental studies of the copper activation mechanisms for selective flotation of the sulfide minerals, sphalerite and pyrite”, by A.P. Chandra and A.R. Gerson, 2009, *Advances in Colloid and Interface Science*, 145, 99. Copyright 2009 Elsevier Science Ltd. Reprinted with permission

Covellite ( $\text{CuS}$ ) and chalcocite ( $\text{Cu}_2\text{S}$ ) have been considered as the end products of copper activation of sphalerite. (Buckley, 2007). The activated sphalerite surface has been described as a “copper-substituted sphalerite lattice with the formation of a metal-deficient sulphide”. The equation for the reaction is



X-ray absorption spectroscopy (XAS), identified the existence of the tetrahedrally coordinated form of copper, bonded to three sulphur atoms and one oxygen atom, on samples of dry activated sphalerite surface at pH 10-12. Hence chemi-adsorbed water may be present on the adsorbed copper atoms in a wet slurry. With the addition of xanthate, the oxygen of the Cu-O bond is replaced by sulphur and covellite forms. (Patrick, et al., 1999).



Other studies using XAS, showed that at under mildly acidic conditions, copper is coordinated with three sulphur atoms in a distorted trigonal planar geometry. (Figure 2.24)

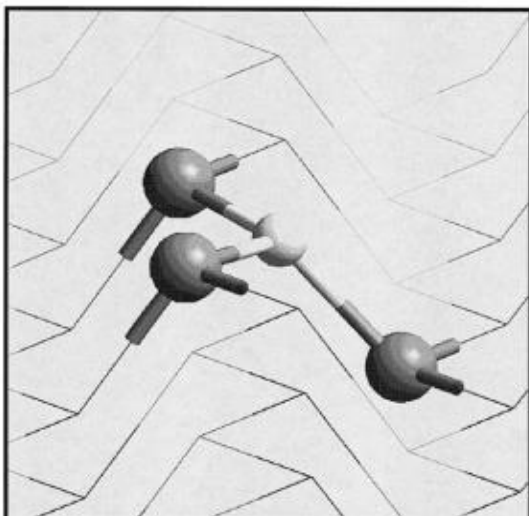


Figure 2.24. The position of the Cu on the surface of the sphalerite lattice is shown as indicated by the XAFS results, i.e., the Cu has replaced one Zn and is in a distorted trigonal planar position between three S with a Cu–S bond length of 2.27 Å. The ZnS surface structure shown in this figure is of the (110) surface the major sphalerite cleavage plane and assumes no surface relaxation has taken place. The Cu is indicated by the light grey sphere, the surrounding sulphurs by darker grey spheres or grey lines and the zinc atoms by black lines.

Reprinted from “The mechanism of copper activation of sphalerite”, by A.R. Gerson et al., 1999, *Applied Surface Science*, 137, 219. Copyright 1999 by Elsevier Science Ltd.

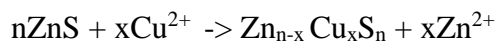
Reprinted with permission

This geometry may be attributed to the fact that the measurements were carried out on a wet slurry. Buckley et al. (2007), confirmed that the copper on the activated surface, consisted of Cu(I), with some Cu(II) ions associated with oxygen, due to chemisorbed water on the sphalerite surface.

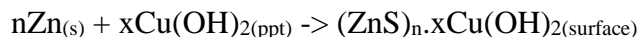
### 2.7.2 Cu(OH)<sub>2</sub> activation

Prestidge et al. (1997), analyzed by XPS synthetic sphalerite conditioned for 30 minutes at pH 9 at high copper concentrations and observed that the sphalerite surface was covered with

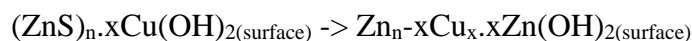
$\text{Cu}(\text{OH})_2$ . This was confirmed by Gerson et al. (1999) using SIMS at high pH and high nominal copper coverage. Rather than the following equation for acidic conditions:



Prestidge et al. (1997), suggested that the following equations are more representative of the reaction in alkaline conditions with  $\text{Cu}^{2+}$  as the activator.



The Cu(II) from the hydroxide may then exchange with the Zn(II) from the sulphide.



The zinc hydroxide when dissolved, controls the hydrophobicity (Fornasiero, D. and Ralston, 2006)(Prestidge et al., 1997). The Cu(II) sulphide then undergoes redox to form Cu(I) sulphur products. These products may then form Cu(I)-xanthate when xanthate is used as a collector. (Patrick et al., 1999). At increased copper concentrations, the copper-substituted zinc sulphide layer become coated with an inhibiting copper hydroxide overlayer (Prestidge et al., 1997).

The hypothesis that the photoreduction of Cu(II) to Cu(I), in the vacuum conditions of XPS analysis has been shown to only apply to  $\text{Cu}(\text{OH})_2$  over-layers and does not affect the Cu(II) associated with activation (Skinner et al., 1996).

### 2.7.3 Zeta potential and isoelectric point (iep)

Popov and Vucinic (1990) found that sphalerite had a positive zeta potential in acidic conditions which became negative in alkaline conditions with an isoelectric point of pH 6.5. The same phenomenon was exhibited when sphalerite was conditioned with xanthate.

However, when conditioned with copper sulphate, a different set of zeta potential-pH curves were recorded. The zeta potential of sphalerite was negative for all copper concentrations below pH 6, which indicated an exchange of Cu(II) and Zn(II) in the sphalerite lattice. (Popov, and

Vucinic, 1990). Popov and Vucinic, (1990) found that there were two charge reversals when the copper concentration was  $8 \times 10^{-4} \text{ mol dm}^{-3}$  (Figure 2.25).

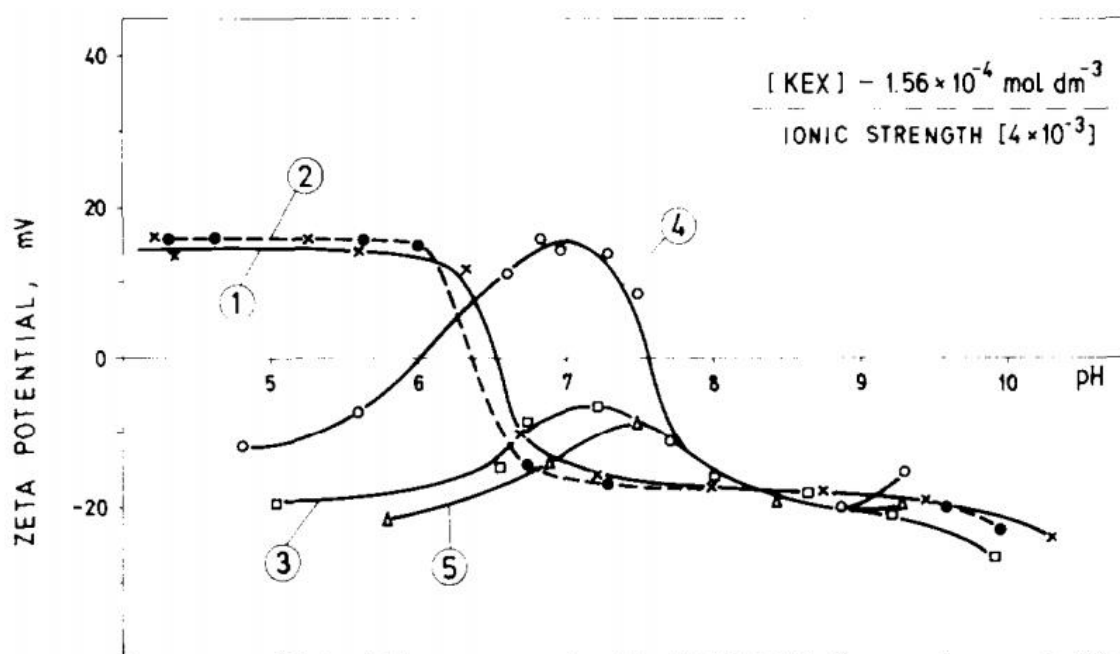


Figure 2.25. Zeta potential of sphalerite at increasing pH and 1=without reagents; 2=Potassium ethyl xanthate (KEX); 3= $1.56 \times 10^{-4} \text{ mol dm}^{-3} \text{ CuSO}_4$ ; 4= $8.0 \times 10^{-4} \text{ mol dm}^{-3} \text{ CuSO}_4$ ; 5= $8.0 \times 10^{-4} \text{ mol dm}^{-3} \text{ CuSO}_4$  (decantation) + KEX. Reprinted from “The ethyl xanthate adsorption on copper-activated sphalerite under flotation-related conditions in alkaline media”, by S.R. Popov and D.R. Vucinic, *International Journal of Mineral Processing*, 30, 236. Copyright Elsevier science Ltd. Reprinted with permission.

The charge reversal from negative to positive at pH 6, is due to adsorption and precipitation of positive hydrolysed ion species ( $\text{Cu}_2(\text{OH})_2^{2+}$  and  $\text{Cu}(\text{OH})^+$ ) on the sphalerite surface. The second reversal occurs at pH 7.6 resulting from the deprotonation of the copper hydroxide on the sphalerite surface. When conditioned with xanthate, the zeta potential remained negative from

pH 5.8 to 9.2, with no charge reversals, due most likely to the adsorption of xanthate on the sphalerite surface. (Popov and Vucinic, 1990). Charge reversals such as this are common with mineral oxides, silicates and sulphides in the presence of adsorbing metal ions. (Rao, 2004)

Similar measurements were conducted by Zhang et al. (1992). While following the curves found by Popov and Vucinic, the zeta potentials measured between pH 2-12, were negative for the entire range and the iep was measured at pH 2.5. The difference was attributed to the iron content of the samples used. Popov and Vucinic (1990), used a natural sphalerite with an iron content of 13% by weight, whereas Zhang et al. (1992) used a natural sphalerite containing only 2.5% by weight.

#### 2.7.4 Effect of sphalerite iron concentration on copper activation.

Pure sphalerite (ZnS), will contain (by weight), 67% Zn, and 33% S. However, natural sphalerite will contain various amounts of Fe substituted for Zn ions in the lattice (Chandra and Gerson, 2009). Sphalerite, which is a natural insulator, will have its reactivity affected by the presence of iron, reducing its band gap (Harmer et al., 2008)

The attachment of xanthate to copper activated sphalerite, decreases as the iron content of the sphalerite increases, mainly due to the reduced sites available in the sphalerite lattice for copper exchange (Solecki and Komosa, 1979) (Szczyba et al., 1980).

Boulton et al. (2005) found that the reduction of exchange sites for  $\text{Cu}^{2+}$ , was more pronounced for coarser sizes, presumably because of the lower surface area to volume ration. Furthermore, there was no change in maximum recovery at low copper concentrations (Boulton et al., 2005). Conflicting studies found that copper activated iron-rich sphalerite, preferentially absorbs xanthate. However, there was no direct correlation between the floatability, iron content and copper concentration (Gigowski et al., 1991).

The number of surface defects and steps increases with the iron content of the sphalerite lead to an increase in the size of the surface oxidation products. The increased surface defect sites allow more  $\text{Cu}^{2+}$  to be adsorbed than when the iron content is lower, because there are less defect sites. At the same time, the higher iron content sphalerite, experience a more rapid oxidation than with lower iron content. In this way, iron assists in the adsorption of  $\text{Cu}^{2+}$  ions (Harmer et

al.,2008). Surface oxidation of sphalerite prior to activation, has a greater effect on copper adsorption onto the lower iron-rich sphalerite in comparison to the iron-rich sphalerite (Solecki et al.,1979) Similarly, copper/xanthate adsorption is much greater on unoxidized sphalerite surfaces than oxidized surface for both high and low iron-rich sphalerite.(Szczypa et al., 1980). Whereas, the iron content was more influential on the copper activation than the degree of oxidation (Gigowski et al., 1991)

### 2.7.5 Copper activation of pyrite.

Unlike sphalerite, pyrite does not need to be activated to adsorb xanthate ions before flotation. In fact, pyrite may be inadvertently activated by copper ions in the slurry. In addition to  $\text{Cu}^{2+}$  ions, pyrite may be activated by  $\text{Pb}^{2+}$ ,  $\text{Fe}^{2+}$  and  $\text{Ca}^{2+}$  ions, all of which are present in complex sulphide ores.

Xanthates may be adsorbed onto the pyrite surface without activation in the pH 5 to pH 7 range. Flotation recoveries of 80-90% may be obtained without activation in the lower end of the pH range; iron-xanthate with dixanthogen were present on the pyrite surfaces which were unactivated. (Leppinen, 1990).

Adsorption of xanthate onto un-activated pyrite surfaces increases with increased aqueous  $\text{Fe}^{2+}$ . The surface oxidation of xanthate to dixanthogen results in a reduction of surface Fe(III) hydroxide, with the conversion to  $\text{Fe}^{2+}$ . Figure 2.26. (Valdivieso et al., 2005).

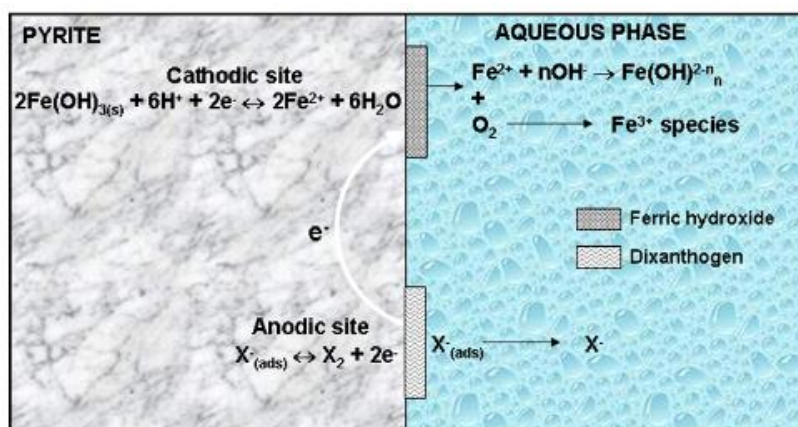


Figure 2.26 Adsorption and dixanthogen formation on unactivated pyrite surface.

Reprinted from “A review of the fundamental studies of the copper activation mechanisms for selective flotation of the sulfide minerals, sphalerite and pyrite”, by A.P. Chandra and A.R. Gerson, 2009, *Advances in Colloid and Interface Science*,145, 104. Copyright 2009 Elsevier Science Ltd. Reprinted with permission

According to the above model, as hydrophobic dixanthogen forms on the pyrite surface, there is a subsequent reduction in the hydrophilic surface hydroxide.

### 2.7.6 Cu(II) and Cu(OH)<sub>2</sub> activation.

The structure and electronic characteristics between pyrite and sphalerite are different, so it is to be expected that the activation mechanisms of the two minerals, will also be different. Firstly, the exchange between pyrite and sphalerite during activation, is not 1:1 as it is with chalcopyrite. Ion exchange as the adsorption mechanism is thus ruled out. (Weisener and Gerson, 2000b). Pyrite activation occurs in a single fast step, involving Cu(II) adsorption onto the reactive sulphur sites at the surface only, with no penetration into the pyrite lattice.(Weisener and Gerson, 2000b). During adsorption, Cu(II) is reduced to Cu(I) with subsequent oxidation of the sulphide surface.

Copper sulphide-like products resembling Cu<sub>2</sub>S or CuS, were found on the pyrite surface by Fourier transformation spectroscopy employing attenuated total reflection (FTIR-ATR). (Leppinen, 1990). Further study using X-ray absorption fine structure (EXAFS) showed that the copper absorbed onto the pyrite surface had a distorted trigonal planar position between the three sulphur atoms.(Weisener and Gerson, 2000b). Use of time of Flight Secondary Ion Mass spectrometry (ToF-SIMS) found Cu(I) to be present for all pH and copper concentrations studied, with Cu(II) occurring as the hydroxide as an overlay of the Cu(I) activated surface only at alkaline pH (Weisener and Gerson, 2000a).

From zeta potential measurements and FTIR-ATR, it was surmised that copper is chemisorbed on the surface of the pyrite (Zhang et al., 1992). However, Hicyilmaz, C., Emre Altun, N., Ekmecki, Z., Gokagac, (2004) showed that the interaction of copper and pyrite is solely an electrochemical process, whereas, the interaction between activated copper and sodium diisobutyl dithiophosphate (DTPI) is chemical in nature. The interaction of activated pyrite surfaces with ethyl xanthate was shown by internal reflection analysis, to have Cu(I)-xanthate as the dominant activation product, with monolayer coverage.(Leppinen, 1990).

Xanthate adsorption and subsequent pyrite flotation was found to be dependent on copper concentration and pH. With equal amounts of copper and xanthate at pH 7, only copper xanthate was observed, however when copper concentrations dominate, significant amounts of

dixanthogen also forms (Leppinen, 1990). The amount of xanthate adsorbed onto activated pyrite surfaces, increases from a minimum at pH 4-5 to a maximum at pH 8, after which it decreases drastically (Leppinen, 1990).

The percentage recovery of activated pyrite with and without xanthate also decrease after pH 8-9 when the pyrite mineral only was investigated (Dichmann and Finch, 2001). An increase in recovery is only seen in the pH range of 6-10. At mildly acidic pH, a higher than expected recovery of un-activated pyrite is observed, due to the emergence of sulphur rich products from the dissolution of iron (Zhang et al., 1992). The hydrophobicity of pyrite increases at low pH regardless of copper activation or collector addition. (Hicyilmaz et al., 2004)

The pulp oxidation potential (Eh) has been found to be an important factor in determining recoveries and speciation on pyrite surfaces, with maximum recoveries obtained at the potential of 35 mV (SHE) at pH 9. Eh influences the production of hydrophilic iron oxides and hydroxides and hydrophobic Cu(I)-S species. The presence and relative abundance of such species has a corresponding effect on pyrite recovery (He et al., 2005).

The range of collector and copper concentrations, depends on the ore mineralogy and the economic minerals. Most references quoted have conducted tests using single minerals in concentrations similar to industry usage, whereas mineral processing mills have a mixed mineral system with galvanic processes which are non-existent in a single mineral test.(Chandra and Gerson, 2009).

### 2.7.7 Mixed pyrite and sphalerite flotation

Separation of pyrite and sphalerite with activated flotation, normally take place at a high pH (Shen et al., 1998), although some mills such as Teck Cominco, use a lower pH (Harmer et al., 2008). Pyrite has a higher rest potential than sphalerite leading to the pyrite surfaces becoming coated with  $\text{OH}^-$  products from the reduction of  $\text{O}_2$  because of the galvanic coupling, making the pyrite surface less hydrophobic and increasing the selectivity of sphalerite.(Harmer et al., 2008)

The galvanic coupling can be suppressed by using nitrogen gas instead of air in the flotation process. This causes the pulp potential to be reduced due to reduced oxygen activity (Rao,

2004). The use of  $N_2$  gas can be used to reduce galvanic interactions in the reverse flotation of pyrite from sphalerite (Finch et al., 2007).

Activated pyrite flotation is depressed in the presence of sphalerite at all values of pH, with recovery decreasing to approximately 2% at pH 11 (Zhang et al., 1992). Flotation without copper activation has no effect on pyrite recovery as sphalerite does not combine with xanthate without copper (Zhang et al., 1997). During mixed flotation, sphalerite preferentially consumes copper and xanthate while pyrite becomes depressed in the presence of sphalerite. The addition of copper increases galvanic coupling between sphalerite and pyrite grains which favours xanthate adsorption on sphalerite while pyrite becomes coated with hydrophilic hydroxide ions (Dichmann and Finch, 2001). This galvanic coupling has been put into practice at Agnico-Eagle's Laronde mine and the former Noranda Mattagami-Bell Attard property (Finch et al., 2007).

XPS and ToF-SIMS studies have shown that in mixed pyrite-sphalerite flotation, hydrophilic species of ferric hydroxide/sulphate obscure the pyrite surface. The iron hydroxide layer appears to inhibit copper and collector adsorption onto the pyrite. Hydrophobic species, such as cuprous sulphide and collector, were found on the sphalerite surface (Boulton et al., 2005). Increasing the copper concentration increased the sphalerite recovery, while increasing the collector concentration increased the pyrite recovery. Testing also revealed that the loss of Zn was a result of fine sphalerite reporting to the tails due to the lower probability of combining with gas bubbles during flotation (Boulton et al., 2005).

Grinding using mild steel media, also reduces the pulp potential as corrosion of steel consumes oxygen. The corrosion of the grinding media is accelerated by the galvanic reaction between the steel balls and the mineral grains, with cathodic reduction of the oxygen occurring on the mineral surfaces (Woodcock et al., 2007; Xia et al., 2017). The metal surface is left rich in hydrophilic hydroxyl products which affect selectivity as they are a significant source of iron contamination (Finch et al., 2007).

Depressants, such as sodium sulphite, sulphur dioxide or sodium metasilphite, may be used to increase selectivity, by preventing collectors adsorbing onto the mineral surface. As no sulphur-



oxygen products are observed on the pyrite surfaces, depression by sulphy species tends to follow an electrochemical mechanism (Rao, 2004.)

Shen et al. (2001) proposed that galvanic interactions occur between the cuprous sulphide layer on the pyrite surface and the pyrite mineral. The cuprous sulphide layer being less cathodic, is oxidized to produce cupric ions while  $O_2$  is reduced at the pyrite surface, producing hydroxide ions. Sodium sulphite with  $O_2$ , induces more hydroxide to form on the pyrite surfaces than on the sphalerite, because pyrite is more cathodic than the sphalerite.

Sodium cyanide can also depress pyrite, by inhibiting xanthate adsorption and its subsequent oxidation (Rao, 2004). This happens through the formation of an insoluble iron-cyanide complex through an electrochemical mechanism. (Fuerstenau et al., 2007; Wang and Forsberg, 1996). Cyanide can also displace xanthate already adsorbed on to pyrite surfaces by an exchange mechanism (Wang and Forsberg, 1996).

In addition, cyanide may lead to the inadvertent activation of sphalerite when added as a pyrite depressant in the flotation of chalcopyrite. This inadvertent activation occurred in the grinding circuit of a mill in Quebec, when the copper was leached out of chalcopyrite by the cyanide and sufficient anodic pulp potential resulted in the activation of sphalerite (Finch et al., 2007). The activation was reversed when the pulp potential became cathodic and the copper existed in the  $Cu^+$  oxidation state in solution and was therefore unable to exchange with the divalent state from the sphalerite. (Rao, Nasset, and Finch, 2007)

Another source of inadvertent activation arises from the water used in the flotation process. The water may contain dissolved minerals and oxidation products, such as  $Fe^{2+}$ ,  $Cu^{2+}$ ,  $Pb^{2+}$ ,  $Na^+$ ,  $K^+$ ,  $Ca^{2+}$  and  $Mg^{2+}$ , along with variations in pH and temperature, which can lead to non-selective adsorption of xanthate and dixanthogen. This contamination may be complicated when recycled water tailings and thickener overflows are added to the mill process water. Not only can these water properties effect the selectivity of the sulphide minerals, but can lead to increased reagent consumption.

### 2.7.8 Summary

Sphalerite and pyrite can both be activated by divalent metal ions, such as  $\text{Cu}^{2+}$ ,  $\text{Fe}^{2+}$ ,  $\text{Pb}^{2+}$  in solution. However, it is copper that is most used for activation, as it commercially more viable than the others.

Copper activation of sphalerite occurs when there is a 1:1 exchange of  $\text{Cu}^{2+}$  with  $\text{Zn}^{2+}$  in the first couple of atomic layers of the sphalerite surface, following which, the sulphide is oxidized to a Cu(I)-S species. The first step is relatively rapid and the second step where the copper diffuses into the bulk structure displacing the  $\text{Zn}^{2+}$  is slow and steady. The copper sulphide species on the surface is hydrophobic and can induce collectorless flotation under low pH conditions. Pyrite activation is a single fast step of copper adsorption onto the pyrite surface without an ion exchange with the iron in the mineral lattice. The adsorbed copper does not migrate into the pyrite lattice. Pyrite, unlike sphalerite, responds well to thiol collectors and will float well without copper activation because of the activating nature of the  $\text{Fe}^{2+}$  ions which are naturally present on the pyrite surface. It is these ions that react with xanthates to form iron-xanthate and dixanthogen. This occurs at low pH as the surface  $\text{Fe}^{2+}$  forms iron hydroxide species at higher pH, which slows the adsorption of the collector.

When sphalerite and pyrite are individually activated with copper and conditioned with xanthate collector, Cu(I)-xanthate is formed, which migrates into the sphalerite lattice, even at very low concentrations. The adsorbed xanthate may form hydrophobic dixanthogen at low pH and low copper concentrations. Xanthate, reacting with Cu inadvertently adsorbed on gangue mineral surfaces, along with the formation of dixanthogen, may result in their flotation.

At high pH, colloidal  $\text{Cu}(\text{OH})_2$  will precipitate on the mineral surfaces, causing loss of selectivity. The colloidal  $\text{Cu}(\text{OH})_2$  may also obscure the Cu(I)-sulphide layer, reducing surface hydrophobicity. An ion exchange between the  $\text{Cu}(\text{OH})_2$  and the  $\text{Zn}^{2+}$  on the surface may result in the reduction of the copper to Cu(I) and, with time, migrate into the bulk of the mineral. This exchange does not take place with pyrite, with some of the  $\text{Cu}(\text{OH})_2$  migrating back into solution.

The iron content of sphalerite reduces its band gap, thus increasing the reactivity of the sphalerite, by aiding in the electron transfer reactions. A high iron concentration in the sphalerite lattice, will decrease the adsorption of copper and subsequently higher xanthate adsorption. This results from the fact that high iron sphalerite oxidizes faster than sphalerite with lower iron content and at high pH is likely to be covered by hydroxides possibly at sites which are near to steps and defects. Apart from augmenting the electrochemical reactions, iron may promote the adsorption of copper by preferentially exchanging with copper and may combine directly with the sulphur in xanthate. With high pH or controlled surface oxidation, surface reactive sites become hidden by oxidation with similar conditions, low iron sphalerite adsorbs more copper or xanthate due to its less reactive nature.

## 2.8. Amine flotation of potash ores.

For many years there was difficulty in using flotation in the beneficiation of apatite ores, as the minerals in the ore were soluble. This section reviews the use of amines as the collector for potash ores and the different adsorption mechanism of amines compared to sulphide flotation using thiol-based collectors, as the amines are immiscible in water and are transported to the mineral surface by collector-coated bubbles (Burdukova and Laskowski, 2009).

The flotation of potash ores differs from the flotation of sulphide ores in a number of ways. Firstly, the valuable minerals, sylvite (KCl) and halite (NaCl) are water soluble and as such are extracted from a brine solution. Secondly, the selective flotation of sylvite from halite is a high ionic system and unlike for example, the low ionic systems, the hydrophobicity attributed to the sylvite does not result from an absorption mechanism where the collector ions or their molecules are diffused onto the mineral surfaces. When an adsorbed collector concentration exceeds the critical micelle concentration, flotation stops. In the case of sylvite, no flotation is observed until precipitation of the amine occurs in the solution (Burdukova and Laskowski, 2009).

The solubility of long chain amines in water is extremely low and even lower in brine. The solubility of the ionic surfactant is a combination of temperature and the Krafft point. The Krafft point is the temperature above which the solubility of the surfactant becomes high enough for the

formation of micelles (Moroi, Matuura, Kuwamura and Inokuma, 1986). By definition, micelles cannot form at temperatures below the Krafft point.

In commercial flotation operations, C16-C22 long chain primary amines are melted by heating to 70-90°C and neutralized by hydrochloric or acetic acids, converting the amine to its ammonium salt (Burdukova and Laskowski, 2009). The hot amine is then mixed with the flotation brine at 24-32°C, cooling the hot amine dispersion to below the Krafft point rapidly. A white precipitate immediately appears and deposits on the brine surface, (Burdukova, and Laskowski, 2009), but no particle-bubble attachment takes place.. However, when the solution is stirred for a short time, KCl particles are picked up by the bubbles. Without this stirring, the amine added to the flotation pulp is not able to perform its function. (Leja, 1983).

When contact angle tests were performed on flat surfaces of KCl treated with amine, the surface was not very hydrophobic, with a contact angle of approximately 40°. When a bubble was created with a coating of the amine collector, the contact angle increased to 50-60°, and when the amine was mixed with methyl isobutyl carbinol (MIBC) as a frother, the hydrophobicity of the surface increased (Leja, 1983). The frother helps spread the collector across the liquid/gas interface and lowers the induction time (Burdukova and Laskowski, 2009). The use of a frother will also assist in the creation of smaller bubbles, increasing the total bubble surface area, giving a greater probability of bubble particle collision.

An analogy to use of amines for the flotation of sulphides is the use of aliphatic nitriles (Lewis and Lima, 2018). This is a new collector series about which little is known and is the subject of research by the author.

## 2.9. Conclusions

The chemistry and physics of flotation is a complex subject with little agreement on a unified theory of the process. This results from the fact that each mineral species reacts differently from the next. This difference even occurs from one mineral association to another,

even within the same ore body. Consequently, research has intended to concentrate on finding a solution to a particular problem in processing the ore from the deposit, with the theory then being developed to fit the empirical results of the research. (Adamson and Gast, 1997).

The research that is conducted, often produces contradictory results due to the different media that are used. The media may vary from the elemental metals, laboratory samples of the pure minerals to samples of the mineralogy. The first two will therefore, totally ignore the effects of interaction between the minerals in the deposit, such as the galvanic interaction between sulphide minerals

This chapter, started with a study of the contact angle between the mineral surface and the liquid gaseous interface, despite the difficulties in obtaining good measurements because of the particle size and roughness, the contact angle is important in understanding the attachment and detachment of the mineral particle to and from the air bubble. The chapter discussed the thermodynamics and kinetics of the efficiency of the attachment and detachment of the mineral particles to the gas bubble.

The chapter continued with a review of the theory of the chemistry of the mineral surface and the electrochemical effects of immersion in water, which becomes crucial to the floatability of the mineral.

The chemistry of the chemicals used to induce hydrophobicity of metal sulphide surfaces was discussed, with emphasis on the xanthate family, the most commonly used collector in the minerals industry.

Often, the sulphide minerals of iron and zinc are found together. This combination of minerals has been widely studied, with a variety results because of the reason expressed above. These studies have been reviewed.

## 2.10. References.

- Adam, N. K. (1938). *The Physics and Chemistry of Surfaces* (Second). Oxford: Carendon Press.
- Adamson, A. and Gast, A. P. (1997). *Physical Chemistry of Surfaces* (6th ed.). New York: John Wiley & Sons.
- Allahkarami, E., Poor, A.Z., Rezai, B. (2017). Pyrite flotation in the presence of galena. Study of galvanic interaction. *Iwasaki, I, Reid, K J, Lex, H A and Smith, K A, Hysicochem. Probl. Miner. Process.*, 53(2), 846–858.
- Allison and Finkelstein, N.P., S. A. (1971). Products of Reaction between Galena and Aqueous Xanthate Solutions. *Trans. I.M.M.*, 80, C235-239.
- Aplan, F.F., and Fuerstenau, D. W. (1962). Principles of Nonmetallic Mineral Flotation. In D. W. Fuerstenau (Ed.), *Froth Flotation. 50th Anniversary Volume* (p. 177). New York, New York: American institute of Mining, Metallurgical and Petroleum Engineers.
- Beischer, D. E. (1953). Radioactive Monolayers: A new approach to surface research. *Journal of Physical Chemistry*, 57(2), 137.
- Boulton, A. Fornasiero, D., Ralston, J. (2005). Effect of iron content in sphalerite on flotation. *Minerals Engineering*, 18, 1120–1122.
- Buckley, A.N, Woods, R., Wouterlood, H. J. (1989). An XPS Investigation of the Surface of Natural Sphalerites under Flotation-Related Conditions. *International Journal of Mineral Processing*, 26, 29–49.
- Buckley, A.N., et al. (2007). Examination of the proposition that Cu(II) can be required for charge neutrality in a sulfide lattice — Cu in tetrahedrites and sphalerite1. *Can.J. Chem.*, 85, 767–781.

- Buckley, A.N. and Woods, R. (1997). Chemisorption - the thermodynamically favoured process in the interaction of thiol collectors with sulfide minerals., *International Journal of Mineral Processing*, 51, 15–26.
- Burdukova, E. and Laskowski, J. S. (2009). Effect of Insoluble Amine on Bubble Surfaces on Particle-Bubble Attachment in Potash Flotation. *Can. Jour. of Chem. Eng.*, 87, 441–447.
- Cassie, A.B.D. and Baxter, S. (1944). Wettability of Porous surfaces. *Trans. Faraday Soc.*, 40, 546–551.
- Chander, S., Wie, J.M., Fuerstenau, D. W. (1975). On native floatability and the surface properties of naturally hydrophobic solids., In R. B. Somasundaran, P.,Grievies (Ed.), *Advances in Interfacial Phenomena of Particulate/ Solid/Gas Systems*, (pp. 183–188). New York: Am. Inst. Chem. Engrs.,
- Chandra, A.P. and Gerson, A. R. (2009). A review of the fundamental studies of the copper activation mechanisms for selective flotation of the sulfide minerals, sphalerite and pyrite. *Advances in Colloid and Interface Science*, 145, 97–110.
- Chau, T. T., Bruckard, W. J., Koh, P. T. L., & Nguyen, A. V. (2009). A review of factors that affect contact angle and implications for flotation practice. *Advances in Colloid and Interface Science*. <https://doi.org/10.1016/j.cis.2009.07.003>
- Chehreh Chelgani, S. and Hart, B. (2014). TOF-SIMS Studies of Surface Chemistry of Minerals Subjected to Flotation Separation. *Minerals Engineering*, 57, 1–11.
- Chidley, F. (2019). Personal Communication.
- Crabtree, E.H., Vincent, J. D. (1962). *Froth Flotation. 50th Anniversary Volume*. (D. W. Fuerstenau, Ed.). New York: American institute of Mining, Metallurgical and Petroleum Engineers.
- Crawford, R. and Ralston, J. (1988). The Influence of Particle Size and Contact Angle in Mineral Flotation. *International Journal of Mineral Processing*, 23, 1–24.

- Dai, Z., Fornasiero, D., & Ralston, J. (2000). Particle-bubble collision models - a review. *Advances in Colloid and Interface Science*, 85(2), 231–256. [https://doi.org/10.1016/S0001-8686\(99\)00030-5](https://doi.org/10.1016/S0001-8686(99)00030-5)
- de Bruyn, P.L. and Agar, G. . (1962). Surface Chemistry of Flotation. In D. W. Fuerstenau (Ed.), *Froth Flotation. 50th Anniversary Volume* (pp. 91–138). New York, New York: American institute of Mining, Metallurgical and Petroleum Engineers.
- Derjaguin, B.V. and Dukhin, S. S. (1961). Theory of flotation of small and medium size particles. *Trans. I.M.M.*, 70, C221-246.
- Dichmann, T.K. and Finch, J. A. (2001). The Role of Copper Ions in Sphalerite-Pyrite Flotation Selectivity. *Minerals Engineering*, 14, 217–225.
- Eadington, P. and Prosser, A. P. (1968). Oxidation of Lead Sulphide in Aqueous Suspensions. *Trans. I.M.M.*, 78, C74-82.
- Finch, J.A., Rao, S.R., Nasset, J. E. (2007). Iron control in mineral processing. In *39th annual meeting of the Canadian Mineral Processors*. Ottawa: Canadian institute of Mining, Metallurgy and Petroleum.
- Finkelstein, N. P. (1967). Kinetic and thermodynamic Aspects of the interaction between Potassium Ethyl Xanthate and Oxygen in Aqueous solution. *Trans IMM*, 76, C51-59.
- Finkelstein, N. P. (1997). The activation of sulphide minerals for flotation: a review. *International Journal of Mineral Processing*, 52, 81–120.
- Fleming, M.G. and Kitchener, J. A. (1965). Development of the Theory of the Flotation of Sulphide Ores. *Endeavor*, 24, 101–105.
- Fornasiero, D. and Ralston, J. (2006). Effect of surface oxide/hydroxide products on the collectorless flotation of copper-activated sphalerite. *International Journal of Mineral Processing*, 78, 231–237.
- Fossberg, E, Sundberg, S. and Hongxin, Z. (1988). Influence of different grinding methods on



- floatability. *International Journal of Mineral Processing*, 22, 183–192.
- Fuerstenau, D.W. and Urbina, R. H. (1988). Flotation Fundamentals. In P. Somasundaran (Ed.), *Reagents in Mineral Technology* (pp. 1–38). New York: Routledge.
- Fuerstenau, M. C., Graeme, J., & Yoon, R. H. (2007). Froth Flotation: A Century of Innovation. *Flotation Chemistry*.
- Gardner, J. R. and, & Woods, R. (1974). An Electrochemical Investigation of Contact Angle and of Flotation in the Presence of Alkylxanthates . I Platinum and Gold Surfaces, (224).
- Gaudin, A. M. (1932). *Flotation* (1st ed.). New York: McGraw-Hill.
- Gerson, A.R., Lange, A.G., Prince, K.E., Smart, R. S. C. (1999). The mechanism of copper activation of sphalerite. *Applied Surface Science*, (137), 207–223.
- Gigowski, B., Vogg, A., Wierer, K., Dobias, B. (1991). Effect of Fe-lattice ions on adsorption, electrokinetic, calorimetric and flotation properties of sphalerite. *International Journal of Mineral Processing*, 33, 103–120.
- Greet, C.J., Kinal, J., Steiner, P. (2005). Grinding Media-Its Effect on Pulp Chemistry and Flotation Behaviour-Fact or Fiction? In *Centenary of Flotation Symposium* (pp. 697–971).
- Hagihara, H. and Uchikoshi, H. (1954). Adsorption of Alkyl Xanthate and Dithiophosphate on a Cleavage Face of Galena as revealed by Electron Diffraction. *Nature*, 174(July 10, 1954), 80–81.
- Harmer, S.L., Mierczynska-Vasilev, A., Beatty, D.A., Shapter, J. G. (2008). The effect of bulk iron concentration and heterogeneities on the copper activation of sphalerite. *Minerals Engineering*, 21, 1005–1012.
- Hart, B.R., Dimov, S., Xia, L. (2014). REE bearing mineral recovery: a microflotation and surface chemistry study using hydroxamate collectors and citric acid. In *IMPC 2014*.
- Hart, B. (2011). ACST in Mineral Processing.

- He, S., Fornasiero, D., Skinner, W. (2005). Correlation between copper-activated pyrite flotation and surface species: Effect of pulp oxidation potential. *Minerals Engineering*, 18, 1208–1213.
- Hewitt, D., Fornasiero, D., Ralston, J., Fisher, L. R. (1993). Aqueous film drainage at the quartz/water/air interface. *L. Chem. Soc. Faraday Trans.*, 89, 817–822.
- Hicyilmaz, C., Emre Altun, N., Ekmecki, Z., Gokagac, G. (2004). Quantifying hydrophobicity of pyrite after copper activation and DTPI addition under electrochemically controlled conditions. *Minerals Engineering*, 17, 879–890.
- Isaacson, A. E. (1989). *Effect of sulphide minerals on ferrous alloy grinding media corrosion*.
- Iwasaki, I., Natarajan, K A, Riemer, S C and Orlich, J N. (1985). Corrosion and abrasive wear in ore grinding,. *Wear*, 103, 253–262.
- Iwasaki, I, Reid, K J, Lex, H A and Smith, K A. (1983). Effect of autogenous and ball mill grinding on sulphide flotation,. *Mining Engineering*, 35, 253–262.
- Jameson, G.J., Nguyen, A.V., Ata, S. (2007). The flotation of fine and coarse particles. In R.-H. Fuerstenau, D.W., Jameson, C.J., Yoon (Ed.), *Froth Flotation: A Century of Innovation*. (pp. 329–351). Denver: SME.
- Konigsmann, K. V. (1973). Aeration in Plant Practice. In *Proc. 5th Annual Meeting, Can. Min. Processors* (pp. 299–332). Ottawa.
- Laskowski, J. S. (1989). Thermodynamic and kinetic flotation criteria. *Mineral Processing and Extractive Metallurgy Review*, 5(1–4), 25–41.
- Laskowski, J. S. (2007). Flotation Thermodynamics: Can we learn anything from it? *Can. Metall. Q.*, 46(3), 251–258.
- Leja, J., Little, L.H., Poling, G. W. (1963). Xanthate Adsorption Studies using Inferred Spectroscopy, Part II, Evaporated Lead Sulphide, Galena and Metallic Lead Substrates. *Trans. I.M.M.*, 72, C414-423.

- Leja, J. and Schulman, J. H. (1954). Flotation Theory: molecular Interactions Between frothers and Collectors at solid-Liquid-air interfaces. *Transactions AIME*, 199, 221–228.
- Leja, J. (1982). *Surface Chemistry of Froth Flotation* (First). New York: Plenum.
- Leja, J. (1983). *On the Action of Long Chain Amines in Potash Flotation*. (R. M. McKercher, Ed.). Toronto: Pergamon Press.
- Leppinen, J. O. (1990). FTIR and flotation investigation of the adsorption of ethyl xanthate on activated and non-activated sulfide minerals. *International Journal of Mineral Processing*, 30, 245–263.
- Lewis, A., Bolin N-J., Malm, Svensson, M., Lima, O. (2019). Analysis of the rougher-scavenger bank using Tecflote S11 at Boliden Aitik. In *Flotation '19*.
- Lewis, A. and Lima, O. (2018). Tecflote- New collector for Sulfide Flotation. In *Procemin Geomet* (pp. 321–333). Santiago, Chile.
- Manor, O., Vakarelski, I.U., Stevens, G.W., Grieser, F., Dagastine, R.R., Chan, D. Y. C. (2008). Dynamic Forces between Bubbles and Surfaces and Hydrodynamic Boundary Conditions. *Langmuir*, 24, 11533–11543.
- Mellgren, O. (1966). No Heats of Adsorption and Surface reactions of Potassium Ethyl Xanthate on Galena. *Trans. AIME*, 235, 46–60.
- Moroi, Y., Matuura, R., Kuwamura, T., Inokuma, S. (1986). Anionic Surfactants with Divalent Gegenions of separate Electric Charge Solubility and Micelle Formation. *J. Coll.Int. Sci.*, 113, 225–231.
- Nagaraj, D.R. and Farinato, R. S. (2016). Evolution of flotation chemistry and chemicals: A century of innovations and the lingering challenges. *Minerals Engineering*, 96–97, 2–14.
- Nagaraj, D. R., & Farinato, R. S. (2016). Evolution of flotation chemistry and chemicals: A century of innovations and the lingering challenges. *Minerals Engineering*.  
<https://doi.org/10.1016/j.mineng.2016.06.019>

- Newcombe, G., and R. Gerson (1994). Bubble spreading kinetics and mineral flotation. *Minerals Engineering*, 7(7), 889–903.
- Nguyen, A.V. and Evans, G. M. (2004). Movement of fine particles on an air bubble surface studied using high-speed video microscopy. *Journal of Colloid and Interface Science*, 273, 271–277.
- Nguyen, A. V. (2003). New method and equations for determining attachment tenacity and particle size limit in flotation. *International Journal of Mineral Processing*, 68, 167–182.
- Patrick, R.A.D., England, K.E.R., Charnock, J.M., M. J. F. W. (1999). Copper activation of sphalerite and its reaction with xanthate in relation to flotation: an X-ray absorption spectroscopy (reflection extended X-ray absorption fine structure) investigation. *International Journal of Mineral Processing*, 55, 247–265.
- Plaskin, I. N. (1957). *Electrical Phenomena and Solid/Liquid Interfaces*. London: Butterworths.
- Poling, G. W. (1976). Reactions between thiol reagents and sulphide minerals. In *Flotation A. M. Gaudin Memorial Volume* (pp. 334–363). New York: American institute of Mining, Metallurgical and Petroleum Engineers.
- Popov, S.R. and Vucinic, D. R. (1990). The ethylxanthate adsorption on copper-activated sphalerite under flotation-related conditions in alkaline media. *International Journal of Mineral Processing*, 30, 229–234.
- Prestidge, C.A., Skinner, W.M., Ralston, J. S. R. S. C. (1997). Copper(II) activation and cyanide deactivation of zinc sulphide under mildly alkaline conditions. *Applied Surface Science*, 108(3), 333–334.
- Pryor, E. J. (1965). *Mineral Processing* (3rd.). London: Elsevier Publishing Co. Ltd.
- Qin, W. et al. (2015). Electrochemical characteristics and the collectorless flotation behavior of galena: With and without the presence of pyrite. *Minerals Engineering*, 74, 99–104.
- Ralston, J., Fornasiero, D., & Hayes, R. (1999). Bubble-particle-attachment-and-detachment-in-

flotation\_1999\_International-Journal-of-Mineral-Processing, 1–32. Retrieved from  
papers2://publication/uuid/3C27F5FC-1466-43FF-A100-9331C29D75E0

Rao, S., Nasset, J.E., Finch, J. A. (2007). Activation of sphalerite by Cu ion produced by cyanide action on chalcopyrite. In G. N. Khosla, N.K., Jadhav (Ed.), *Proceedings of the International Seminar on Mineral Processing Technology (MPT)*. New Delhi: Allied Publishers.

Rao, S.R., Finch, J. A. (1988). Galvanic interaction studies on sulphide minerals. *Can. Metall. Q.*, 27(4), 253.

Rao, S. R. (2004). *Surface Chemistry of Froth Flotation* (Second). New York: Plenum.

Reid, E. E. (1962). *Organic chemistry of Bivalent Sulfur*. New York: Chemical Publishing Co.

Rimstidt, D. D., & Vaughan, D. J. (2003). Pyrite oxidation: A state-of-the-art assessment of the reaction mechanism. *Geochimica et Cosmochimica Acta*, 67(5), 873–880.  
[https://doi.org/10.1016/S0016-7037\(02\)01165-1](https://doi.org/10.1016/S0016-7037(02)01165-1)

Senior, G.D., Trahar, W. J. (1991). The influence of metal hydroxides and collector on the flotation of chalcopyrite. *International Journal of Mineral Processing*, 33, 321–341.

Shen, W.Z., Fornasiero, D., Ralston, J. (1998). Effect of collectors, conditioning pH and gases in the separation of sphalerite from pyrite. *Minerals Engineering*, 11, 145–158.

Shen, W.Z., Fornasiero, D., Ralston, J. (2001). Flotation of sphalerite and pyrite in the presence of sodium sulfite. *International Journal of Mineral Processing*, 63, 17–28.

Skinner, W.M, Prestidge, C.A., Smart, R. St. C. (1996). Irradiation Effects During XPS Studies of Cu(II) Activation of Zinc Sulphide. *Surface and Interface Analysis*, 24, 620–626.

Smart, R.St.C, Jasieniak, M., Prince, K.E., Skinner, W. M. (2000). SIMS studies of oxidation mechanisms and polysulfide formation in reacted sulfide surfaces. *Minerals Engineering*, 13, 857–870.

Solecki, J., Komosa, A., S. J. (1979). Copper ion activation of synthetic sphalerites with various

- iron contents. *International Journal of Mineral Processing*, 6, 221–228.
- Somasundaran, P. (2004). *Encyclopedia of Surface and Colloid Science, Volume 1* (Second). New York: Marcel Dekker.
- Stechemesser, H. and Nguyen, A. V. (1999). Time of gas–solid–liquid three-phase contact expansion in flotation. *International Journal of Mineral Processing*, 56, 117–132.
- Sutherland, K.L. and Wark, J. W. (1955). *Principles of Flotation*. Melbourne: Aust. I.M.M.
- Sutherland, K. L. (1948). Physical chemistry of Flotation XI. Kinetics of the Flotation Process. *J. Phys. Chem*, 52(2), 394–425.
- Szczypa, J., Solecki, J., Komosa, A. (1980). Effect of surface oxidation and iron contents on xanthate ions adsorption of synthetic sphalerites. *International Journal of Mineral Processing*, 7, 151–157.
- Tolun, R., and Kitchener, J. A. (1964). Electrochemical study and Thermodynamic Equilibria of the Galena-Oxygen-Xanthate Flotation System. *Trans. I.M.M.*, 73, C313-322.
- Toperi, D., and Tolun, R. (1969). Electrochemical Study and Thermodynamic Equilibria of the Galena-Oxygen-Xanthate Flotation System. *Trans. I.M.M.*, 78, C191-197.
- Valdivieso, L.A., Sanchez-Lopez, A.A., Song, S. (2005). On the cathodic reaction coupled with the oxidation of xanthates at the pyrite/aqueous solution interface. *International Journal of Mineral Processing*, 77, 154–164.
- Verrelli, D. I., Koh, P. T. L., & Nguyen, A. V. (2011). Particle-bubble interaction and attachment in flotation. *Chemical Engineering Science*, 66(23), 5910–5921.  
<https://doi.org/10.1016/j.ces.2011.08.016>
- Wang, X.H., Forssberg, K. S. E. (1996). The solution electrochemistry of sulfide-xanthate-cyanide systems in sulfide mineral flotation. *Minerals Engineering*, 9, 527–546.
- Weisener, C. and Gerson, A. (2000a). An Investigation of the Cu (II) Adsorption Mechanism on Pyrite by ARXPS and SIMS. *Minerals Engineering*, 13, 1329–1340.

- Weisener, C. and Gerson, A. (2000b). Cu(II) adsorption mechanism on pyrite: an XAFS and XPS study. *Surface and Interface Analysis*, 30, 454–458.
- Wenzel, R. N. (1949). Surface roughness and contact angle,. *J. Phys. and Colloid Chem.*, 53, 1466–1467.
- Wills and Finch. (2015). *Mineral Processing Technology* (8th ed.). Butterworth-Heinemann.
- Wills, B. A. (1997). *Mineral Processing Technology*. (Wills B.A., Ed.) (6th ed.). Boston. MA: Butterworth-Heinemann.
- Winter, G., and Woods, R. (1973). The Relation of Collector Redox potential to flotation Efficiency: Monothiocarbonates. *Separation Science*, 8, 261–267.
- Woodcock, J.T., Sparrow, G.J, Bruckard, W. J. (2007). Flotation of Precious Metals and Their Minerals. In R. . Fuerstenau, M.C., Jameson, G., Yoon (Ed.), *Froth Flotation: a century of innovations*. Colorado: Society for Mining, Metallurgy and Exploration, Inc.
- Woods, R. (2007). Electrochemistry of Sulfide Flotation. In *Flotation A. M. Gaudin Memorial Volumetation: A.M. Gaudin Memorial Vol 1* (pp. 298–333).
- Xia, L., Hart, B., Chen Z., Furlotte M., Gingras G., and Laflamme, P. (2017). ToF-SIMS investigation on correlation between grinding environments and sphalerite surface chemistry: implications for mineral selectivity in flotation. *Surface and Interface Analysis*, 49(13), 1397–1403.
- Yopps, J.Y. and Fuerstenau, D. W. (1964). Zero point of charge of alpha alumina,. *J. Coll .Sci.*, 113, 61–71.
- Zhang, Q., Rao, S.R., Finch, J. A. (1992). Flotation of sphalerite in the presence of iron ions. *Colloids and Surfaces*, 66, 81–89.
- Zhang, Q., Xu, Z., Bozkurt, V. (1997). Pyrite flotation in the presence of metal ions and sphalerite. *International Journal of Mineral Processing*, 52, 187–201.

## 3 Methodology

### 3.1 Materials used

#### 3.1.1 Sulphide Minerals

All tests were performed with a synthetic ore of chalcopyrite, pyrite and a common gangue phase that consisted mainly of quartz. A mineralogical assessment and identification of the gangue minerals was not performed. The sulphide minerals from Mexican sources, were purchased from Ward's Scientific, Rochester N.Y. The proportions of the three components in the test synthetic ores varied dependent on the type of test being conducted. The synthetic ore compositions are listed in Table 3.1. All synthetic ores were ground to  $-75 \mu\text{m} + 34 \mu\text{m}$ . Synthetic ores were used to limit the number of experimental variables and exclude interactions between other minerals, which may be present in a natural polymetallic ore.

Ore designation	Composition	Use and comments
Synthetic Ore 1.	1 g. Chalcopyrite, 1 g. Pyrite and 3 g. gangue minerals	Used for conditioning tests, to account for potential mineral interactions.
Synthetic Ore 2.	~0.03 g. Chalcopyrite, ~0.03 g Pyrite and ~0.88 g. gangue minerals	Mixture for micro-flotation (1 g.) with a 2% Cu grade as found in a Volcanogenic Massive Sulphide (VMS) ore deposit.
Synthetic Ore 3.	1 g. Chalcopyrite and 1 g. gangue minerals	Mixture for column tests to build on tests performed by (Schach et al. 2019)

Table 3.1. Composition of "synthetic ores" used in investigations.



## 3.2 Research Methodology

The following experiments were conducted:

- Conditioning tests to determine the amount of collector adsorbed onto the mineral surfaces and the relative degree of collector discrimination between the mineral species where TECFLOTE S11 was adsorbed onto the mineral surfaces.
- Micro-flotation tests, to ascertain the relationship between Tecflote S11 adsorption on the chalcopyrite surface and flotation recoveries.
- Column flotation tests to identify potential distribution mechanisms of TECFLOTE S11 as a collector in the flotation of sulphide minerals.

### 3.2.1 Conditioning tests

The best practice in base metal sulphide flotation, is to condition the ground ore with a mixture of reagents including a pH modifier, collector(s) and other activators or depressants, prior to the flotation circuit (Konigsmann, 1973). This step, referred to as conditioning, serves two purposes: to ensure that the ore slurry is aerated and to distribute the chemicals throughout the slurry promoting adsorption onto the mineral surfaces. The conditioning tests were designed to emulate this process and to determine the extent of TECFLOTE S11 adsorption on the mineral surfaces.

The sulphide minerals in synthetic ore 1 were lightly hand-ground separately in an agate mortar and pestle to expose fresh mineral surfaces and avoid galvanic interactions associated with wet grinding (Greet et al., 2005). Sample conditioning began immediately after the grinding was completed to avoid oxidation or contamination of the prepared surfaces. The conditioning tests consisted of adding 100 ml of de-ionized water to the mineral mixture in a 250 ml PYREX beaker, with one drop of TECFLOTE S11 delivered from a syringe. The mixture was vigorously stirred using a BARNAT stirrer for 5 minutes. The vigorous stirring was designed to disperse the immiscible collector throughout the liquid mixture, as described by Leja (1983).

After the mixing, the liquid was decanted, and the remaining solids were double-washed in de-ionized water to remove excess collector. A sample of the post-conditioning synthetic ore

consisted of approximately 12 individual grains of each of sulphides and gangue was collected with a needle and transferred to a piece of indium foil for examination by Time of Flight Secondary Ion Mass Spectrometry (ToF-SIMS). The particle selection was performed while the grains were immersed in the wash solution in order to minimize contact with the atmosphere. The wet sample was subsequently introduced into the sample transfer chamber of the TOF-SIMS to avoid oxidation of the mineral grain surface prior to analysis. The water was pumped off in the vacuum chamber of the ToF-SIMS.

In the selective flotation of minerals in a polymetallic ore, copper sulphate is commonly added to activate sphalerite or pyrite surfaces so that the collector will be adsorbed and render the surfaces hydrophobic. To simulate this the conditioning tests were repeated with the addition of copper sulphate at the equivalent concentration of 100 g per tonne of minerals to observe the adsorption of TECFLOTE S11 on Cu activated pyrite surfaces.

### 3.2.2 Micro-flotation Tests

The flotation behaviour of the inherent minerals in a metal sulphide ore, is evaluated from laboratory flotation tests. Where the amount of the ore available is limited, the tests are carried out with a small (approximately 1g) sample in a micro-flotation cell. Where larger samples are available (several kilograms) the tests are performed using various sizes of bench flotation cells.

The micro-flotation tests were performed using a Siwek micro-flotation tube (Figure 3.1.) Micro-flotation is an accepted technique (Hart et al., 2014) to evaluate the links between variable experimental conditions and the recovery of the defined mineral phases. The relative weighted recovery is expressed as the concentration of the element of interest in the floated defined material (concentrate) as a percentage of the concentration of the element of interest in the total weight of the same material used in the test (feed). A metallurgical balance was estimated using energy dispersive X-ray (EDX) analyses of the various flotation products (feed, concentrate and tails), as described below.

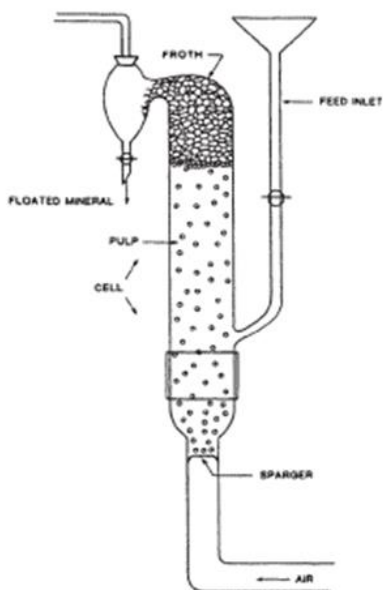


Figure 3.1 Siwek micro-flotation tube. From (Leja, 1982). Reprinted from *Surface Chemistry of Surfaces* (p.46), by S.R. Rao, 2004, Plenum. Copyright Springer Nature 2004. Reprinted with permission.

The Siwek tube is constructed of glass and consists of two parts, the lower gas dispersion unit and an upper enclosed flotation column and concentrate collection bulb. The lower part has an air or gas inlet leading to a frittered glass plate. The column has a feeding tube above the frittered glass plate and a bulb is located at the top of the column into which the floated material runs and is collected.

The tests were carried out using approximately 1g of synthetic ore 2. This synthetic ore was lightly hand-ground in an agate mortar and pestle to create fresh mineral surfaces and mixed with 100ml de-ionized water. The test was repeated at various pH values adjusted to approximately 6.7, 8.1, 9.5 and 10.9 with sodium hydroxide. The slurry was added to a 250 ml PYREX beaker, 1 drop of TECFLOTE S11 was added from a syringe and the slurry vigorously stirred for 5 minutes. The contents of the PYREX beaker were transferred to the Siwek tube, through the feed tube. The liquid level was raised to just below the lip leading to the collection bulb with pH adjusted de-ionized water, and the water level maintained by addition of pH adjusted de-ionized water to replace that entrained in the froth during the tests. The pH was measured using a hand-held CORNING Checkmate 90 pH meter. The meter was calibrated before each test with two buffer solutions at pH 7 and 4 or 10. Air was introduced through the mineral solids sitting on top of the frittered glass plate at a rate of 24.2 ml/sec. The mineral particles that attached themselves

to the air bubbles overflowed into the collection bulb. After 1 minute, the air flow was stopped and the concentrate and tail components were collected.

A small fraction of both flotation products (concentrate and tails) was used for analysis with the ToF-SIMS. The remainder of the concentrate and tails portions were filtered, dried, weighed and analyzed for metal content, using scanning electron microscopy coupled with energy dispersive X-ray spectroscopy (SEM/EDX).

Because TECFLOTE S11 is immiscible with water and only slightly soluble (10%) in acetyl nitrile, it was difficult to vary the concentration of Tecflote S11 used for the tests in this study. The minimum dosage that could be introduced to the mineral sample was one drop administered from a syringe. Even with this small dosage, it far exceeded the relative amounts used in commercial flotation operations. The excessive dosage used with the small mineral samples (1g), may have unanticipated effects on the flotation performance of the tests, as discussed in Chapter 4.

### 3.2.3 Column flotation tests

The only source of turbulence imparted to the mineral sample in a Siwek tube in the micro-flotation tests is from the air flow through the frittered glass plate in the gas diffusion unit of the Siwek tube. The air flow needs to be controlled to prevent the inadvertent reporting of gangue to the concentrate collection bulb. Consequently, the shear forces of a production flotation cell, which contribute to the adhesion and separation of mineral grains to a rising air bubble, cannot be duplicated in the Siwek tube. As TECFLOTE S11 tends to disperse along the air/water interface, a test was designed to allow the TECFLOTE S11 to spread across the air/water interface before the ore was introduced to the air water mix, to compare the adsorption levels of TECFLOTE S11 between the different methods of introducing the collector to the mineral surface.

The gas dispersion unit of the Siwek tube (Figure 3.1), was fitted with an approximately 5.5 cm plastic cylinder to form a 40 ml flotation column. The gas dispersing unit was also fitted with a magnetic stirrer to induce turbulence in the column.

The column was filled with approximately 30 ml of de-ionized water adjusted to pH 9.5 with sodium hydroxide and air introduced at a rate of 105 ml./sec. One drop of TECFLOTE S11 along with two drops of Methyl isobutyl carbinol frother (MIBC) were added by syringe to the vortex of the solution. A 2 g sample of synthetic ore 3 was then added to the solution. De-ionized water with a pH adjusted to 9.5 was sprayed on the top of the mineral laden froth to remove entrained gangue minerals and to raise the liquid level of the froth sufficiently to overflow the lip of the flotation column. A sample of the overflowed froth was collected, with mineral grains selected for ToF-SIMS analysis as per the previously described method. The test was repeated, with the floated concentrate being triple washed with de-ionized water to remove any unabsorbed TECFLOTE S11.

### 3.2.4 Time of Flight Secondary Ion Mass spectrometry (ToF-SIMS)

ToF-SIMS has a proven record of determining species on mineral surfaces towards providing some understanding regarding potential factors linked to the flotation behaviour of minerals in both flotation tests and plant operations. (Chelgani, and Hart, 2014; Smart, et al., 2000)

The ToF-SIMS at Surface Science Western uses a bismuth primary ion beam to bombard the surface of the sample causing the emission of neutral, positively and negatively charged secondary ions from surfaces. A mass spectrum is produced by plotting the secondary ion intensity in counts /sec against the atomic mass of the ions in atomic mass units (amu) (Figure 3.2). The secondary ions are then analyzed using a time of flight mass spectrometer. The measured positive and negatively charged ions are derived from both the matrix of the mineral phase and the various species which are adsorbed on its surface. The ions represent a variety of organic and inorganic components. The typical detection limit for TOF-SIMS is in the low ppm range.

An atomic mass unit or Dalton, is defined as one twelfth of the mass of a <sup>12</sup>carbon atom ([https://www.lexico.com/definition/atomic\\_mass\\_unit](https://www.lexico.com/definition/atomic_mass_unit)).

With this technique the top 1-10 atomic layers of the surface are analyzed without significant destruction of the sample surface. The instrument used in this work was an ION-TOF, TOF SIMS IV, located at Surface Science Western. The data was recorded with full mass spectra in 256 x 256-pixel format using a high current bunched mode  $^{209}\text{Bi}^{3+}$  cluster ion beam. Typically, the ion beam is rastered over the sample for 100 shots with the final spectrum representing a summation of the 100 spectra generated from the region. Charging of the sample was compensated for by using an electron flood gun. Each ToF-SIMS spectrum was calibrated using the atomic weight units of H, C and  $\text{C}_2\text{H}_5$ . An animated clip of a ToF-SIMS may be viewed at <https://www.ifg.kit.edu/img/tofsims.gif>

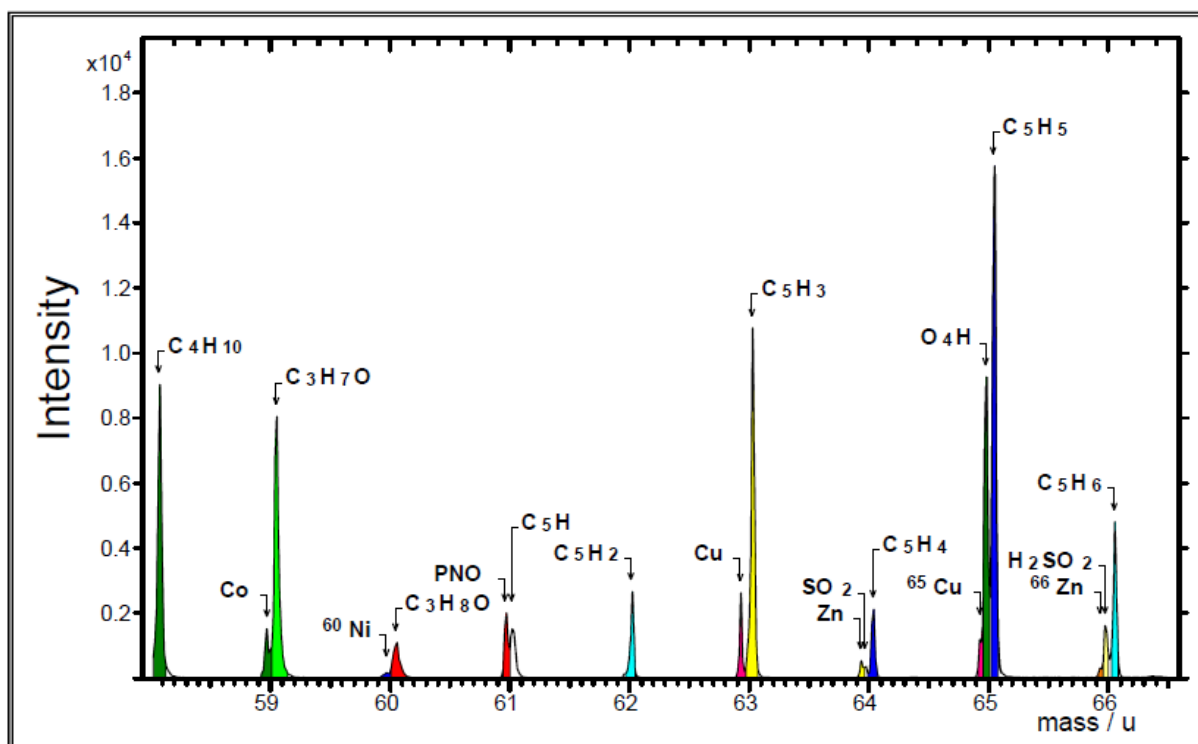


Figure 3.2. Mass spectrum in the region from 58 to 66.5 amu showing the mass positions for various organic fragments and Co, Ni, Cu and Zn along with the isotopes for Cu and Zn. Reprinted from “ACST in Mineral Processing” by B.R. Hart. Unpublished. Reprinted with permission.

The ion beam conditions were:

- Ion source: 25 keV, ion beam: cluster of 3  $\text{Bi}^{3+}$  ions
- Current  $\sim 0.3$  pA
- Pulse: 1ns

- Beam spot size  $\sim 1\mu\text{m}$
- Raster area: generally,  $300 \times 300\ \mu\text{m}$  (variable)
- Mass range 1-850 amu

### 3.2.5 Scanning Electron Microscope-Energy Dispersive X-ray Spectroscopy (SEM-EDX)

The scanning electron microscope with an energy dispersive X-ray system (SEM-EDX) was used to measure the elemental composition of mineral samples. As opposed to the ToF-SIMS, which uses an ion beam to stimulate emission of secondary ions, SEM uses a tungsten filament-based electron gun to stimulate the release of secondary electrons from the sample by rastering the electron beam across the sample surface. These electrons are collected by detectors, allowing the surface morphology to be examined. In this investigation mineral grain evaluation was performed using both secondary electron (SEI) and back-scattered electron (BSE) images.

The interaction of the electron beam with the sample surface also generates X-rays. Energy dispersive X-ray (EDX) spectroscopy uses a silicon drift detector to measure the X-rays emitted from the sample. The data that is generated from the EDX analysis produces a spectrum that contains peaks corresponding to the different elements in the sample. The technique can be used to generate element maps for example Fe and Cu element maps showing the distribution of pyrite (Fe), chalcopyrite (Fe and Cu) grains in the tests performed on the various ores.

The SEM-EDX used in this study was a Hitachi SU 3500 variable pressure tungsten filament SEM coupled with an Oxford X-Max 50 mm X-ray detector located at the Surface Science Western laboratories in London, Ontario. Analyses were performed at an excitation voltage of 15kV, the pressure maintained at 20 Pa and the samples were not coated.

## 3.3 Data Generation and Presentation

### 3.3.1 ToF-SIMS

During the course of the ToF-SIMS analysis, images and spectra are saved with the detailed evaluation of the data performed post analysis. To analyze the data, the images are reviewed and regions of interest (ROI) are selected based on elevated concentrations of the desired element(s) (Figure 3.3). Both positive and negative ion spectra are collected from these ROI and thus represent information from the surface of the grains of interest only. From both the calibrated positive and negative ion spectra intensities of defined peaks are collected. In order to account for variability in ROI size the intensity at each mass position is normalized to the total ion yield generated for that particular ROI.

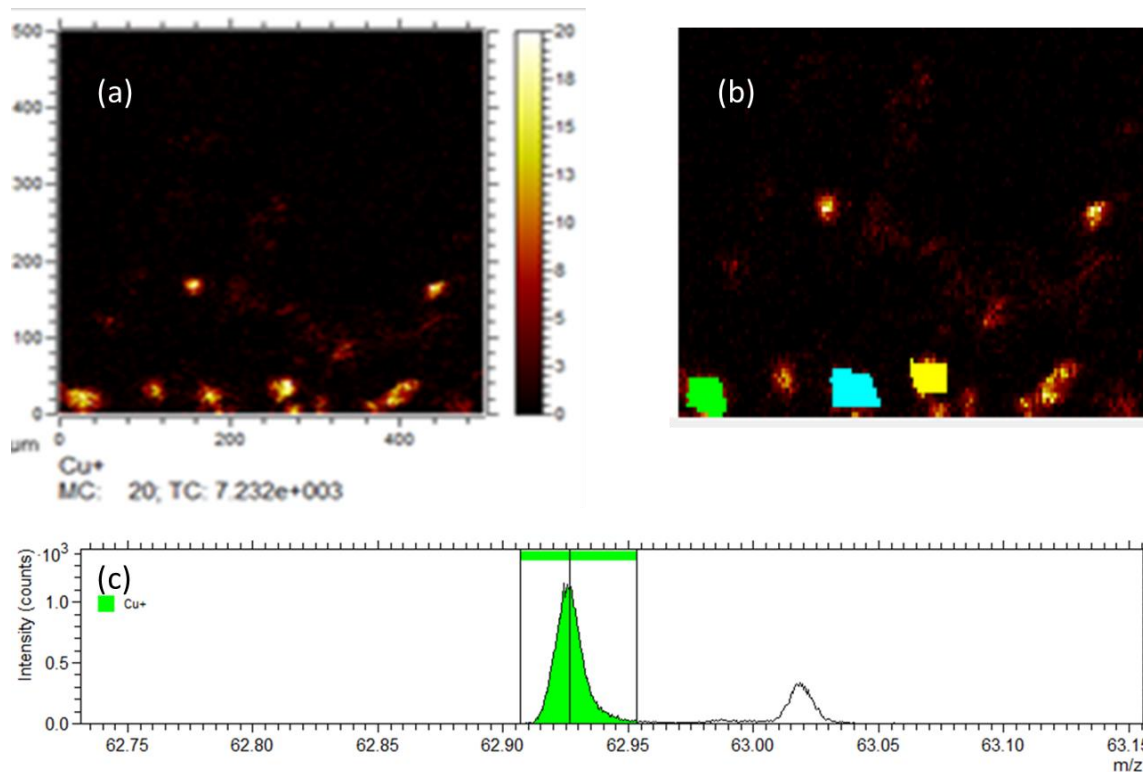


Figure 3.3. ToF-SIMS output: (a) Distribution of Cu<sup>+</sup> ions on grain surfaces; (b) Coloured areas are selected Regions Of Interest; (c) Spectrum of Cu<sup>+</sup> of green ROI.



The software embedded in the ToF-SIMS (SURFACELAB 7) can perform a variety of multivariate statistical analyses on the data generated. Quantification of the ion intensity is not possible using this technique, without the use of matrix matched standards, but the comparison of the intensities of species from a statistically relevant number of regions of interest can provide information regarding the potential factors influencing the flotation characteristics of the mineral phases. The comparison of the normalized intensity is presented as box and whisker plots in the results section of this thesis.

### 3.3.2 TOF-SIMS surface chemistry data presentation

The intensity of selected species, Cu (arbitrary units) in the example below, detected on the grain surfaces (also referred to as a region of interest ROI), as negative ions are presented in vertical box plots (Figure 3.4). All TOF-SIMS data presented (counts) are normalized by the total ion intensity (counts of the recorded total mass spectrum) for the region of interest. The normalization allows for comparison of different sized grains (ROIs).

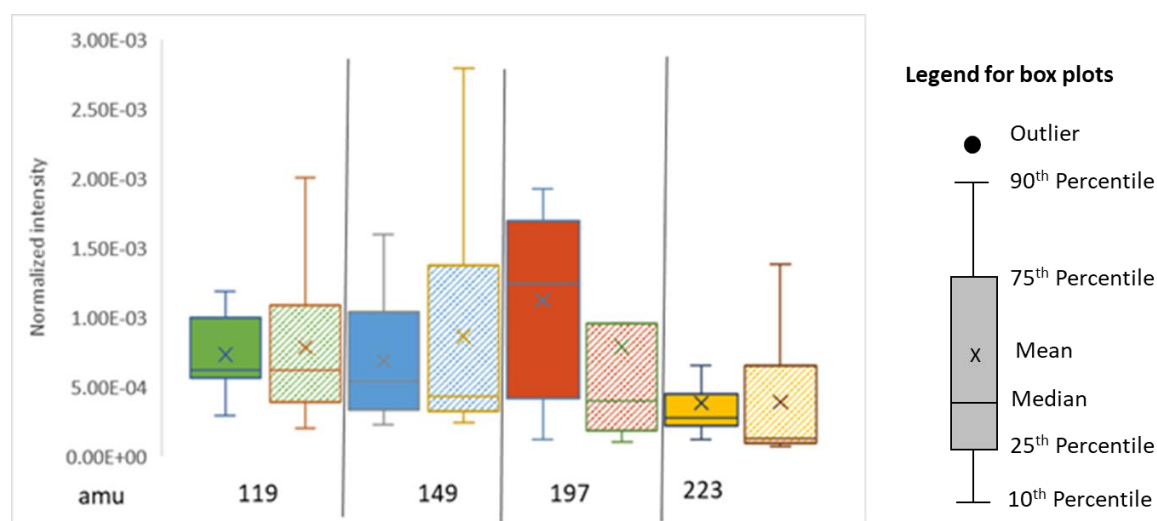


Figure 3.4. Example of box and whisker plot with explanation of the legend displayed on the right.

As the data reflects analysis of the surface from +20 grains the data is typically highly variable. Therefore, for the comparative analysis between test samples, the normalized intensity data, plotted as vertical box plots, illustrates the relative changes in surface specie abundance for the mineral grain examined in the sample. The discussion refers to a relative increase or decrease in measured specie intensity between grains in the test samples. Relative differences in the discussion are based on the **median values** indicated in the figures. It is the opinion of the author that the median values better reflect the data as the mean has a tendency to show greater influence by outliers in the data set. In the vertical box plots, the median is plotted as the solid line across the box whereas the mean is plotted as an X. An illustration of a box plot showing the various components is given above

### 3.3.3 SEM-EDX

In order to evaluate the results of microflotation testing the Scanning Electron Microscope combined with Energy Dispersive X-ray spectrometry, was used to obtain the metal content of the micro-flotation products. After conducting the micro-flotation tests, it was obvious that there was insufficient volume of concentrate to provide a reasonably sized sample for analysis and thus the metal content of the concentrate could not be measured.

To estimate the Cu content of the feed sample it was assumed that the source of copper in the feed to the tests was entirely due to the copper content of the chalcopyrite. This was later confirmed by analyzing pyrite grains in the sample which had no evidence of Cu. Using a stoichiometric amount of 34.6% Cu by weight in chalcopyrite, the Cu content of the feed can be reasonably estimated. Knowing the Cu content of the feed and, by EDX analysis measuring the Cu content of the flotation tailings the Cu content of the concentrate could be estimated and thus the copper recovery of the tests calculated.

To determine the Cu content of the flotation tailings a sample of the tailings from each test was dried, homogenized and a fraction distributed as a single layer on a carbon adhesive disc and analyzed by EDX for its copper content. For the analysis, 6 to 7 regions approximately 300 x 300 microns of the disk were scanned. It was estimated that on the order of 30-40 mineral particles

were analyzed per region and the average of the copper content (Table A49) of the grains taken as an estimate for use in the recovery calculations.

If the copper content of the chalcopyrite differed from the assumed stoichiometric amount, then the same error would be replicated for all tests. As the tests were designed to evaluate the relative recoveries of the desired element (Cu) at the different pH values of the tests, the effects of the assumptions on the conclusions were deemed to be minimal.

A sampling of the EDX results are from the analysis of the flotation tailings is presented in Table 3-3. Full analysis results are shown in Table A50, with average, minimum, maximum values and standard deviation ( $1\sigma$ ).

	O	Na	Mg	Al	Si	S	K	Ca	Fe	Cu	Total
Spectrum 31	52.3	2.4	0.1	5.1	31.4	2.0	2.0		3.4	1.2	100
Spectrum 32	48.6	1.9	0.6	12.2	28.8	1.1	2.1	0.7	3.6	0.5	100
Spectrum 33	52.1	2.6	0.6	5.9	29.0	1.1	3.0	0.9	4.8	0.0	100
Spectrum 34	51.2	1.9	0.5	4.9	30.8	1.9	2.9	0.9	3.8	1.1	100
Spectrum 35	51.7	2.1		5.3	30.7	2.2	2.9	1.0	3.2	1.0	100
Spectrum 36	52.0	2.3		4.8	31.7	1.6	2.5	1.5	2.6	0.8	100
Statistic	O	Na	Mg	Al	Si	S	K	Ca	Fe	Cu	
Max	52.3	2.6	0.6	12.2	31.7	2.2	3.0	1.5	4.8	1.2	
Min	48.6	1.9	0.1	4.8	28.8	1.1	2.0	0.7	2.6	0.0	
Average	51.3	2.2	0.5	6.4	30.4	1.7	2.6	1.0	3.6	0.8	
Standard Deviation	1.4	0.3	0.2	2.9	1.3	0.5	0.4	0.3	0.7	0.5	

Table 3.2 Elemental content of sample of the tailings from micro-flotation test, conducted at pH 6.7, with statistics, as measured by EDX used in estimating the recoveries.

### 3.4 Metallurgical balances

In any metallurgical process, the accounting of weights may be expressed as;

$$F=C+T, \quad (1)$$

Where: F =Total weight of material in the feed.

C= Total weight of material reporting to the concentrate (valuable product)

And T= Total weight of material reporting to the tailings (valueless or rejected product)

(Pryor, 1965)

The metal balance for any metal in the process, may be expressed as

$$F_f = C_c + T_t \quad (2)$$

Where, f, c and t are the metal values of the feed, concentrate and tailings, respectively, in appropriate units (Pryor, 1965). Note: For this thesis, where required, EDX analysis was used to estimate the Cu contents of the test samples, rather than chemical assays.

The efficiency of the process, is referred to as the recovery, in other words, the amount of the desired mineral reporting to the concentrate as a percentage of the amount of the desired mineral in the feed to the process as a percentage

From formula (2), the recovery of the valuable metal may be calculated as;

Recovery =  $C_c/F_f$  %.

Example where not all values are known.

#### **Known values:**

Measured weight of feed	1.012g
Measured weight of chalcopyrite in feed	0.059g.
Measured weight of filtered and dried tailings	0.846g.
% Cu in tails estimated from EDX analysis	0.76%

#### **Calculations:**

Weight of Cu in Feed       $0.059 * 0.346 = 0.020414g$  where 34.6% is the stoichiometric percentage of Cu in chalcopyrite.

Weight of Cu in Tails  $0.846 \times 0.0076 = 0.00643\text{g}$

Weight of Cu in Concentrate = Weight of Cu in Feed – Weight of Cu in Tails =  $0.020414 - 0.00643 = 0.014122\text{g}$

Recovery (not corrected for mass of material recovered into the concentrate) = Weight of Concentrate \* % Cu in concentrate / Weight of Feed \* % Cu in Feed =  $(0.166 \times 0.0853 / 1.012 \times 0.0206) \times 100 = 68.71\%$

Weighted Recovery (corrected for mass of material recovered into the concentrate) = Mass of concentrate x weight% of Cu in Concentrate / Mass of feed x weight% of Cu in Feed =  $(0.166 \times 0.0141 / 1.012 \times 0.0203) \times 100 = 11.25\%$

And Concentrate grade = Weight of Cu in concentrate / Weight of concentrate =  $0.014122 / (1.012 - 0.846) = 0.0141 / 0.166 = 8.53\%$

### 3.5 References

Chehreh Chelgani, S. and Hart, B. (2014). TOF-SIMS Studies of Surface Chemistry of Minerals Subjected to Flotation Separation. *Minerals Engineering*, 57, 1–11.

Greet, C.J., Kinal, J., Steiner, P. (2005). Grinding Media-Its Effect on Pulp Chemistry and Flotation Behaviour-Fact or Fiction? In *Centenary of Flotation Symposium* (pp. 697–971).

Hart, B.R., Dimov, S., Xia, L. (2014). REE bearing mineral recovery: a microflotation and surface chemistry study using hydroxamate collectors and citric acid. In *IMPC 2014*.

Hart, B. (2011). ACST in Mineral Processing.

Konigsmann, K. V. (1973). Aeration in Plant Practice. In *Proc. 5th Annual Meeting, Can. Min. Processors* (pp. 299–332). Ottawa.

Leja, J. (1982). *Surface Chemistry of Froth Flotation* (First). New York: Plenum.

Leja, J. (1983). *On the Action of Long Chain Amines in Potash Flotation*. (R. M. McKercher, Ed.). Toronto: Pergamonn Press.

Pryor, E. J. (1965). *Mineral Processing* (3rd.). London: Elsevier Publishing Co. Ltd.

Smart, R.St.C, Jasieniak, M., Prince, K.E., Skinner, W. M. (2000). SIMS studies of oxidation mechanisms and polysulfide formation in reacted sulfide surfaces. *Minerals Engineering*, 13, 857–870.

## 4. Results and Discussion.

The results from the various tests described in Chapter 3 are discussed within the general thesis objective, to better understand the role of the collector TECFLOTE in the flotation recovery of the sulphide minerals chalcopyrite and pyrite. A detailed evaluation of the results will be used to develop a model of the mechanism by which the aliphatic nitrile TECFLOTE S11 is delivered to the surface of the sulphide minerals.

To determine the intensity of the TECFLOTE S11 that existed on mineral grain surfaces, a spectral fingerprint of TECFLOTE S11 was prepared by depositing small several drops of the reagent on a silicon wafer and then analyzing it by ToF-SIMS; +ve and -ve ion spectra were recorded. A sample of the -ve ion spectra of TECFLOTE S11 is shown below in Figure 4.1 The spectra of the TECFLOTE S11 exhibited 5 peaks with the most intense peak at the center of a group of peaks. The first group of peaks is centered at 118.98 amu. Subsequent groups of peaks occur at intervals of approximately 15 amu, suggesting a loss of  $\text{CH}_3$ , with decreasing intensity at higher amu. For purposes of this research; to evaluate the adsorption of TECFLOTE S11 on sulphide mineral surfaces, only four peak groupings were used to illustrate the test results. The groups were numbered for ease of reporting as listed in Table 4.1. This nomenclature is used throughout the thesis and in the data tables in Appendix 1. The spectra from the mineral grain analyses were compared to the reference TECFLOTE S11 spectra to determine the presence of the reagent and the variability of its intensity on the mineral surfaces. The mean TECFLOTE S11 normalized ion intensity at amu 119 on the micro-flotation concentrate is in the order of  $1.15 \times 10^{-3}$  compared to  $3.96 \times 10^{-6}$  on the tailings. The typical detection limits for TOF-SIMS are in the low ppm range.

<b>Name</b>	<b>Actual AMU</b>	<b>Nominal AMU</b>
*TECFLOTE 1	118.99	119
TECFLOTE 2	133.8	133
*TECFLOTE 3	148.99	149
TECFLOTE 4	162.89	163
TECFLOTE 5	176.98	177
*TECFLOTE 6	196.93	197
TECFLOTE 7	208.96	209
*TECFLOTE 8	223.03	223

Table 4.1 TECFLOTE S11 labels and associated amu. \* denotes spectrum used for illustrative purposes.



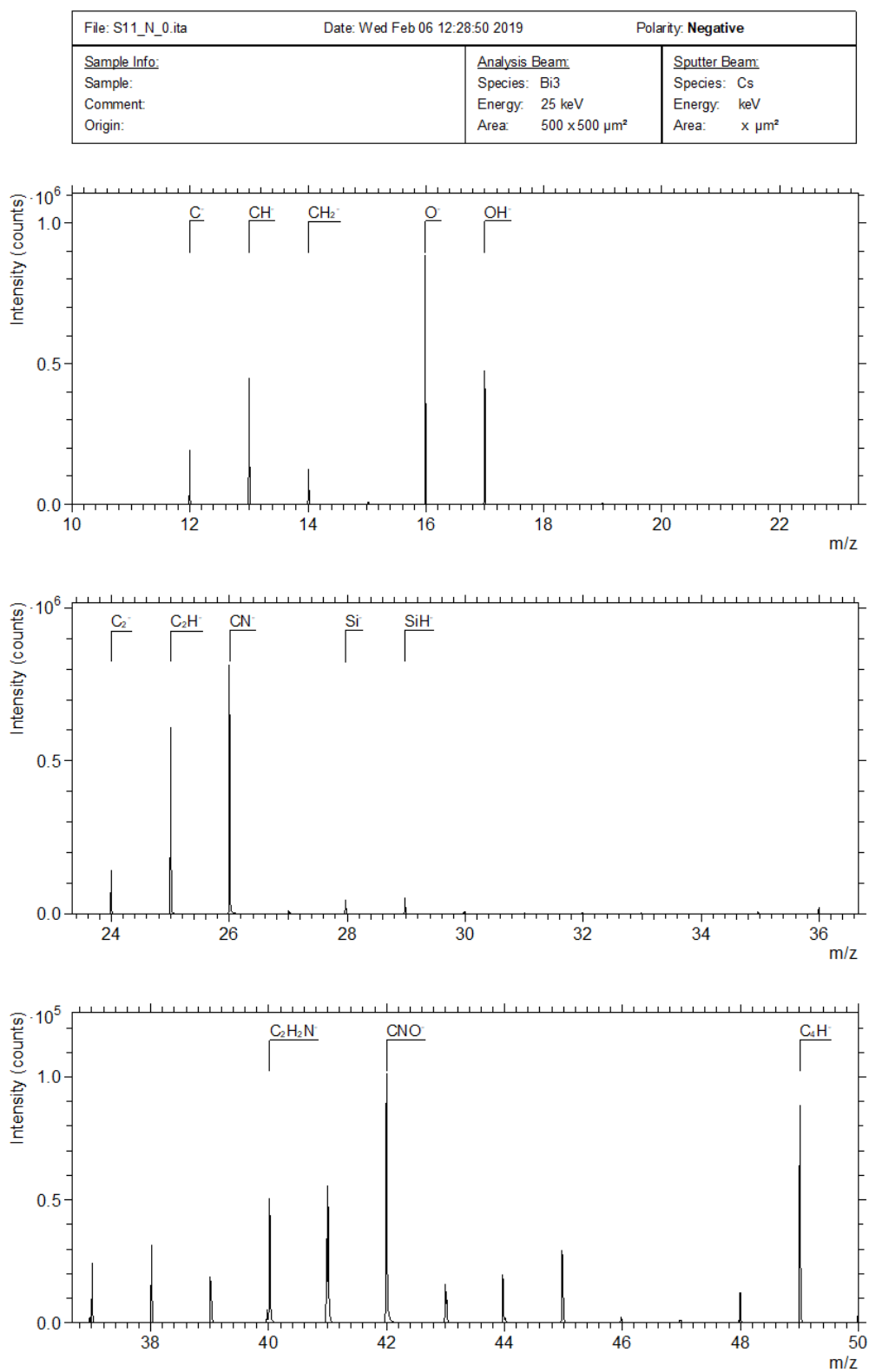


Figure 4.1 (a) ToF-SIMS spectra of TECFLOTE S 11 showing negative secondary ion fragments between amu 0 and 50

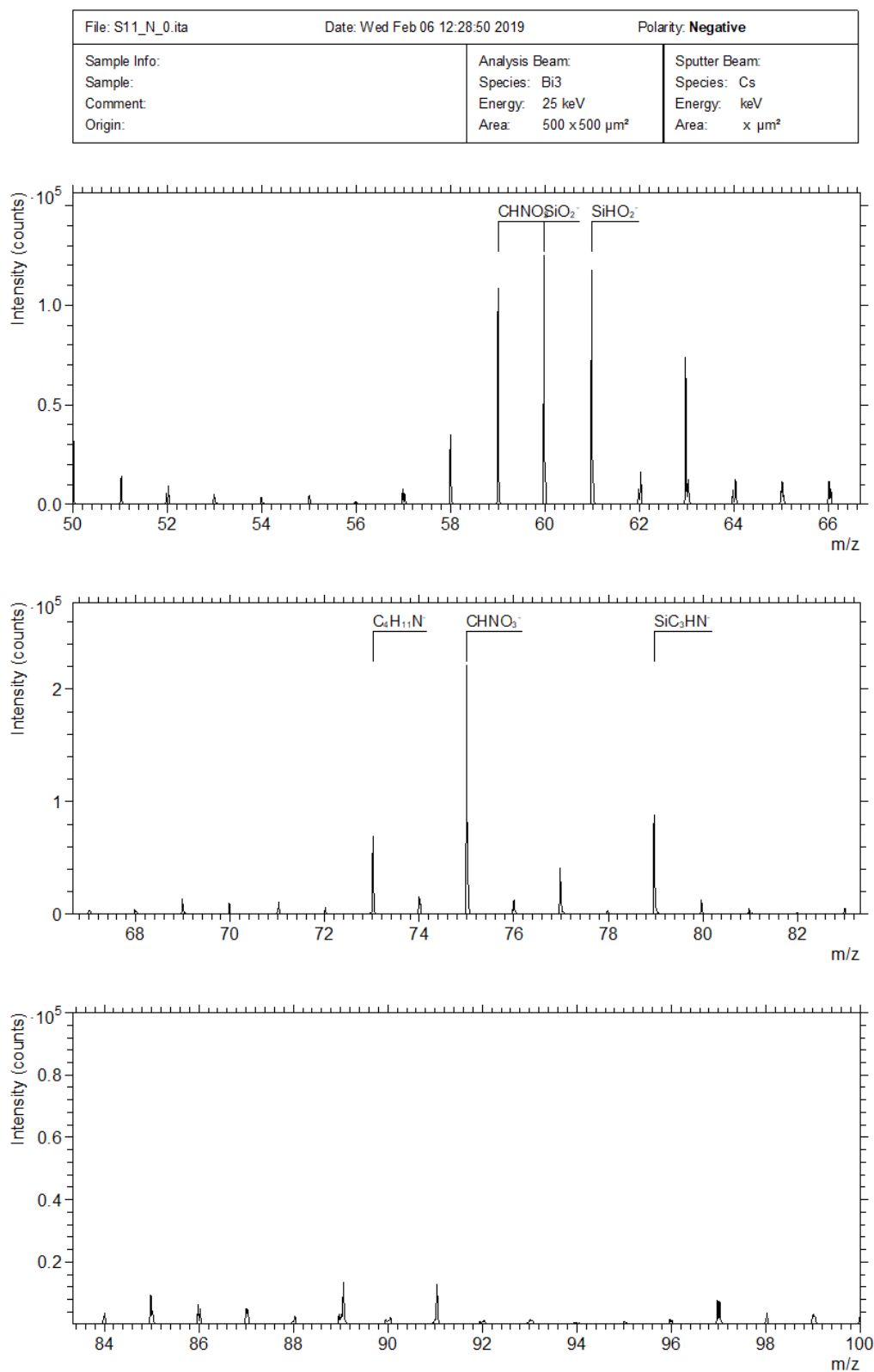


Figure 4.1 (b) ToF-SIMS spectra of TECFLOTE S 11 showing negative secondary ion fragments between amu 50 and 100

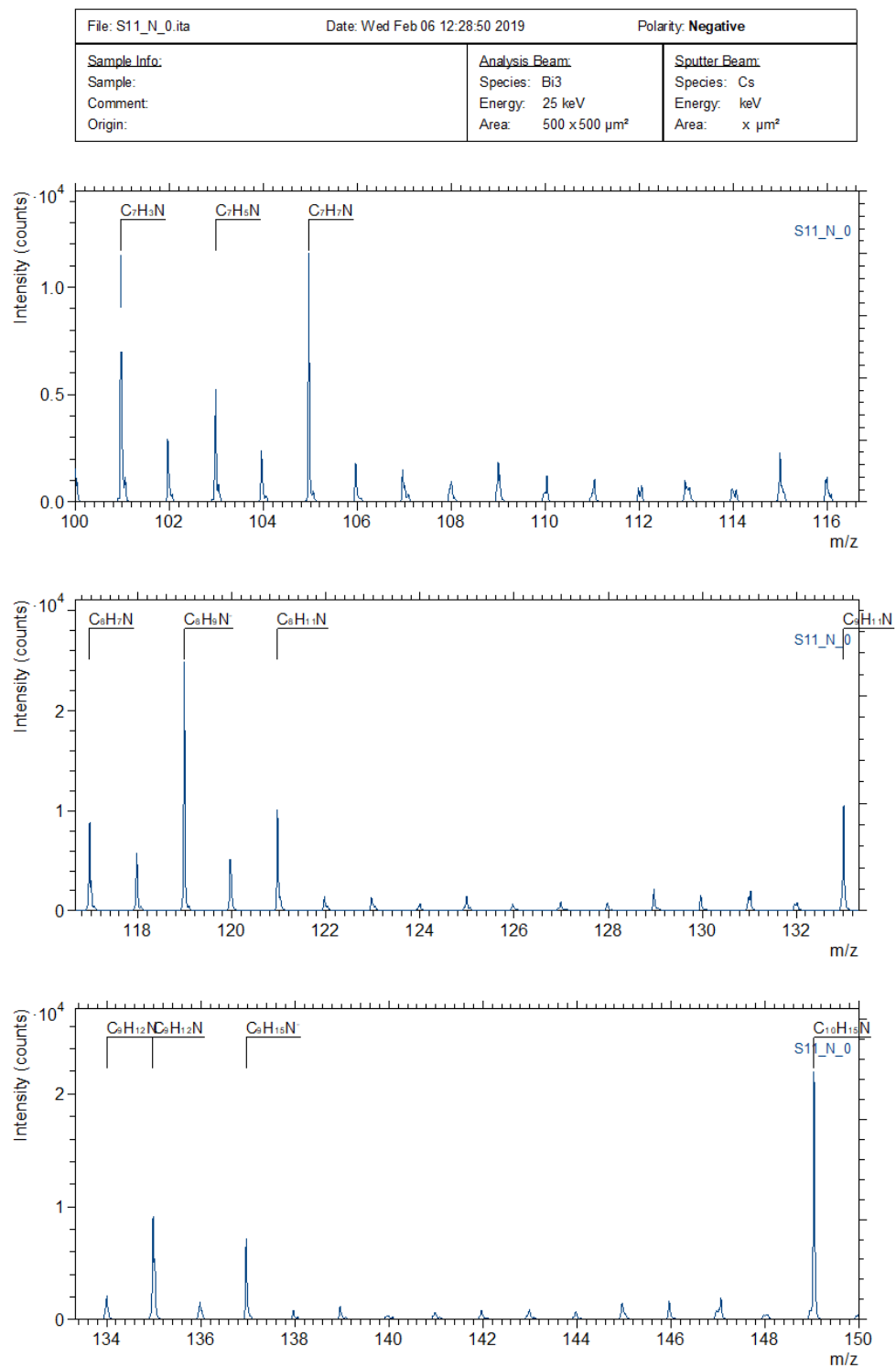


Figure 4.1 (c) ToF-SIMS spectra of TECFLOTE S 11 showing negative secondary ion fragments between amu 100 and 150

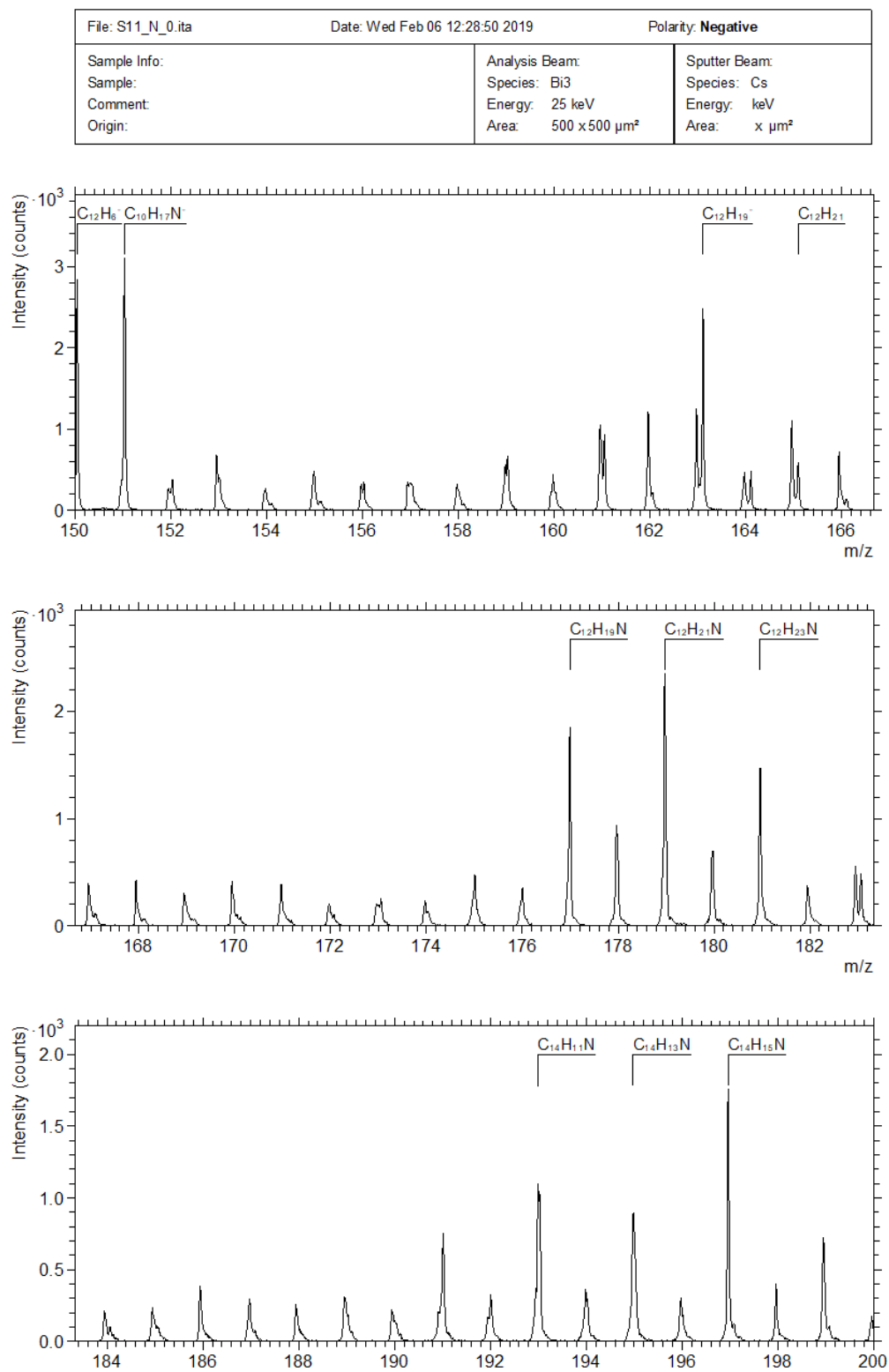


Figure 4.1 (d) ToF-SIMS spectra of TECFLOTE S 11 showing negative secondary ion fragments between amu 150 and 200.

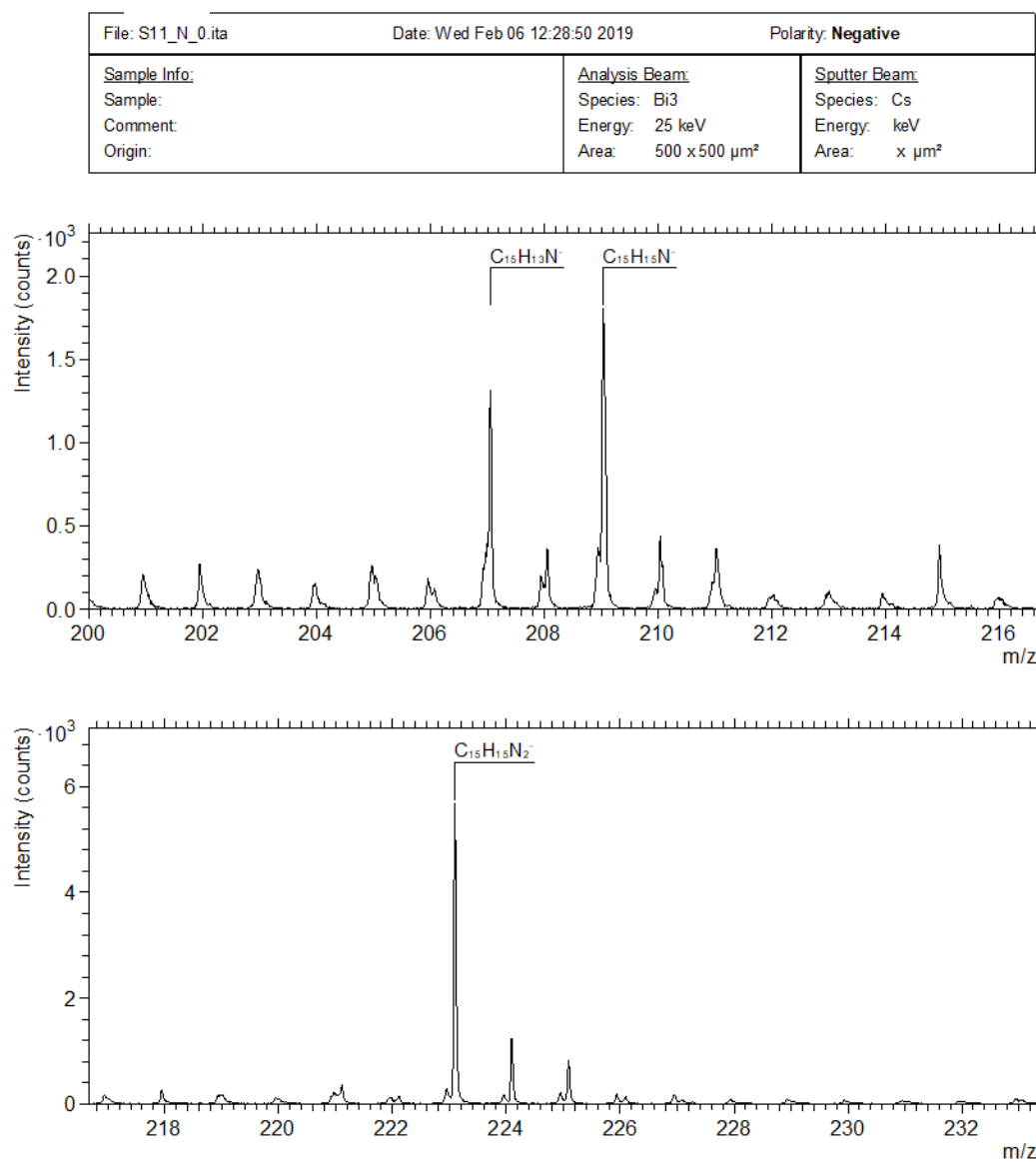


Figure 4.1 (e) ToF-SIMS spectra of TECFLOTE S 11 showing negative secondary ion fragments between amu 200 and 233.

## 4.1 Experimental results

### 4.1.1 Conditioning tests

In flotation using xanthates as collectors, it is common ore-milling practice to mix the ground ore slurry with the collector, pH modifier, frother(s) and non-value mineral depressants prior to introducing the slurry to the flotation banks. This approach, known as conditioning, has been shown to increase both the selectivity and recovery of sulphide minerals from a polymetallic ore (Konigsmann, 1973).

A synthetic ore 1 consisting of ground chalcopyrite, pyrite and gangue minerals was conditioned with de-ionized water and TECFLOTE S11, as described in Chapter 3 was used to emulate this processing approach. The mixture was vigorously stirred to ensure that the TECFLOTE S11 collector was well adsorbed along the air/liquid interface. The requirement for vigorous stirring was identified by Leja (1983), who observed that where amine collectors were introduced to a potash ore slurry without stirring, the amine was not adsorbed on the mineral surfaces even after 36 hours, but that adsorption occurred almost instantaneously with vigorous stirring.

In this study the slurry was allowed to settle after 5 minutes of conditioning, the supernatant liquor decanted and the solids were double-washed with de-ionized water to remove any collector that was not adsorbed onto the mineral surfaces. A sample of the conditioned mineral particles was mounted on indium foil and introduced into the ToF-SIMS where surface analysis of individual mineral particles was performed.

A comparison of the TECFLOTE S11 adsorbed on the chalcopyrite and pyrite grains for selected TECFLOTE S11 ion spectra is shown in Figure 4.2. Surface analysis of the pyrite and chalcopyrite grains from the conditioning tests indicate that the normalized intensity of TECFLOTE S11 markers are higher on the surface of the chalcopyrite

relative to the pyrite (Figure 4.2). The data indicates that the TECFLOTE S11 favours attachment to the surface of chalcopyrite over pyrite.

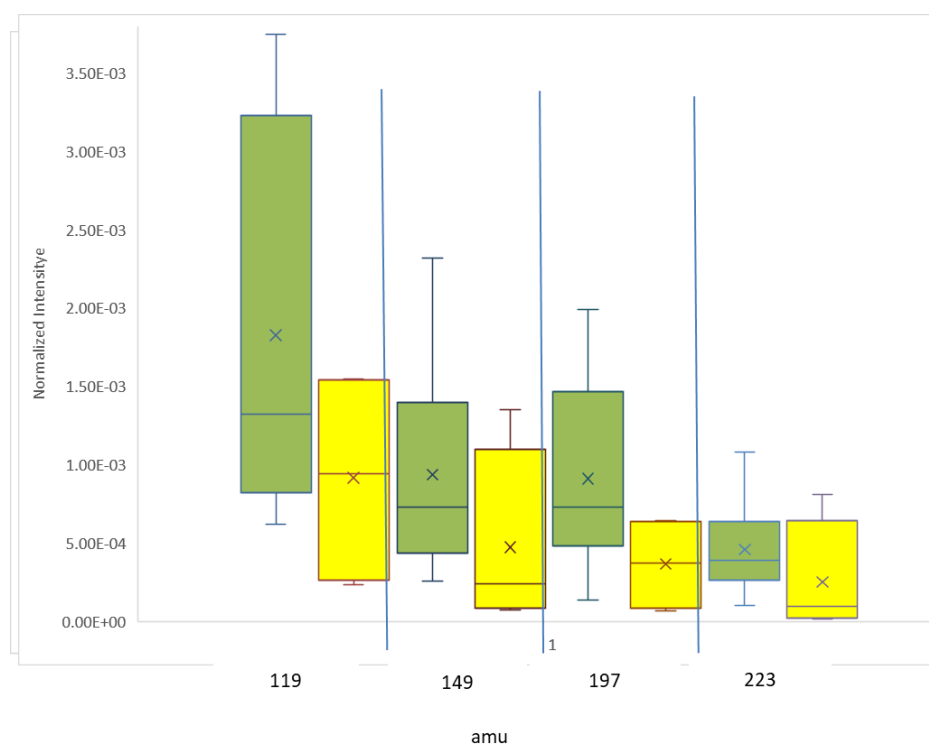


Figure 4.2. Box plots showing normalized intensity for mass positions identified as representative of TECFLOTE S11 on Chalcopyrite (green bars) and Pyrite (yellow bars). Explanation of the Box and whisker legend is found in section 3.3.2

Although the selectivity of TECFLOTE S11 towards chalcopyrite has been established, it is necessary to determine if the observed increased intensity of the TECFLOTE S11 identifier mass positions are truly indicative of the collector or some other compound that developed on the surface of the chalcopyrite during the test. To this end, the conditioning tests were repeated without the addition of TECFLOTE S11 to the slurry and the surfaces of chalcopyrite grains was examined by ToF-SIMS. The results are presented below in Figure 4.3.

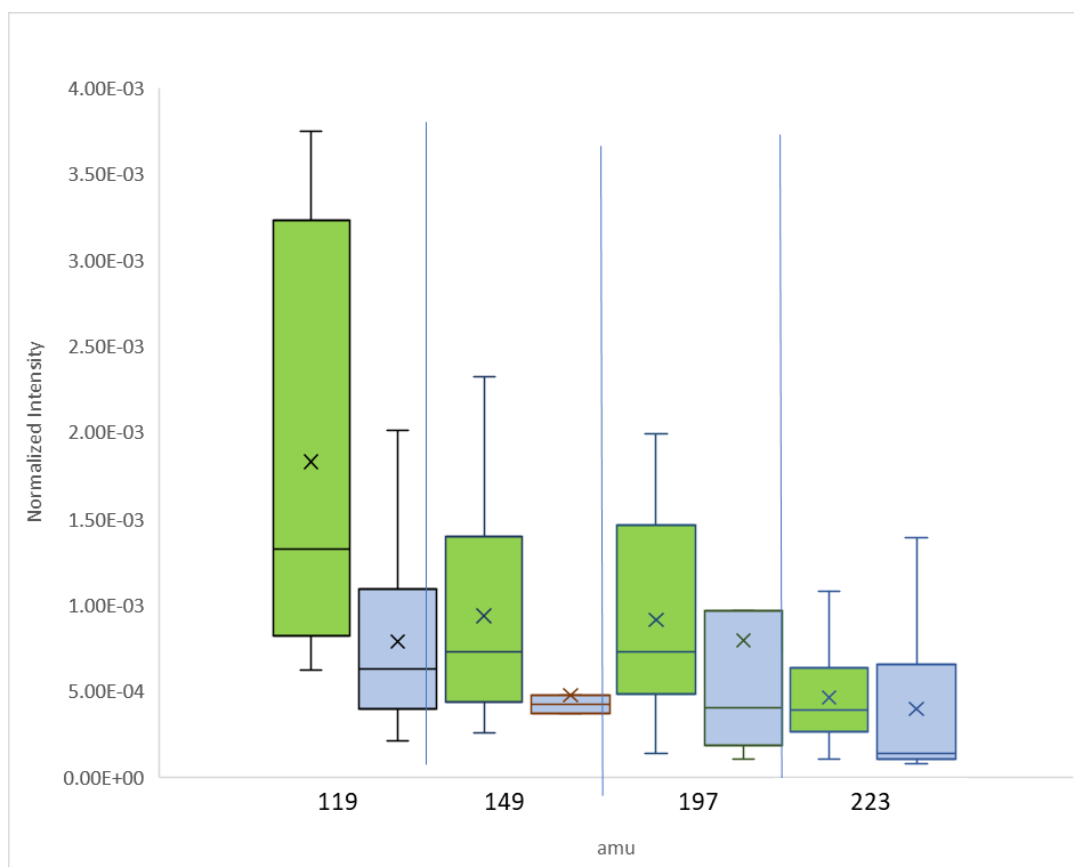


Figure 4.3. Box plots showing the normalized intensity of negative ion mass positions indicative of TECFLOTE S11 on chalcopyrite grains from conditioning tests performed with TECFLOTE (green) and no TECFLOTE S11 chalcopyrite (blue).

The higher normalized intensities of TECFLOTE S11 on the conditioned chalcopyrite particles relative to the unconditioned chalcopyrite (Figure 4.4) indicates that at the mass positions identified for TECFLOTE S11, there is a higher adsorption of the TECFLOTE S11 on the chalcopyrite surfaces that were conditioned with the TECFLOTE S11 than where there is no TECFLOTE S11 added to the mineral slurry. The comparison data (Figure 4.4) illustrates that, at the mass positions used to identify TECFLOTE S11, the increase in intensity reflects surface adsorption of the collector rather than a surface alteration that was generated during the tests.



Where xanthates are used as collectors, pyrite may be rendered hydrophobic by the surface adsorption of Cu ions either by transfer from Cu sulphides or the addition of copper sulphate to the slurry. The Cu ions act as an activator for pyrite to which the xanthate will attach. To investigate whether a similar phenomenon will be observed with TECFLOTE S11 as the collector, the conditioning tests were repeated with the addition of 100g/tonne of  $\text{CuSO}_4$ .

The surface analysis results from these tests are shown in Figure 4.4.

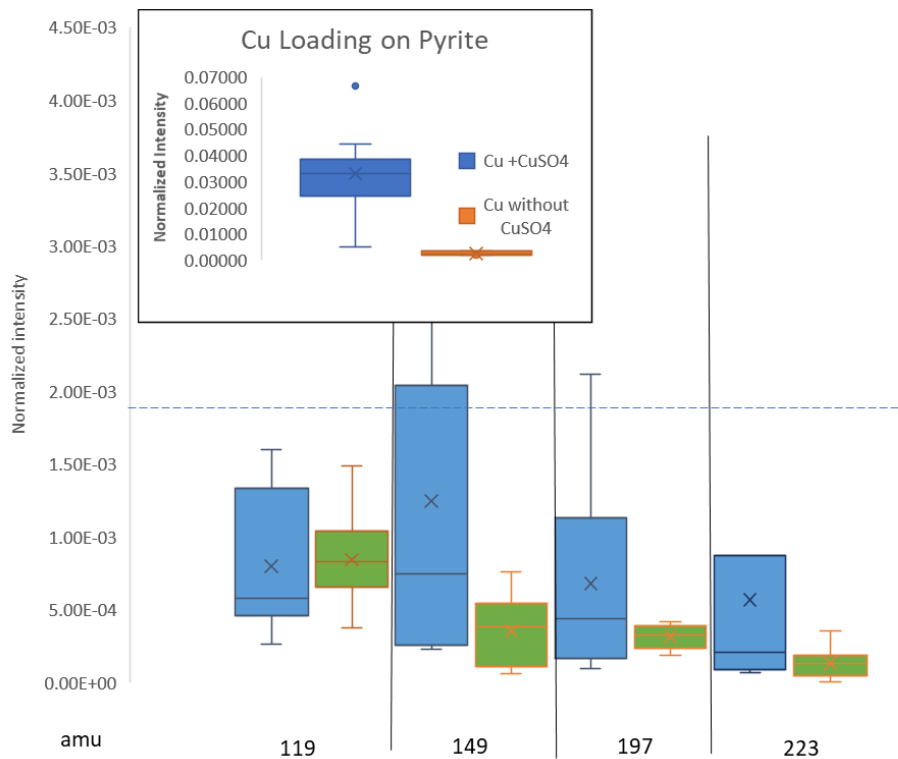


Figure 4.4. Box plot of TECFLOTE S11 ion intensities on pyrite grains with (green) and without  $\text{CuSO}_4$  (blue) TECFLOTE S11 conditioning. Inset. Box plot of copper ion intensity on pyrite grains with  $\text{CuSO}_4$  conditioning and without conditioning. The horizontal blue dashed line shows the approximate average normalized intensity of TECFLOTE S11 (amu 119) on the surface of TECFLOTE S11™ conditioned chalcopyrite.

The median intensity of TECFLOTE S11 on the pyrite grains at 119 amu is higher if  $\text{CuSO}_4$  is present, whereas for the other peak positions indicative of TECFLOTE, the intensity without the  $\text{CuSO}_4$  addition appears higher on the pyrite grain surfaces. The data for the adsorption of TECFLOTE S11 on the pyrite surfaces is inconclusive and the addition and surface adsorption of Cu ions may or may not be facilitated by TECFLOTE S11, as seen for the adsorption of xanthate collectors. This could have ramifications in the processing of polymetallic ores, where  $\text{CuSO}_4$  is used to promote selectivity between the copper and other metal sulphides, such as sphalerite

#### 4.1.2 Column tests

Leja and Schulman (1954) proposed that for mineral flotation to occur the xanthate collector is not only adsorbed onto the mineral surface from the collector dispersed in the slurry, but also from the surface of the bubble. To test the relevance of their proposed theory in the context of TECFLOTE S11, column tests were designed to introduce the TECFLOTE S11 to the air/liquid interface before the bubbles were in contact with the mineral surfaces.

Schach et al. (2019) used a KAI Ultra Turrax system to conduct qualitative flotation tests on a mixture of chalcopyrite, pyrite and quartz. The KAI Ultra Turrax system allowed the TECFLOTE S11 to be added to the airflow instead of the material slurry. However, from these tests it was not possible to determine if the hydrophobic surface of the chalcopyrite was caused by direct adsorption of the TECFLOTE S11 on the chalcopyrite from solution or was imparted by the particle-bubble contact from the liquid-air interface.

Because of the closed design of the Siwek tube (Chapter 3, Figure 3.3), the collector is introduced into the mineral slurry through a feeding tube, which is located above the location where air is introduced into the mineral/liquid mixture. In order to allow for immediate contact of the air with the mineral slurry, the air dispersion unit at the bottom of the Siwek tube was removed and fitted with an open-ended plastic tube. The length of

the tube was chosen to allow a froth column to build above the frittered glass plate. Full description of the modifications and tests are presented in Chapter 3.

As soon as the synthetic ore 3 was added to the TECFLOTE S11 charged air-water vortex in the column, the separation of the chalcopyrite from the other minerals was visually apparent. An optical examination of the floated material, using a binocular ZEISS optical microscope, showed that the floated “concentrate” was mainly chalcopyrite. A detailed chemical assessment of the degree to which the Cu in the concentrate was upgraded however, was not performed. Floated chalcopyrite grains collected from the froth in the column were analyzed by TOF-SIMS. The grains that were immediately extracted from the froth are compared to those which were washed with de-ionized water on Figure 4.5.

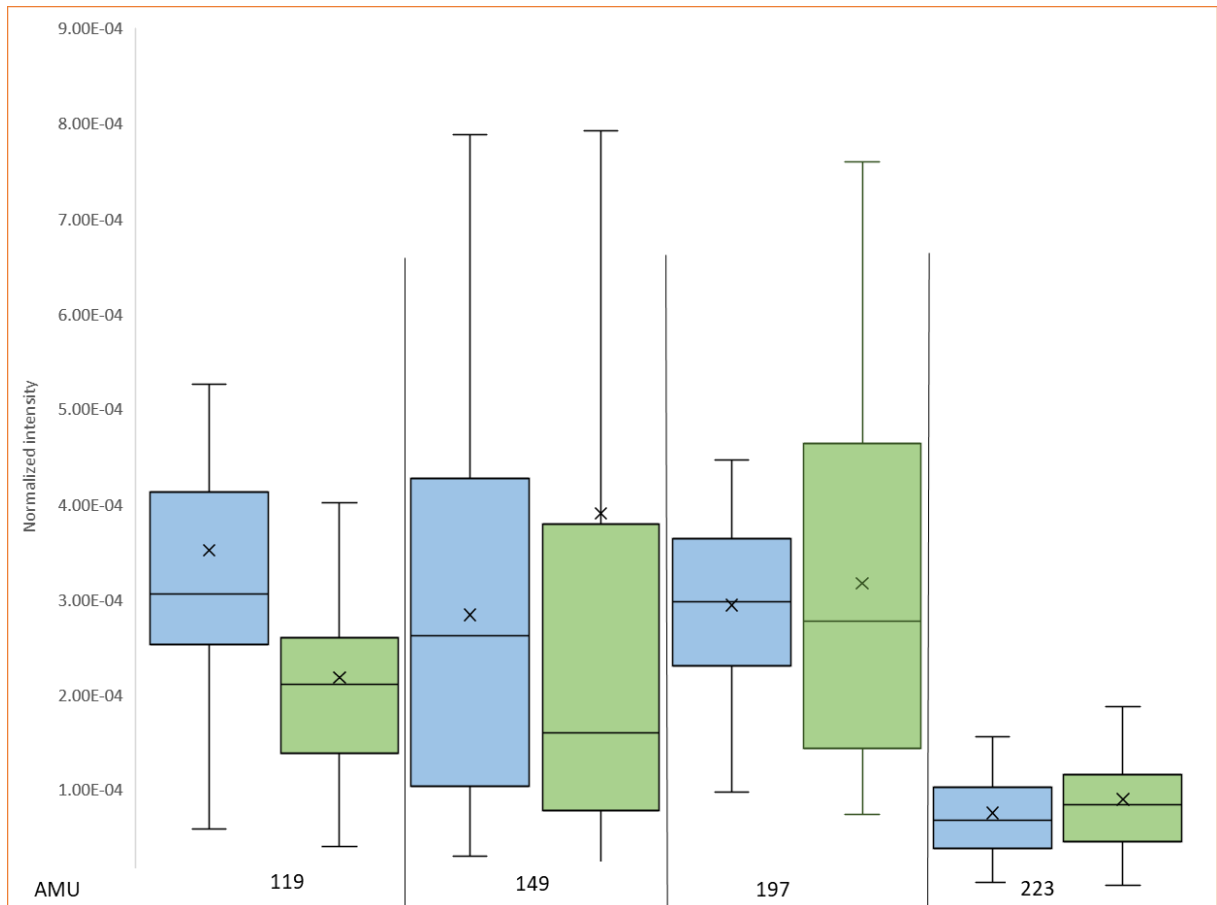


Figure 4.5. Comparison of TECFLOTE S11 intensity on chalcopyrite grains from column flotation tests. Before (blue) and after washing (green)

The TECFLOTE S11 ion intensity on the chalcopyrite particles was higher in the tests where the floated particles were not washed (blue), than where the particles were washed (green) to remove TECFLOTE S11 that was not adsorbed onto the chalcopyrite surfaces (Figure 4.5). With the exception of mass 223, the median values for each TECFLOTE S11 ion intensity fragment is higher for the unwashed particles than the washed particles. The spread between the 1<sup>st</sup> and 3<sup>rd</sup> quartile values is approximately the same for each pair of tests (washed and unwashed), infers that flotation was achieved in response to the adsorption of TECFLOTE S11 on the chalcopyrite. Given the hydrophobic nature of the

TECFLOTE S11 and that it is immiscible in water (Schach et al., 2019; Lewis et al, 2018), the transfer to the mineral particle surface was most probably from contact with the surface of air bubbles loaded with TECFLOTE S11.

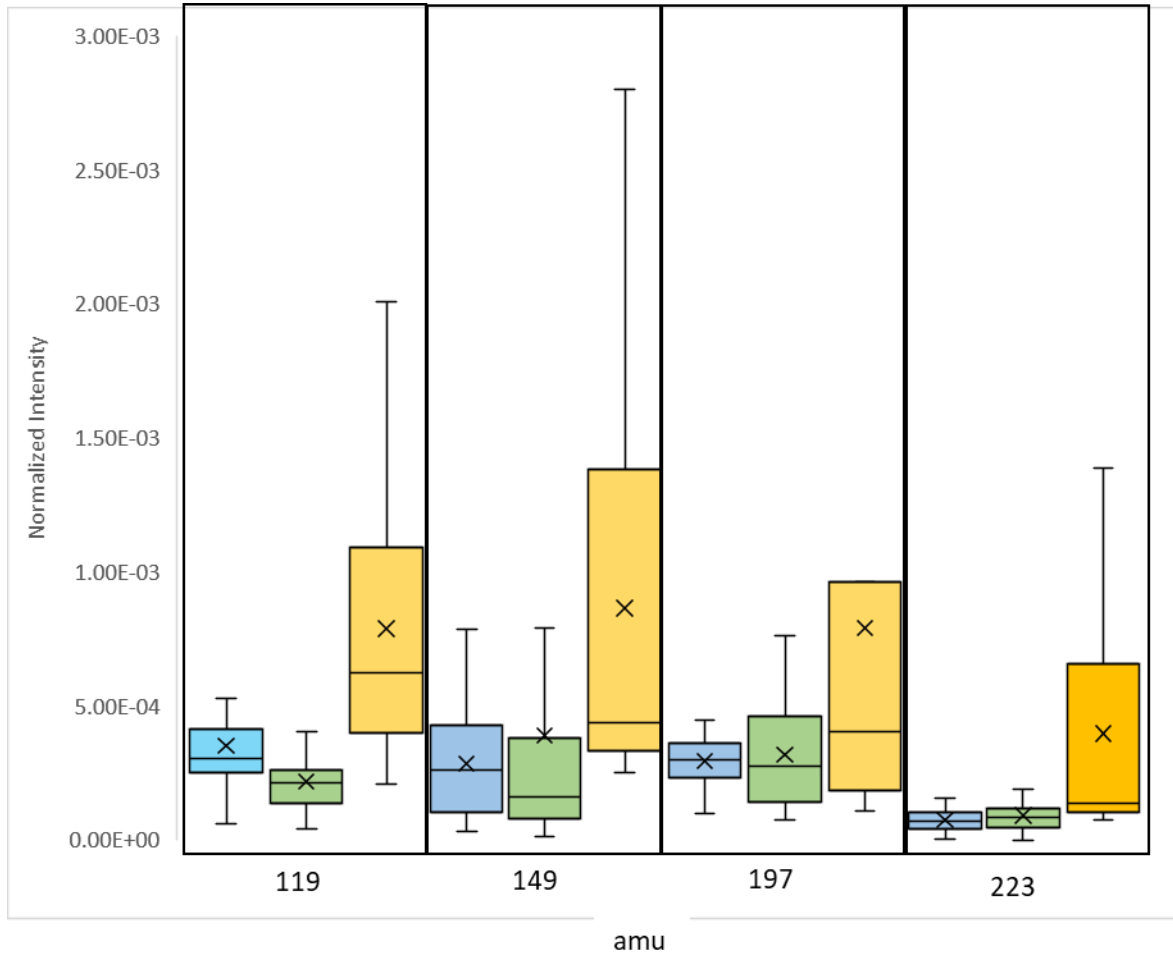


Figure 4.6. Comparison of TECFLOTE S11 intensities obtained in column flotation tests, before washing (blue) and after washing (green) with conditioning tests (yellow).

The column test results show that TECFLOTE S11 is adsorbed onto the chalcopyrite surfaces but at a lower intensity than in the conditioning tests (Figure 4.6). The fact that TECFLOTE S11 is immiscible in water and is adsorbed on the floated chalcopyrite grains suggests that the transfer of the reagent to the mineral surface is likely by particle bubble contact (Leja and Schulman, 1954). TECFLOTE S11 thus acts in a manner

similar to the adsorption of immiscible amine collectors in potash flotation (Burdukova and Laskowski, 2009). The lower adsorption of TECFLOTE S11 through the column tests may be due to the length of time that the mineral surfaces were in contact with the TECFLOTE S11; 5 minutes for the conditioning tests compared to 1 to 2 minutes for the column tests.

#### 4.1.3 Micro-flotation tests

Micro-flotation tests at pH values of 6.7, 8.1, 9.5 and 10.9 were performed to evaluate the relationship between the adsorption of TECFLOTE S11 on chalcopyrite and the metallurgical performance as measured by the recovery, as described in Chapter 3. The minerals recovered from the flotation tests were examined by ToF-SIMS to determine the surface intensity of TECFLOTE S11. Metallurgical balances from the flotation tests were calculated, as per the method outlined in Chapter 3 and are summarized in Table 4.2

pH	Calculated Feed Grade % Cu	Mass recovery con (%)	Mass recovery tail (%)	Calculated grade % Cu	Calculated % Cu recovery	Weighted % Cu recovery
6.7	2.03	16.4	84.6	8.5	68.7	11.3
8.1	2.05	25.2	75.6	4.5	55.1	13.8
9.5	2.03	17.1	84	8.7	72.2	12.2
10.9	2.06	5.2	95.6	33.8	83.9	4.3

Table 4.2. Metallurgical results from the microflotation tests.

Mass recovery of the concentrate, tails and the calculated Cu grade and recovery for the microflotation test samples performed at the four different pH values are given in Figure

4.7. The data shows that the Cu grade in the samples is highest at pH 10.9, where only a small fraction of the feed sample was collected as a concentrate (5.2%), and lowest at pH 8.1 where close to 25% of the feed sample reported to the concentrate.

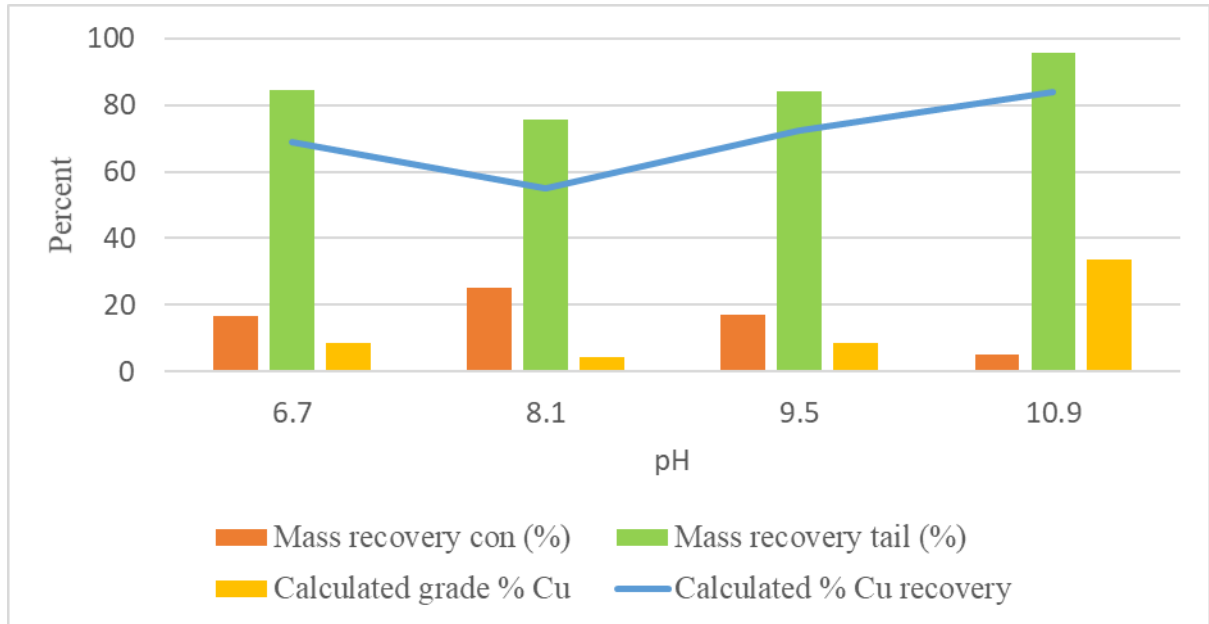


Figure 4.7. Mass recovery of the concentrate and tails, the Cu grade and the non-mass corrected Cu recovery for the microflotation test samples performed at four different pH's.

The TOF-SIMS results from the analysis of flotation concentrates and tails grains are given in Figure 4.8. With the exception of mass positions 149 amu at pH 6.7 and 223 amu at pH 9.5, the TECFLOTE S11 intensities were overall higher on ore particles reporting to the concentrate, or floated material, relative to those from the tailings or residue. (Figure 4.7). This difference in TECFLOTE S11 intensity displayed between the grains from the concentrate relative to those from the tails was more pronounced in the tests performed at low pH.

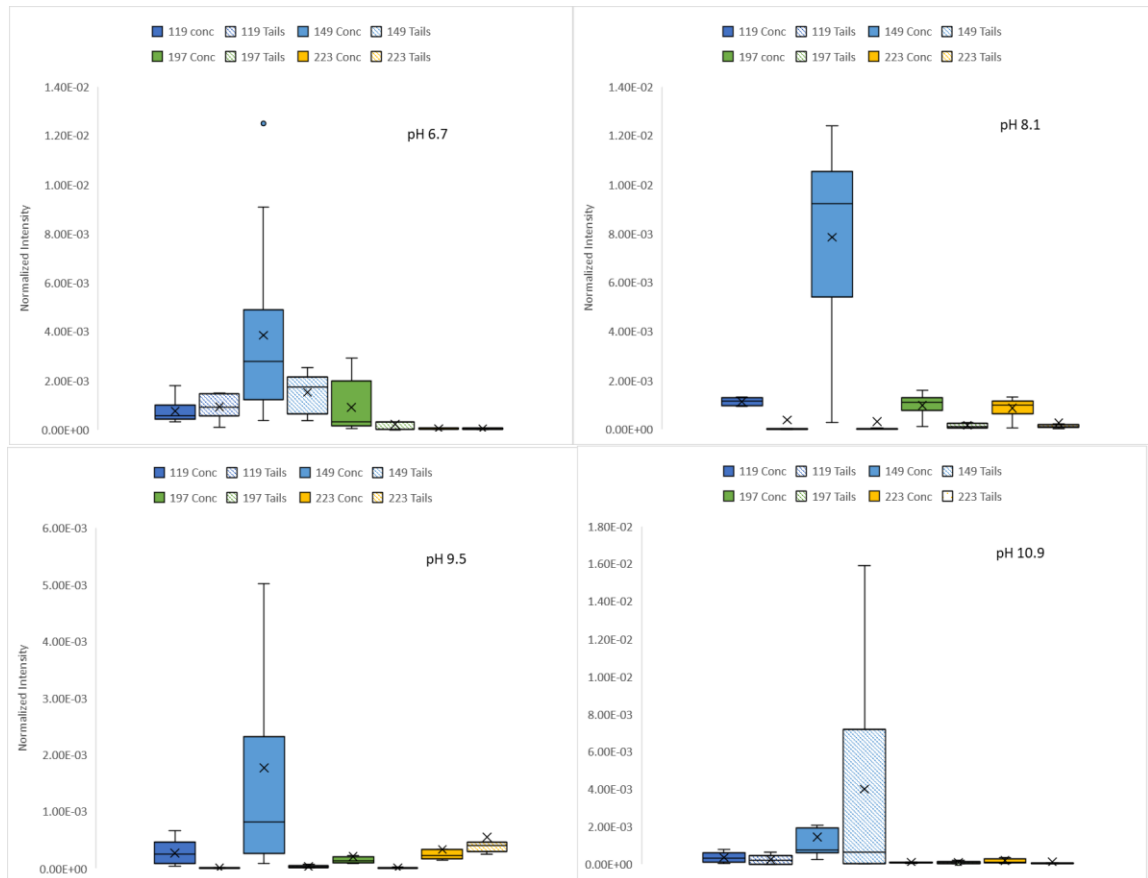


Figure 4.8. TECFLOTE S11 ion intensities on concentrate and tailings portions from micro-flotation tests at (a) pH 6.7, (b) pH 8.1, (c) pH 9.5 and (d) pH 10.9.

To understand the interaction of the Cu recovery in relation to mass recovery, the weighted recovery was calculated (Table 4.2) and is shown in Figure 4.9. The calculation includes the various masses of material reporting to the flotation concentrate and that remaining in the feed. Consequently, the weighted or mass-corrected recovery provides an accurate representation of the desired material recovered in the float. The weighted recovery is highest in the tests below a pH of 10 and shows a significant drop at a pH of 10.9. The highest weighted recovery at pH 8.1 also coincides with the highest measured ion intensity for TECFLOTE S11 on chalcopyrite grains reporting to the concentrate.



Note that at pH 8.1 and 9.5 the measured intensity of TECFLOTE S11 on chalcopyrite surfaces from the tails is very low.

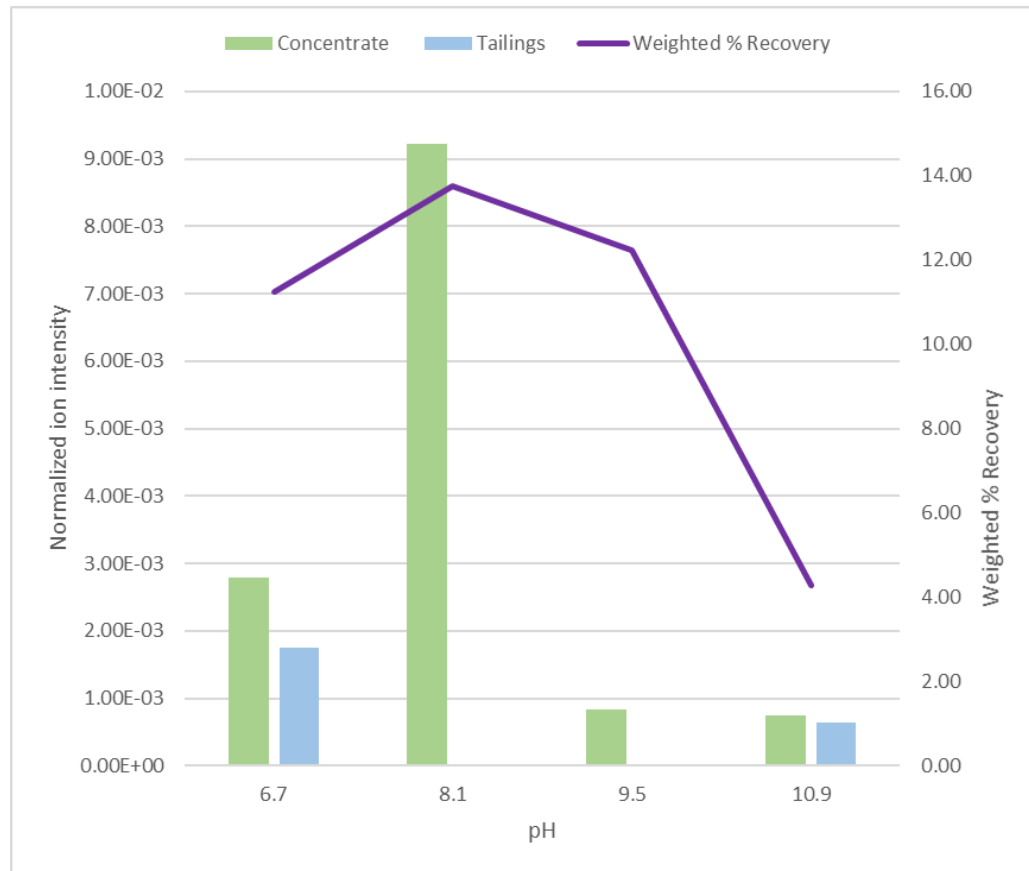


Figure 4.9. Median ion intensity of TECFLOTE S11 at amu 149, on microflotation concentrate (green), tailings (blue) compared to weighted % recovery (purple line)

The difference in the trend of mass corrected and non-mass corrected recovery is striking (compare Figure 4.7 and 4.9) and reflects the relative difference in mass recoveries to the concentrates in the tests performed at the different pH values. For example, comparing the tests performed at pH 8.1 and 10.9, the former had a mass recovery to the concentrate of 25% whereas the later had a mass recovery of only 5%. This difference in mass recovery reflects the inclusion of gangue phases in the flotation process, which decreases the grade of the concentrate. In this example, the mass non-corrected Cu recovery was

55% in 25.2% of the material in the feed at a pH 8.1, whereas the non-corrected Cu recovery was 84% in only 5.2% of the mass of material in the feed in the test performed at a pH of 10.9. Using a mass-corrected recovery, the chalcopyrite recovered to the concentrate at pH 8.1 was 13.8% versus 4.3% at pH 10.9. This illustrates the importance of the concentrate grade which reflects the performance of mineral flotation selectivity in the process. In industrial practice, a metallurgist seeing the decline in concentrate grade at pH 8.1, would instinctively increase the collector dosage, but as seen from Figure 4.9, this would result in more gangue material reporting to the concentrate, rather than an increase in concentrate grade.

As TECFLOTE S11 is water immiscible at room temperature and has no known solvent, it was impossible to accurately control the amount of TECFLOTE S11 used in the micro-flotation tests. One drop of the TECFLOTE S11 from the syringe, weighed 0.0013 g. This is the equivalent of 1300 grams per tonne of "ore", which is two orders of magnitude greater than the collector dosages used in plant trials (Lewis and Lima, 2018). Such dosages of TECFLOTE S11 at pH values of 6.7 and 8.1 may have provided sufficient collector to promote flotation but also may have induced the development of hemi-micelles still attached to the mineral surface providing a significantly higher intensity of collector. The nature of a collector (Figure 4.10), is that the functional headgroup is essentially hydrophilic, has an affinity for water and easily attaches to a mineral surface, whereas the hydrocarbon chain is hydrophobic. Hemi-micelles (aggregates of surfactant molecules) are formed when the hydrophobic headgroups link together, remaining in contact with the solution surrounding the hydrocarbon chains tail regions of the collector. Hemi-micelles can form at high collector concentrations by the linking of collector molecules while maintaining attachment to the mineral surface.

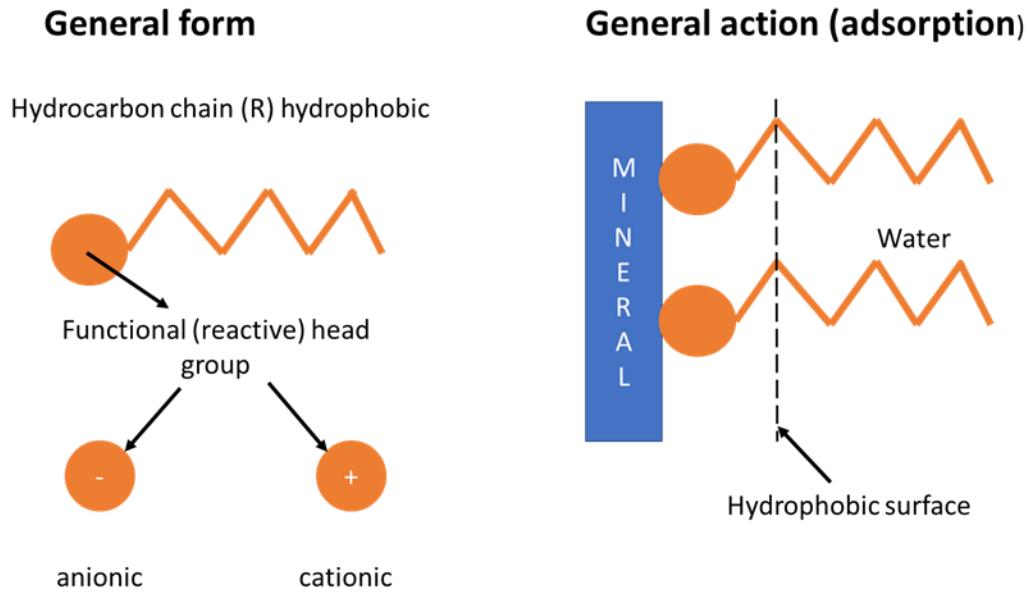


Figure 4.10. General structure and adsorption mechanism of flotation collector Adapted from J.A. Finch, 2019 Slide 16

The discrimination between the concentrate and tailings is due to the difference in adsorption of TECFLOTE S11 on the mineral surfaces. At both the micro-flotation tests performed at high and low pH the discrimination in surface intensity of the collector between concentrate and tailings decreases, with the least discrimination occurring at pH 10.9, when the highest grade of concentrate is reported. The almost identical median ion intensity on the concentrate at pH 9.5 and 10.9, would suggest that this is the minimum adsorption required to float the chalcopyrite, higher intensities on grains from the concentrates or tails might indicate the development of hemi-micelles.

Although there is no direct evidence from the ToF-SIMS studies that suggests a mechanism for TECFLOTE S11 adsorption and the intensity on chalcopyrite surfaces from the concentrate's apparent decreases with increasing pH, it is evident that there is a change in absorption at pH 8.5, with the almost complete disappearance of TECFLOTE S11 on the tailings component (Figure 4.9).

At pH 10.9, the adsorption discrimination between the surface of the concentrate and tailings is less pronounced than at lower pH, but the grade of the concentrate is higher, indicating that although it is likely that less TECFLOTE S11 is adsorbed on the gangue materials as very few are recovered. This behaviour at the high pH may make TECFLOTE S11 a good collector for the cleaner section of the floatation circuit. The decrease in mass recovery with an increase in concentrate grade is similar to what was observed in plant trials at the Aitik mine in Boliden, Sweden (Lewis et al., 2019). The data provided by the microflotation tests agrees with that from the plant trials reported by the manufacturer (Lewis and Lima, 2018), in that the highest grade concentrates are achieved at pH values above 9.

The difference between the column flotation tests and the microflotation test is likely related to the manner in which the TECFLOTE S11 is delivered to the mineral surfaces. With the micro-flotation tests, the TECFLOTE S11 is added to the slurry, similar to the fashion that xanthates are added in an industrial setting. With the column test, the collector is added to a stream of bubbles in the water before the mineral mix is added, so that the collector is carried to the mineral surface by the air bubbles, similar to the manner in which amines are used in the flotation of potash (Burdukova, E. and Laskowski, 2009; Leja, 1983).

A comparison of the mineral surface TECFLOTE S11 intensities on to the concentrate grains from both the micro-flotation tests and the column flotation tests at approximately the same pH (9.5) are given in Figure 4.11. The column flotation tests showed a higher surface intensity of TECFLOTE S11 at amu 119 and 149 before the grains of chalcopyrite were washed than on the surface of the micro-flotation test concentrate, by a factor of approximately 3.5. However, at amu 197 the surface intensities are essentially the same whereas for amu 223, with the ion intensity is greater in the micro-flotation test than the column test. While there is no evidence to explain this reversal, it is suspected that the data, particularly at amu 223 may be affected by a peak overlap, from some

compound not included in the TECFLOTE S11 standard spectrum, causing the intensity measured from the microflotation test to be significantly higher. Aside from the peak at amu 223 the adsorption intensity of the TECFLOTE S11 is higher on the concentrate from the column tests than from the micro-flotation tests, which indicates that the air bubble is a better delivery system than that typically used in the xanthate flotation process (Figure 4.11).

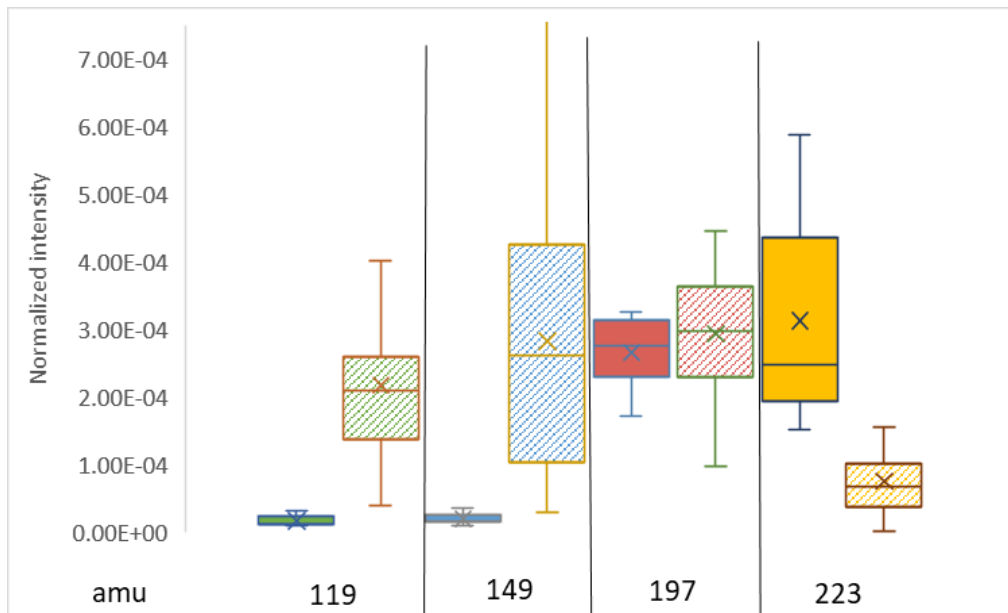


Figure 4.11. Comparison of TECFLOTE S11 surface intensities on chalcopyrite grains from concentrates between the micro-flotation tests (solid colour) and column tests before washing (hashed areas) areas at approximately pH 9.5

A comparison between TECFLOTE S11 on chalcopyrite surfaces from conditioning tests and microflotation test concentrates performed at pH 6.7 are given in Figure 4.12. The data shows that TECFLOTE S11 intensities on chalcopyrite surfaces from the microflotation tests are very slightly higher than those on the grains from the conditioning tests. As the micro-flotation test started with minerals that had been conditioned with TECFLOTE S11 prior to flotation, it is expected that chalcopyrite

grains from the two tests would have similar levels of intensity of TECFLOTE S11 on their surfaces. The difference in TECFLOTE S11 intensity on the chalcopyrite grains from the microflotation concentrate may be related to a longer period of contact with the collector at the air/liquid interface from bubble contact allowing for a greater degree of TECFLOTE S11 adsorption.

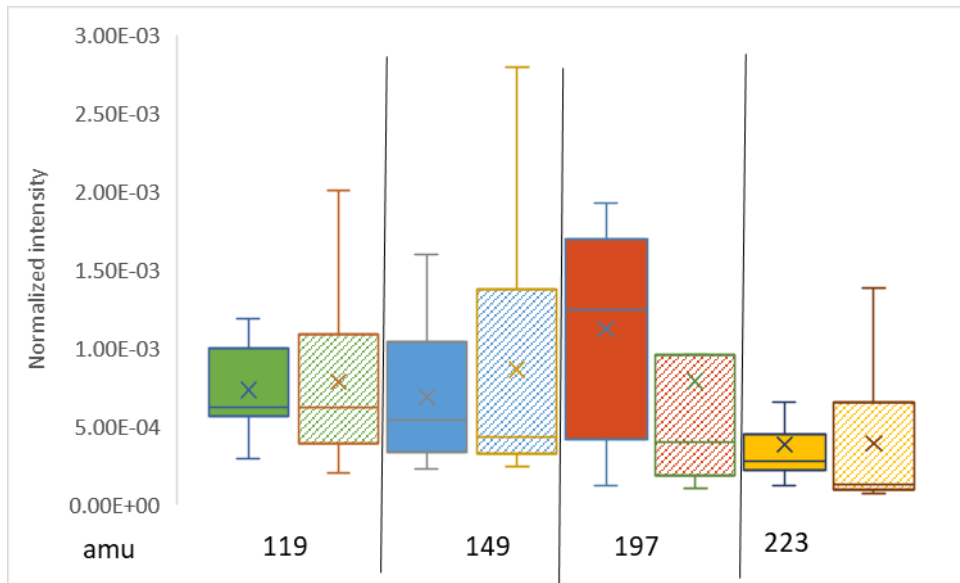


Figure 4.12. Comparison of TECFLOTE S11 surface intensities on chalcopyrite grains from concentrates between micro-flotation tests (solid colour) and conditioning tests (hashed colours) at pH 6.7

## 4.2 Discussion.

### 4.2.1 Distribution mechanism

The model for all collector surface adsorption consists of two parts, the delivery of the collector to the metal sulphide surface and the method of attachment of the collector to the sulphide surface. There are two models for the delivery of collectors currently used in the mineral processing industry; each is specific to the nature of the reagent in use. The mechanisms of attachment are certainly collector specific but are also significantly

affected by the surface chemistry of the various mineral phases in the flotation system. The data in this research has been used to identify the most probable way in which the collector TECFLOTE S11 is delivered to the mineral surface along with some speculation as to how the collector is attached to the mineral surface. The models outlined below have provided some practical guidance towards developing a model for the delivery and adsorption mechanism of TECFLOTE S11 on sulphide mineral surfaces.

**The thiol model.** This model is used with thiol collectors, for example xanthates, which are the most widely used collector in the processing of base metal sulphides. In this model, xanthates which are water soluble, are typically added at the milling and conditioning stage before the flotation circuit. This method has the advantage of allowing early contact of collectors and various activators with the relatively fresh mineral surfaces to be rendered hydrophilic at the front end of the flotation circuit (Konigsmann, 1973). The xanthates being water soluble, are adsorbed onto the sulphide surfaces from the solution where they are typically chemisorbed onto the surface with subsequent formation of metal xanthates or dixanthogen causing the sulphide surface to become hydrophobic (Finkelstein, 1997).

**The amine model.** This model describes the use of amine collectors in the flotation of potash and similarly describes the mechanisms for a number of oily collectors used in the flotation of both sulphides and non-sulphides. The collector is immiscible with water and is introduced as a stirred collector-gas-liquid mixture into the potash ore slurry. The collector spreads across the water/air interface, resulting in bubbles that are coated with the collector. This process only works if the slurry is vigorously stirred, otherwise there is limited opportunity for the collector at the bubble water interface to contact the potash mineral surface (Leja, 1983). The delivery of the collector to the mineral surface then is at the air/water interface through contact with the bubbles.

From the conditioning tests, it appears that the TECFLOTE S11 follows the thiol model, in that when conditioned with TECFLOTE S11 in a vigorously stirred environment, TECFLOTE S11 is adsorbed onto the sulphide mineral surfaces. Surface analysis

identified that chalcopyrite surface showed a greater intensity of TECFLOTE S11 over pyrite, indicating a degree of collector selectivity for the chalcopyrite likely resulting in its preferential recovery over pyrite.

With the column tests, where the only source of the TECFLOTE S11 is from the bubble surface, there was clearly a greater intensity of the TECFLOTE S11 on the chalcopyrite surface over the intensity on the chalcopyrite surface in the conditioning tests. This suggests that the TECFLOTE S11 carried by the air bubbles is delivered to the mineral surface more efficiently where introduced as a collector-bubble-liquid mixture rather than being introduced to the microflotation cell as a liquid followed by vigorous stirring. Therefore, it would appear that the TECFLOTE S11 on the surface of the sulphide minerals from a concentrate is likely transferred through a hybrid of the thiol and amine models. However, as the collector is considered immiscible, delivery to the mineral surface is most probably dominated by the contact with bubbles.

#### 4.2.2 Adsorption mechanism

The adsorption mechanism of the more common flotation collectors, such as xanthates or TECFLOTE S11 is either by chemisorption, or physisorption. In the former, the anionic headgroup attached to the long chain hydrocarbon, forms a chemical bond with the surface of the mineral. In the case of xanthate and chalcopyrite, the collector typically attaches to the copper atom forming a metal-xanthate or dixanthogen, which renders the chalcopyrite surface hydrophobic.

For TECFLOTE S11, which has a  $\text{CN}^-$  ion attached to the hydrocarbon chains, one might expect that there would be a compound of copper and cyanide formed at the site of the TECFLOTE S11 adsorption and that there would be a higher ion intensity of the  $\text{CN}^-$  or  $\text{CNO}^-$  (isocyanate) ions and certainly a higher intensity on the concentrate than on the tailings surfaces in the micro-flotation tests. The ToF-SIMS spectra for these specific ions did not show any appreciable difference in the ion intensity of the  $\text{CN}^-$  or  $\text{CNO}^-$  ions



between the micro-flotation products, leading to the conclusion that the adsorption may not be chemical in nature.

With physisorption, it is speculated that the collector is adsorbed onto the mineral surface by electrostatic attractions or possibly similar to Van der Waals attraction. These forces are generally very weak and, within a rather aggressive flotation environment, seem unlikely to be the dominant mechanism for attachment. Furthermore, as TECFLOTE S11 is described by the manufacturer as non-ionic (Lewis and Lima, 2018), one would not expect the adsorption mechanism to be electrostatic in nature.

However, the surface analysis from the microflotation test products clearly showed higher intensities of the peaks definitive of the collector on the surface of the chalcopyrite grains reporting to the concentrates over the tails. This indicates that there is indeed some mechanism of attachment. Furthermore, there appears to be some link between mineral recovery and pH, which suggests that variabilities in mineral surface charge in response to changes in pH may lead to an electrostatic attraction of the collector (Kosmulski, M., 2020). Given the above, it is apparent from this research that, no clear mechanism for collector attachment to the mineral surface could be identified.

The extremely high proportion of TECFLOTE S11 on the surface of chalcopyrite in the microflotation concentrates and high proportion of gangue minerals recovered to the concentrate at pH 8.1 may be linked to a high dose of collector and the development of collector aggregates. Hemi-micelles (aggregates of surfactant molecules) are formed when the hydrophobic headgroups link together, remaining in contact with the solution surrounding the hydrocarbon chains tail regions of the collector. In cases where excess collector exists in solution, colloidal-sized groups of organic ions can be formed where chains associate in tight clusters pointing inwards whereas the functional headgroups remain pointing outwards into the water. The shape of the hemi-micelles is determined by the equilibrium of the forces of attraction of the hydrocarbon chains and forces of repulsion of the functional headgroups of the collector ions (Aplan and Fuerstenau, 1962). As the number of hemi-micelles increase, they eventually reach a concentration

where flotation becomes diminished (Dobias, 1986). This is referred to as the Critical Micelle Concentration (CMC) and identifies a concentration where a significant proportion of the collector hydrophobic reports to the tails, regardless of whether the headgroup is adsorbed on the mineral surface, and are no longer effective to induce flotation. The development of multiple collector layers, rather than a single mono-layer on mineral surfaces, generated in a similar fashion to hemi-micelles has been suggested to affect flotation recovery of minerals (Rao, 2004). Hemi-micelle formation on the chalcopyrite surface may explain the behaviour at pH 8.1, where the results from the surface analysis show higher intensity of the mass fragments representative of the TECFLOTE S11 collector on the mineral surface.

Furthermore, with an overabundance of TECFLOTE S11 in the flotation test, the excess is available for adsorption by the gangue minerals. These inadvertently activated grains then report to the concentrate, lowering the grade of the concentrate, evident in the tests performed below pH10. The adsorption of TECFLOTE S11 on gangue phases along with the potential development of hemi-micelles would deplete the collector leaving little to be adsorbed and measured on minerals in the tailings, accounting for the very low measured intensities on the surface of the minerals in the tails from the tests performed at pH 8.1 and 9.5.

#### 4.2.3 Selectivity of TECFLOTE S11 for chalcopyrite instead of pyrite.

In industrial mineral processing settings, the selective separation of chalcopyrite from pyrite is achieved by the addition of lime ( $\text{Ca}(\text{OH})_2$ ) or NaOH and conducting the flotation at high pH > 10 (Yan et al., 2018). This practice induces pyrite hydrophobicity by promoting partial surface oxidation and the adsorption of  $\text{OH}^-$  ions onto the 100 plane of the pyrite crystal, inhibiting the development of a hydrophobic surface (Yan et al., 2018). Furthermore, surface analysis from numerous studies has identified layers of hydrophylic hydroxides formed on pyrite surfaces at alkaline pH, for example Han, et al.

(2020). If this mechanism is indeed operative in tests performed in this study it would be expected that there would be a higher  $\text{OH}^-$  ion intensity on the pyrite surface from the tailings for the micro-flotation test carried out at pH 10.9, than at lower pH values. The pyrite surface analysis showed that median  $\text{OH}^-$  ion intensities are approximately the same at pH 6.7 and pH 10.9 (Tables A17 and A37). These data indicate that the absorption of  $\text{OH}^-$  on pyrite surfaces is not the dominant cause of the preferential selectivity of TECFLOTE S11 of chalcopyrite over pyrite.

The preferred selectivity of TECFLOTE S11 for chalcopyrite over pyrite may possibly be explained by the physical differences of the two minerals. More specifically, the difference in breakage of the two minerals. The breakage characteristics are important because it has been found that areas of mineral surfaces that are broken or etched have higher surface free energies and are more likely to be chemically reactive (Prosser, 1969). This was supported by Beischer (1953) who identified stronger adsorption of stearic acid on quartz surfaces in areas where it was scratched as opposed to the fresh surfaces.

Pyrite has an isometric structure and fractures conchoidally (Hurlburt and Klein, 1985a). Chalcopyrite on the other hand, has a tetrahedral structure and fractures irregularly and unevenly (Hurlburt and Klein, 1985b). The rougher surfaces of the chalcopyrite will likely have a higher surface free energy and greater number of sites for collector attachment over the pyrite. The increased adsorption of TECFLOTE S11 on the chalcopyrite grains due to the higher surface free energy, will contribute to the increased contact angle of the mineral surface (You et al., 2020) rendering the chalcopyrite surface more hydrophobic than pyrite promoting a higher recovery of chalcopyrite during flotation.

### 4.3 Summary

In summary, the tests performed in the investigation allow some conclusions to be drawn regarding the objectives of the investigation.

The conditioning test demonstrated that TECFLOTE S11 was adsorbed onto the mineral particle surfaces from a vigorously stirred slurry. The TECFLOTE S11 show a preference for chalcopyrite surfaces rather than pyrite surfaces. It is postulated that this preference is a result of the difference in fracturing characteristics between the two minerals and the resultant surface free energy of the broken surfaces, which is linked to preferential collector adsorption on chalcopyrite.

In the column flotation tests, the mineral mixture was delivered directly into the water/air/ collector interface, as opposed to the conditioning test where the collector was delivered to the mineral/ water interface. In the column tests, the rapid flotation of the chalcopyrite to the froth zone along with the lower TECFLOTE S11 ion intensity compared to that from the conditioning tests demonstrates that the TECFLOTE S11 was rapidly delivered to the mineral surface likely through contact with the bubble. The lower level of ion intensity on the minerals floated in the column tests compared to the conditioning tests, is probably due to the difference in the time required to induce chalcopyrite flotation between the two tests.

From the micro-flotation tests, data about the relationship between the adsorption of TECFLOTE S11 on chalcopyrite and the metallurgical performance as measured by the weighted recovery, was collected. The highest grade of the concentrate was found at pH 10.9, while the lowest grade was found at pH 8.1, where the highest mass recovery was measured. The high mass recovery at pH 8.1 also coincides with the highest measured TECFLOTE S11 ion intensity on the surface of chalcopyrite and is speculated to be the result of hemi-micelles forming on the chalcopyrite surfaces. The high mass recovery is believed to be related to excess TECFLOTE S11 in the system being adsorbed onto the

surface of the gangue minerals, allowing them to report to the concentrate instead of the tailings.

## 4.4 References

- Aplan, F.F., and Fuerstenau, D. W. (1962). Principles of Nonmetallic Mineral Flotation. In D. W. Fuerstenau (Ed.), *Froth Flotation. 50th Anniversary Volume* (p. 177). New York, New York: American institute of Mining, Metallurgical and Petroleum Engineers.
- Beischer, D. E. (1953). Radioactive Monolayers: A new approach to surface research. *Journal of Physical Chemistry*, 57(2), 137.
- Burdukova, E. and Laskowski, J. S. (2009). Effect of Insoluble Amine on Bubble Surfaces on Particle-Bubble Attachment in Potash Flotation. *Can. Jour. of Chem. Eng.*, 87, 441–447.
- Dobias, B. (1986). Adsorption, Electrokinetic, and flotation Properties of Concentration Minerals above the Critical Micelle. In J. F. Scamehorn (Ed.), *Phenomena in Mixed Surfactant Systems* (ACS Symp., pp. 216–224). Washington D.C.
- Finkelstein, N. P. (1997). The activation of sulphide minerals for flotation: a review. *International Journal of Mineral Processing*, 52, 81–120.
- Han, G., Wen, S., Wang, H., Feng, Q. (2020). Selective adsorption mechanism of salicylic acid on pyrite surfaces and its application in flotation separation of chalcopyrite from pyrite. *Separation and Purification Technology*, 240, 1–9.
- Hurlburt, C.S., Klein, C. (1985a). *Manual of Mineralogy* (20th ed.). New York: John Wiley and Sons.
- Hurlburt, C.S., Klein, C. (1985b). *Manual of Mineralogy* (20 th). New York: John Wiley and Sons.

- Konigsmann, K. V. (1973). Aeration in Plant Practice. In *Proc. 5th Annual Meeting, Can. Min. Processors* (pp. 299–33.2). Ottawa.
- Kosmulski, M. (2020) The pH dependent surface charging and point of zero charge. VIII . Update. *Advances in Colloid and Interface Science*, 275, 102064-102082.
- Leja, J. and Schulman, J. H. (1954). Flotation Theory: molecular Interactions Between frothers and Collectors at solid-Liquid-air interfaces. *Transactions AIME*, 199, 221–228.
- Leja, J. (1983). *On the Action of Long Chain Amines in Potash Flotation*. (R. M. McKercher, Ed.). Toronto: Pergamon Press.
- Lewis, A., Bolin N-J., Malm, Svensson, M., Lima, O. (2019). Analysis of the rougher-scavenger bank using Tecflote S11 at Boliden Aitik. In *Flotation '19*.
- Lewis, A. and Lima, O. (2018). Tecflote- New collector for Sulfide Flotation. In *Procemin Geomet* (pp. 321–333). Santiago, Chile.
- Prosser, A. P. (1969). Influence of mineralogical factors on the rates of chemical reaction of minerals. In *Proceedings of the Ninth Commonwealth Mining and Metallurgical Congress 1969 Vol 3 Vol 3* (pp. 59–79). London: The Institution of Mining and Metallurgy.
- Rao, S. R. (2004). *Surface Chemistry of Froth Flotation* (Second). New York: Plenum.
- Schach, E., Lewis, A., Rudolph, M. (2019). Investigations on the working mechanism of the nitrile based sulfide collector TECFLOTE™. In *Flotation '19*.
- Yan, H., Yuan, Q., Zhou, L., Qiu, T., Ai, G. (2018). Flotation Kinetics and thermodynamic behavior of chalcopyrite and pyrite in high alkaline systems. *Physicochemical Problems of Mineral Processing*, 54((3)), 901–910.
- You, K., Kim, K., Han, S., Kwon, S. (2020). Direct measurement of interaction force between solid surface and air bubble. Relationship between interaction force and contact angle. *Minerals Engineering*, 152, 1–8.

## 5 Conclusions

The overall goal of this thesis is, through surface chemical analysis of pyrite and chalcopyrite from various laboratory-based flotation tests, to identify factors which may contribute to the selective flotation of chalcopyrite over pyrite using the collector TECFLOTE S11 as observed in plant trials. This chapter draws upon the test results presented in the previous chapter, and provides some conclusions regarding the objectives of the investigation. The conclusions are presented here in terms of the three groups of tests performed. It should be pointed out that, for this discussion, the degree to which TECFLOTE S11 is surface adsorbed, or rather its relative surface proportion, is based on surface intensity measurements by TOF-SIMS.

From the conditioning tests, it was found that TECFLOTE S11 was adsorbed onto the mineral surfaces from the vigorously stirred mineral slurry. Furthermore, the adsorption of TECFLOTE S11 was greater on the surface of chalcopyrite than on the pyrite grain surfaces. The adsorption mechanism of TECFLOTE S11 onto the mineral surfaces may be electrostatic in nature and the preference for chalcopyrite may be a result of the differences in mineralogy between the two minerals. The fractured surfaces of the chalcopyrite having a higher surface free energy than the pyrite surfaces, thus adsorbing the TECFLOTE S11 preferentially over the pyrites.

From the column flotation tests, it was found that TECFLOTE S11 was best dispersed through the system on bubble surfaces in a vigorously stirred air/water slurry. Bubble contact with the subsequently added minerals resulted in rapid collector adsorption and flotation, indicating that the TECFLOTE S11 was delivered to the mineral surface through contact with the air bubbles rather than adsorption from solution.

The results from the micro-flotation tests failed to provide some clear conclusions in regards to a relationship between chalcopyrite flotation recovery and pH. The data may however offer some insight to processes that may be happening at the mineral surface.

When the adsorption of TECFLOTE S11 on chalcopyrite surfaces in the test concentrates is highest (pH 8.1), the mass recovery is also highest as an excess of gangue minerals are inadvertently activated and report to the concentrate instead of the tailings. The high proportion of gangue reporting to the concentrate at pH 8.1 may be related to overdosing of the collector but may also be linked to some unknown phenomena on the surface of the gangue minerals at this particular pH. The very high intensity of TECFLOTE S11 on chalcopyrite surfaces at pH 8.1 has been postulated to be a result of the development of hemi-micelles, which may also have partially inhibited chalcopyrite recovery.

At pH 9.5 and 10.9 the level of TECFLOTE S11 on the chalcopyrite grains reporting to the concentrates is very similar may represent the minimum required for flotation. At pH 10.9 the grade of the concentrate is high indicating that there is likely less TECFLOTE S11 adsorbed on the gangue materials making the collector excellent for the cleaner section of the circuit where gangue exclusion is the goal.



## 6 Future Work

The declaration of a pandemic and the subsequent lockdown of the Surface Science Western facilities, resulted in a secession of research activities to the investigations that form a portion of this thesis. If research activities would have continued, the following would have been performed to confirm the findings obtained to that time.

Column flotation test on the synthetic ore 2, with a grade similar to those found in volcano-genic massive sulphide deposits, at the same pH as used in the micro-flotation test to compare the TECFLOTE S11 ion intensities and recoveries to determine if there is a drop in the recovery at pH 8.1, or if the different distribution mechanism does not result in gangue minerals reporting to the concentrate.

To further investigate the surface attachment mechanism of TECFLOTE S11, the surface chemical characteristics of chalcopyrite at variable pH's and the ensuing varying degrees of collector adsorption, should be studied. Suitable techniques for such a study could include TOF-SIMS, Zetapotential, FTIR, XPS or possibly AFM.

Tensiometer studies of the chalcopyrite surface in contact with TECFLOTE S1, should be performed to determine the critical micelle concentration (CMC), to confirm the hypothesis proposed in the previous chapter, that hemi-micelles are formed at pH 8.1. If the CMC study is inconclusive, then further investigation should focus on the electrochemistry of the mineral surfaces during flotation to determine if there is a surface charge change of the constituent minerals in the ore, which would account for the decrease in copper recovery when the surface adsorption of TECFLOTE S11 is highest. This extension of testing, may reveal if the TECFLOTE S11 adsorption is caused by chemisorption or physisorption.

Given that the calculation of the Cu content in the concentrate is based on subtraction of that which is measured by EDX in the tails from that which was calculated in the feed,




factors linked to sample preparation and the EDX technique could introduce a significant degree of error in the results. The use of EDX to estimate the Cu content of the samples, has some limitations, especially when the Cu content of the tailings samples is close to the detection levels of the technique. Reported results for the tailings in the range of detection limits could lead to errors in the range of 100% resulting in a similar error in the calculated Cu concentration in the concentrate samples.









In regards to sample preparation, spreading the tailings grains on the adhesive carbon discs, could introduce a bias into the results. Firstly, a variation in the depth of grains could result in a lowering of the Cu grade because the chalcopyrite grains are hidden below the gangue mineral grains. EDX only scans the topmost microns of the sample surface, so a complete accounting of the chalcopyrite grains in the sample may not have been accomplished in the scans. This would be particularly true when the mass pull is greatest, as the sample will contain more gangue minerals.









Secondly, particle size may create a problem. Coarser particles will probably cause the Cu content to be registered higher than finer particles, because of the bias described above. A predominance of fine particles, will lower the measured Cu content, not only because of the hidden particles, but because of the total surface of the chalcopyrite compared to the surface area of the larger gangue mineral grains.









To counteract the potential bias towards higher Cu content in the EDX results, other techniques should be considered for estimating the Cu content of the samples. Such techniques include, wet chemical assay, atomic adsorption, inductively-coupled plasma mass-spectrometry and X-ray fluorescence.









## Appendix 1. Test data









Table	Description	File
A1	Conditioning tests +ve ions on Chalcopyrite grains: Baseline	 Table A1.xlsx
A2	Conditioning tests -ve ions on Chalcopyrite grains: Baseline	 Table A2.xlsx
A3	Conditioning tests +ve ions on Pyrite grains: Baseline	 Table A3.xlsx
A4	Conditioning tests -ve ions on Pyrite grains: Baseline	 Table A4.xlsx
A5	Conditioning tests +ve ion loadings on Chalcopyrite grains	 Table A5.xlsx
A6	Conditioning tests. -ve ion loadings on Chalcopyrite grains	 Table A6.xlsx
A7	Conditioning tests. +ve ions on Pyrite grains	 Table A7.xlsx

A8	Conditioning tests -ve ions on Pyrite grains	 Table A8.xlsx
A9	Conditioning tests with addition of CuSO4 -ve loadings on Chalcopyrite	 Table A9.xlsx
A10	Conditioning tests with addition of CuSO4 +ve ion loadings on Chalcopyrite grains	 Table A10.xlsx
A11	Conditioning test with addition of CuSO4 -ve ions loading on Pyrite grains	 Table A11.xlsx
A12	Conditioning tests with addition of CuSO4 +ve ion loadings on Pyrite grains	 Table A12.xlsx
A13	Micro-flotation tests -ve ion loadings on concentrate pH 6.7	 Table A13.xlsx
A14	Micro-flotation tests TECFLOTE S11 -ve ion loadings on concentrate pH 6.7	 Table A14.xlsx
A15	Micro-flotation tests +ve ion loadings on concentrate pH 6.7	 Table A15.xlsx




A16	Micro-flotation tests TECFLOTE S11 +ve ion loadings on concentrate pH 6.7	 Table A16.xlsx
A17	Microflotation tests. -ve ions loading on tailings pH 6.7	 Table A17.xlsx
A18	Microflotation tests. TECFLOTE S11 -ve ions loading on tailings pH 6.7	 Table A18.xlsx
A19	Micro-flotation tests. +ve ion loadings on tailings. pH 6.7	 Table A19.xlsx
A20	Micro-flotation tests. TECFLOTE S11 +ve ion loadings on tailings. pH 6.7	 Table A20.xlsx
A21	Micro-flotation tests. -ve ion loadings on concentrate. pH 8.1	 Table A21.xlsx
A22	Micro-flotation tests. TECFLOTE S11 -ve ion loadings on concentrate. pH 8.1	 Table A22.xlsx
A23	Micro-flotation tests. +ve ion loadings on concentrate. pH 8.1	 Table A23.xlsx

A24	Micro-flotation tests. TECFLOTE S11 +ve ion loadings on concentrate. pH 8.1	 Table A24.xlsx
A25	Micro-flotation tests +ve ion loadings on tailings pH 8.1	 Table A25.xlsx
A26	Micro-flotation tests -ve ion loadings on tailings pH 8.1	 Table A26.xlsx
A27	Micro-flotation tests TECFLOTE S11 -ve ion loadings on tailings pH 8.1	 Table A27.xlsx
A28	Micro-flotation tests TECFLOTE S11 +ve ion loadings on tailings pH 8.1	 Table A28.xlsx
A29	Microflotation tests. -ve ion loadings on concentrate. pH 9.5	 Table A29.xlsx
A30	Microflotation tests. TECFLOTE S11 -ve ion loadings on concentrate. pH 9.5	 Table A30.xlsx
A31	Micro-flotation tests. +ve ion loadings on concentrate. pH 9.5	 Table A31.xlsx

A32	Micro-flotation tests. TECFLOTE S11 +ve ion loadings on concentrate. pH 9.5	 Table A32.xlsx
A33	Micro-flotation tests. -ve ion loadings on tailings. pH 9.5	 Table A33.xlsx
A34	Micro-flotation tests. TECFLOTE S11 -ve ion loadings on tailings. pH 9.5	 Table A34.xlsx
A35	Micro-flotation tests. +ve ions loadings on tailings. pH 9.5	 Table A35.xlsx
A36	Micro-flotation tests. TECFLOTE S11 +ve ions loadings on tailings. pH 9.5	 Table A36.xlsx
A37	Micro-flotation tests. -ve ion loadings on concentrate. pH 10.9	 Table A37.xlsx
A38	Micro-flotation tests. TECFLOTE S11 -ve ion loadings on concentrate. pH 10.9	 Table A38.xlsx
A39	Micro-flotation tests. +ve ion loadings on concentrate. pH 10.9	 Table A39.xlsx


A40	Micro-flotation tests. TECFLOTE S11 +ve ion loadings on concentrate. pH 10.9	 Table A40.xlsx
A41	Micro-flotation tests. -ve ion loadings on tailings. pH 10.9	 Table A41.xlsx
A42	Micro-flotation tests. TECFLOTE S11 -ve ion loadings on tailings. pH 10.9	 Table A42.xlsx
A43	Micro-flotation tests. +ve ion loadings on tailings. pH 10.9	 Table A43.xlsx
A44	Micro-flotation tests. TECFLOTE S11 +ve ion loadings on tailings. pH 10.9	 Table A44.xlsx
A45	Column flotation tests -ve ion loadings unwashed grains	 Table A45.xlsx
A46	Column flotation tests. +ve ion loadings unwashed grains	 Table A46.xlsx
A47	Column flotation tests. -ve ion loadings washed grains	 Table A47.xlsx



A48	Column flotation tests. +ve ion loading washed grains	 Table A48.xlsx
A49	Micro-flotation tests tailings EDX values	 Table A49.xlsx
A50	Micro-flotation tests. Metallurgical balance	 Table A50.xlsx

## Appendix 2. Permissions to Reproduce

Figure	Permission
1.1	<a href="https://s100.copyright.com/CustomerAdmin/PLF.jsp?ref=fea5085d-eead-485c-aa40-9f4b4ac7d54b">https://s100.copyright.com/CustomerAdmin/PLF.jsp?ref=fea5085d-eead-485c-aa40-9f4b4ac7d54b</a>
2.3	<a href="https://s100.copyright.com/CustomerAdmin/PLF.jsp?ref=57589133-9178-4730-8c48-c9b4953a91c3">https://s100.copyright.com/CustomerAdmin/PLF.jsp?ref=57589133-9178-4730-8c48-c9b4953a91c3</a>
2.4	<a href="https://s100.copyright.com/CustomerAdmin/PLF.jsp?ref=57589133-9178-4730-8c48-c9b4953a91c3">https://s100.copyright.com/CustomerAdmin/PLF.jsp?ref=57589133-9178-4730-8c48-c9b4953a91c3</a>
2.5	<a href="https://s100.copyright.com/CustomerAdmin/PLF.jsp?ref=dc80df8b-1c35-491f-97e8-fc4d37290109">https://s100.copyright.com/CustomerAdmin/PLF.jsp?ref=dc80df8b-1c35-491f-97e8-fc4d37290109</a>
2.6	<a href="https://s100.copyright.com/CustomerAdmin/PLF.jsp?ref=e8cea1fe-7a44-49dd-8573-7b1c97fef7d5">https://s100.copyright.com/CustomerAdmin/PLF.jsp?ref=e8cea1fe-7a44-49dd-8573-7b1c97fef7d5</a>
2.8	 <p>Figure 2.8 &amp;9.pdf</p>
2.9	 <p>Figure 2.8 &amp;9.pdf</p>
2.18	<a href="https://marketplace.copyright.com/rs-ui-web/mp/checkoit.confirmation-details/bc7cffa-83e2-46af-ad24-c3512629d">https://marketplace.copyright.com/rs-ui-web/mp/checkoit.confirmation-details/bc7cffa-83e2-46af-ad24-c3512629d</a>
2.22	<a href="https://s100.copyright.com/CustomerAdmin/PLF.jsp?ref=9cea9092-9fea-4866-9de8-e031f9ff4721">https://s100.copyright.com/CustomerAdmin/PLF.jsp?ref=9cea9092-9fea-4866-9de8-e031f9ff4721</a>

2.23	<a href="https://s100.copyright.com/CustomerAdmin/PLF.jsp?ref=ac6530be-31c0-4d97-af86-304f1b6e89b3">https://s100.copyright.com/CustomerAdmin/PLF.jsp?ref=ac6530be-31c0-4d97-af86-304f1b6e89b3</a>
2.24	<a href="https://s100.copyright.com/CustomerAdmin/PLF.jsp?ref=b1633008-e03b-4a99-a43c-2e4ad3b5367e">https://s100.copyright.com/CustomerAdmin/PLF.jsp?ref=b1633008-e03b-4a99-a43c-2e4ad3b5367e</a>
2.25	<a href="https://s100.copyright.com/CustomerAdmin/PLF.jsp?ref=95be63cf-5768-4963-8611-18c9dde21197">https://s100.copyright.com/CustomerAdmin/PLF.jsp?ref=95be63cf-5768-4963-8611-18c9dde21197</a>
2.26	<a href="https://s100.copyright.com/CustomerAdmin/PLF.jsp?ref=ac6530be-31c0-4d97-af86-304f1b6e89b3">https://s100.copyright.com/CustomerAdmin/PLF.jsp?ref=ac6530be-31c0-4d97-af86-304f1b6e89b3</a>
3.1	<a href="https://s100.copyright.com/CustomerAdmin/PLF.jsp?ref=4043c6a2-c0fe-4665-b653-83d8010f2179">https://s100.copyright.com/CustomerAdmin/PLF.jsp?ref=4043c6a2-c0fe-4665-b653-83d8010f2179</a>
3.2	 Figure 3.2.pdf

## Curriculum Vitae

**Name:** Trevor Holness

**Post-secondary Education and Degrees:** Imperial College of Science and Technology  
London, England

1965-1968, B.Sc. (Eng.).  
Royal School of Mines  
London, England.

1965-1968, A.R.S.M

University of Western Ontario  
London, Ontario, Canada

1971-1973 M.B.A.

The University of Western Ontario  
London, Ontario, Canada

2018-2020 M.Sc.

**Professional Designation** P. Eng.  
Professional Engineers of Ontario

<b>Honours and Awards:</b>	The University of Western Ontario London, Ontario 1973 Dean's Honour List
<b>Related Work Experience</b>	Teaching Assistant Western University London, Ontario 2018-2020
	Research Assistant Sala Maskinfabrik AB. Sala, Sweden Summer 1966
	Mill Laboratory Assistant Mattagami Lake Mines Matagami, Quebec Summer 1967
	Mill Metallurgist Mines de Poirier Joutel, Quebec

1968-1971

Techno-Economic Analyst

Noranda Research Centre

Pointe-Claire, Quebec

Summer 1972